Anisotropic Plasticity and Viscoplasticity

Vom Fachbereich Mechanik
der Technischen Universität Darmstadt
zur Erlangung des Grades eines

Doktor Ingenieurs
(Dr.-Ing.)

genehmigte

Dissertation

von

Dipl.-Ing. David Schick

aus Ichenhausen

Hauptreferent:	Prof. Dr.-Ing. Ch. Tsakmakis
Korreferent:	Prof. Dr.-Ing. F. Gruttmann
Tag der Einreichung:	31.10.2003
Tag der mündlichen Prüfung:	07.01.2004

Darmstadt 2004

D 17

Die vorliegende Arbeit entstand während meiner Tätigkeit als wissenschaftlicher Mitarbeiter am Institut für Mechanik der Technischen Universität Darmstadt.

Herrn Prof. Dr.-Ing. Ch. Tsakmakis möchte ich herzlich für die hervorragende wissenschaftliche und außerordentlich freundschaftliche Betreuung, sowie für die Übernahme des Hauptreferates danken. Herrn Prof. Dr.-Ing. F. Gruttmann danke ich für das Interesse an dieser Arbeit und für die freundliche Übernahme des Korreferates.

Für die fachlichen Diskussionen und Anregungen möchte ich mich bei meinen Kollegen, insbesondere bei Herrn Dr. rer. nat. P. Grammenoudis, bedanken.

Darmstadt, im Januar 2004 David Schick

Zusammenfassung

Anisotropie, gekoppelt mit inelastischem Fließen spielt in vielen Bereichen der Materialtheorie eine wichtige Rolle. Beispiele dafür sind Stoffgesetze zur Kristallplastizität, zur Beschreibung von Texturen in Blechen usw. Im ersten Teil der vorliegenden Arbeit werden die konstitutiven Materialgleichungen für die Materialantwort bei Orthotropie und kubischer Anisotropie entwickelt. Zu diesem Zweck wird das in Tsakmakis [106] vorgestellte thermodynamisch konsistente konstitutive Materialmodell für Plastizität und Viskoplastizität bei großen Deformationen für diese beiden Fälle der Anisotropie weiter ausgeführt.
Wichtige Bestandteile der Theorie sind die multiplikative Zerlegung des Deformationsgradienten in einen elastischen und inelastischen Anteil sowie die Annahme der Gültigkeit des sogenannten Postulats von Il'iushin für Plastizität. Es wird sowohl eine anisotrope kinematische Verfestigung als auch eine allgemeine Gestaltänderung der Fließfläche berücksichtigt. Die Theorie ist phänomenologisch formuliert und invariant gegenüber beliebigen überlagerten Starrkörperrotationen in der plastischen Zwischenkonfiguration und der Momentankonfiguration.
Die Anisotropie wird mit Hilfe sogenannter Strukturtensoren in der freien Energiefunktion und der Fließfunktion formuliert. Für den Fall der kubischen Anisotropie wurde ein Brinell Kugeleindruckversuch simuliert und qualitativ mit dem Experiment an einer einkristallinen Nickelbasislegierung (CMSX4) verglichen.

Bei einem anfänglich isotropen Material kann durch die plastische Deformation eine Anisotropie induziert werden, was sich insbesondere bei Metallen durch eine Verschiebung, Rotation und Verzerrung (formative Verfestigung) der Fließfläche ausdrückt. Dies wurde auch durch verschiedene experimentelle Untersuchungen unabhängig von der Definition des Fließbeginns bestätigt. Im zweiten Teil der Arbeit wird ein einfaches, thermodynamisch konsistentes Materialmodell für kleine Deformationen entwickelt, das die Evolution der Anisotropie in der Fließfläche beschreibt. Das Modell erfüllt hinreichende Bedingungen für die sogennante Dissipationsungleichung. Abschließend wird die Evolution der Fließfläche für verschiedene Vorbelastungen simuliert und mit den Experimenten von Ishikawa an SUS 304 Edelstahl Rohrproben qualitativ verglichen.

Abstract

Plastic anisotropy effects may be described in a phenomenological model by employing in the constitutive theory a set of internal variables, which are defined suitably. These variables have to model the hardening response of the material under consideration to describe e.g. the rotation of some symmetry axes. Such axes are imagined to be related with the development of the material substructure assumed, or, correspondingly, with the state variables characterizing this development. The objective of the first part of this work is to develop the constitutive equations governing the material response for the case of orthotropic and cubic anisotropy. Therefore the thermodynamically consistent theory for plasticity (and viscoplasticity), recently published by Tsakmakis [106], which accounts for anisotropy effects is presented and extended for the aforementioned cases of anisotropy.
Important features of the theory are the use of the multiplicative decomposition of the deformation gradient tensor as well as the assumption of the validity of Il'iushin's postulate in the case of plasticity. For simplicity, apart from kinematic hardening effects, only orientational evolution of the underlying substructure is regarded. Care is taken that the theory is invariant with respect to rigid body rotations superposed to both, the current and the so-called plastic intermediate configuration.
Anisotropy effects are elaborated in the free energy and the yield function by means of structural tensors. For the case of cubic material symmetry a Brinell hardness indentation test has been simulated and is compared qualitatively with the experiment for a commercially available single-crystal nickel-based superalloy (CMSX4).

Inelastic deformations induce anisotropy in the material response, even if this is initially isotropic. For metallic materials, deformation induced anisotropy is reflected, above all, by translation, rotation and distortion of the yield surface. This has been confirmed by several experimental investigations independent of the way the yield point is defined. In the second part of this work a simple, thermodynamically consistent model is proposed, describing the evolving anisotropy of the yield surface. The model is first theoretically established, based on a sufficient condition for the dissipation inequality to be satisfied. Then, it is applied to predict the subsequent yield surfaces, after various prestressings, which have been observed experimentally by Ishikawa for SUS 304 stainless steel.

Contents

Chapter 1

Introduction

1.1 Objective of the work

A closer view on anisotropic plastic and viscoplastic material behavior reveals – especially for metals – a lot of unclear issues and unsolved problems. Realistic material properties input represents one of the major limitations in computer stress analysis in the plastic range. In spite of some very subtle theoretical treatments of plastic deformation such as for example the approach to dislocation dynamics based on an atomistic understanding of crystal defects and their movement or the crystal plasticity approach relating the behavior of polycrystalline aggregates to the slip behavior in single crystals, the so-called phenomenological theory of plasticity remains the theory used extensively in stress analysis problems.

In the first part of the present work new aspects of a thermodynamic consistent constitutive model for single crystals and large deformation, based on recent works of Tsakmakis [106] and Häusler et al. [43] will be presented. Here materials are considered that have a substructure which may macroscopically be accounted for by employing a set of internal state variables. The constitutive models dealt with are rate-dependent and rate-independent plasticity laws exhibiting anisotropy effects related to kinematic and orientational hardening. (For simplicity isotropic hardening and distortional hardening is not regarded). Such plasticity laws have extensively been discussed by Dafalias (see the comprehensive study in Dafalias [32] and the references cited herein) in the framework of constitutive and related plastic spin concepts. Physically, the mechanical response described may be assigned to initially anisotropic materials as e.g. rolled plates, single crystals or materials in structural geology. Also, such constitutive laws may be viewed as the first step towards describing the material behaviour of polycrystalline materials indicating anisotropy effects of both orientational and distortional type.

Generally, in all plastic anisotropy models some characteristic directions are attached to the material which may rotate due to the deformation process. The spin of this rotation is related to some one of the so-called plastic spin concepts. The latter are often defined e.g. by examining basic kinematical aspects of the deformation or by considering the physical mechanisms of inelastic flow at the crystal level. Publications concerning this subject are, among others the works of Asaro and Rice [8], Asaro [7], Loret [71], Dafalias [26], [29], [31], Dafalias and Rashid [28], Dafalias and Aifantis [30], Loret and Dafalias [72], Cho and Dafalias [20], Aravas and Aifantis [3], Aravas [4], [5], Ning and Aifantis [84], van der Giessen [37], [38], Tuğcu and Neale [107] as well as Tuğcu et al. [108]. The main differences between these works and the present one is in the constitutive equations and the related plastic spin issues governing the model response and in particular the kinematic hardening rule.

To be more specific, a plasticity theory which satisfies the second law of thermodynamics in every admissible process is presented. Following a proposal by Dafalias [31] (cf. also Dafalias [32]), various constitutive spins are introduced, responsible for rotations of axes of symmetry e.g. associated with the elasticity law, the yield function and the kinematic hardening rule, respectively. In the case of crystal plasticity the assumption of the existence of different axes of symmetry e.g. for the elasticity and the kinematic hardening law may be justified by the fact that the lattice is disturbed locally by dislocations or some other kinds of defects. Thus different axes of symmetry can be attributed to different kinds of physical mechanisms. Several important features of the theory are the constancy of volume during plastic flow (pressure independent flow), the existence of a yield surface which designates the stress state at the onset of plastic flow, the hardening rule describing the change in the yield surface with plastic flow and the associated flow rule relating the plastic strain rate with the yield function. The new aspects hereby are the used transformation behavior of so-called structural tensors, describing the evolution of anisotropy in the elasticity law, the yield function and the hardening rule, as well as the conditions for the material parameters for the case of orthotropic and cubic material symmetry, that are worked out explicitly.

In the second part, the aspect of deformation induced anisotropy of the yield surface after various preloadings is elaborated for small deformations. The approach here is identical to that one presented recently in Dafalias et al. [34]. An important feature in the constitutive theory of rate-independent plasticity and rate-dependent (visco-)plasticity is the assumption of the existence of a yield surface in the stress or strain space, which separates purely elastic states from elastic-plastic states (see e.g. Khan and Huang [64], Naghdi [82]). Closely related to the yield surface are also the so-called loading conditions, which decide whether or not inelastic flow has to be involved. These conditions are satisfied for the case of work hardening plasticity if the actual strain or stress state is on the yield surface and the imposed strain or stress increment points outward from the yield surface (see e.g. Casey and Naghdi [15], Dafalias and Popov [23]). On the other hand, when viscoplasticity is concerned, loading conditions are defined commonly to be fulfilled if a non-vanishing, so-called overstress applies. The notion overstress has been introduced by Krempl [67] and Perzyna [87] and is defined as a scalar valued function of a stress state which is outside of the area enclosed by the yield surface in stress space (for more details see Tsakmakis [102]).
Also, the concept of yield surface plays a crucial role if the plastic strain is supposed to obey an associated normality rule, i.e. if the plastic strain rate is positive proportional to the outer normal at the yield surface. Such evolution equations, termed "flow rules", may often be obtained, at least for isotropic material response, from some overall work postulates (a long list of papers dealing with work postulates in plasticity is given in Tsakmakis [103]).

Conformity of the yield surface concept with experimental results has been examined in several works. A good overview of this is given, among others in the works of Hecker [44], [45], Helling et al. [46], Henshall et al. [47], Ikegami [58], Ishikawa [59], Ishikawa and Sasaki [60], [61], Khan and Wang [63], Kowalewski and Śliwowski [65], Miastkowski [79], Miastkowski and Szczepiński [80], Phillips [88], Phillips and Das [89], Phillips and Moon [90], Phillips and Tang [91], Stout et al. [97], Trampczynski [98], Williams and Svensson [110], [111]. Generally there are some differences in the approaches employed to measure yield surfaces. For example, the definition of plastic yielding is not unique. Customary, the method of departure from the linearity (proportional limit), the method of backward extrapolation and the stress at a strain offset by a given small amount are

utilized to determine the initial yield surface as well as subsequent yield surfaces after preloading. The first method is used e.g. in MIASTKOWSKI [79], MIASTKOWSKI AND SZCZEPIŃSKI [80], PHILLIPS AND DAS [89], PHILLIPS AND MOON [90], PHILLIPS AND TANG [91], the second one e.g. in KHAN AND WANG [63], STOUT ET AL. [97], while the offset criterion has been employed e.g. in HELLING ET AL. [46], ISHIKAWA [59], ISHIKAWA AND SASAKI [60],[61], KHAN AND WANG [63], KOWALEWSKI AND ŚLIWOWSKI [65], MIASTKOWSKI [79], MIASTKOWSKI AND SZCZEPIŃSKI [80], TRAMPCZYNSKI [98], WILLIAMS AND SVENSSON [110], [111]. Further references on experimental determination of yield surfaces can be found in the review papers HENSHALL ET AL. [47], IKEGAMI [58], PHILLIPS [88]. As it can be seen from these works, the assumed definition of yielding affects the identified yield surface crucially. Similarly, the form of the measured yield surfaces depends heavily on the loading-unloading-reloading paths chosen. Essentially, after preloadings the subsequent yield surfaces may translate, rotate and distort, even if an initially isotropic yield surface has been recorded. In some cases, when the offset strains are very small, the subsequent yield surfaces have been observed to exhibit a sharpening in the direction of preloading and a flattening on the opposite side. However, when the yield surfaces are measured by partial unloading from the actual stress state to the assumed center of the yield surface, the yield loci referred to plane stress loadings have turned out to form rather ellipses (see ISHIKAWA [59], ISHIKAWA AND SASAKI [60], TRAMPCZYNSKI [98]).

Some effort has been made to describe theoretically the evolution of yield surfaces during plastic flow (see e.g. the literature given in WEGENER AND SCHLEGEL [109]). Because of their simplicity, yield functions which contain a fourth-order state tensor and are quadratic functions of the stress tensor are very attractive. This is the case e.g. for the constitutive models proposed by BACKHAUS [9], BALTOV AND SAWCZUK [10], ISHIKAWA [59], REES [93], WILLIAMS AND SVENSSON [110], [111], WU ET AL. [112] and YOSHIMURA [113]. It is worth noting, that all these works are formulated in a purely mechanical context.

Here a thermodynamic consistent theory is formulated, which is achieved by establishing sufficient conditions for the satisfaction of the so-called dissipation inequality. For the sake of simplicity, the proposed model is outlined for yield surfaces which are initially isotropic and the initial yield surface may be approximated with sufficient accuracy by a VON MISES yield function. This refers to e.g. experiments by ISHIKAWA [59], which will be used in order to discuss the capabilities of the model.

1.2 Outline of the thesis

After introducing some definitions and the notation, the basic kinematic relations, used in this work, will be presented in Chapter 2. The starting point of the theory is the multiplicative decomposition of the deformation gradient tensor into an elastic and an inelastic part. All necessary strain and stress measures are also defined. The evolution equations developed must be invariant under arbitrary rigid body rotations, superposed on both the actual and the so-called plastic intermediate configuration. The formulation of the constitutive theory is completely relative to this configuration.

In Chapter 3, a thermodynamically consistent constitutive model for anisotropic, large deformation plasticity and viscoplasticity is outlined as proposed in Tsakmakis [106]. The thermodynamic consistency is required with respect to the Clausius-Duhem inequality. As a result, an anisotropic elasticity law as well as a dissipation inequality are derived. Making use of the so-called postulate of Il'iushin, a yield condition and a normality rule are obtained. Viscoplasticity of overstress type is assumed to apply. For the sake of simplicity, isotropic hardening will be dropped and only kinematic hardening is considered. The yield function is supposed to exhibit, besides of kinematic hardening, orientational anisotropic behaviour. Following the outlined theory, two special cases of anisotropy are discussed. The first one describes orthotropic anisotropy, applicable for an orthorhombic crystal structure. So-called structural tensors of second-order are introduced that represent local axes of symmetry in the elasticity law, the kinematic hardening and the yield function (cf. Boehler [12], Liu [70]). These, together with the representation theorems for isotropic tensor functions (cf. Spencer [95], Zheng [114]) are used in formulating e.g. the constitutive equations for the free energy and the yield function. The second case addresses cubic material symmetry, which can be treated as a special case of orthotropic symmetry (cf. Billington and Tate [11]). In Chapter 4 the capabilities of the presented constitutive model for cubic anisotropy will be demonstrated. Experimental findings of a Brinell-hardness indentation test for a nickel-based single-crystal superalloy (CMSX4) are compared with a finite element simulation of the indentation test, using the finite element program ABAQUS [1].

Chapter 5 focuses attention on the description of small elastic-viscoplastic (rate-dependent) deformations of polycrystalline materials. Here a phenomenological model, previously presented in Dafalias et al. [34], is discussed, which shows how deformation induced anisotropy of the yield surface may be formulated in a thermodynamically consistent manner. Then, it is applied to predict the subsequent yield surfaces, after various prestressings, of commercially available SUS304 stainless steel, which have been measured experimentally by Ishikawa [59].

1.3 Notation

Only isothermal deformations with a uniform temperature distribution will be considered. We write $\dot{\varphi}(t)$ for the material time derivative of a function $\varphi(t)$, where t is the time. An explicit reference to space will be dropped throughout the work, since deformations are not affected by a space dependency. As usual, a function and the value of that function at a point are described by the same symbol. If different representations of the same functions are used, the symbols for that function will also vary. For real x, $\langle x \rangle$ denotes the function

$$\langle x \rangle := \begin{cases} x & \text{if } x \geq 0 \\ 0 & \text{if } x < 0 \end{cases} \quad . \tag{1.1}$$

Vectors and second-order tensors are denoted by bold-face letters, whereas fourth-order tensors are denoted by bold-face calligraphic letters. In particular, $\mathbf{a} \cdot \mathbf{b}$ and $\mathbf{a} \otimes \mathbf{b}$ denote the inner product and the tensor product of the vectors $\mathbf{a}$ and $\mathbf{b}$, respectively.
For second-order tensors $\mathbf{A}$ and $\mathbf{B}$, $\operatorname{tr} \mathbf{A}$, $\det \mathbf{A}$ and $\mathbf{A}^T$ is written for the trace, the determinant and the transpose of $\mathbf{A}$, respectively, while $\mathbf{A} \cdot \mathbf{B} = \operatorname{tr}\left(\mathbf{A}\mathbf{B}^T\right)$ is the inner product between $\mathbf{A}$ and $\mathbf{B}$ and $\|\mathbf{A}\| = \sqrt{\mathbf{A} \cdot \mathbf{A}}$ is the EUCLIDEAN norm of $\mathbf{A}$. Further,

$$\mathbf{1} = \delta_{ij} \mathbf{e}_i \otimes \mathbf{e}_j \quad , \tag{1.2}$$

$i, j = 1, 2, 3$, represents the identity tensor of second-order, where δ_{ij} is the KRONECKER-delta and $\{\mathbf{e}_i\}$ is an orthonormal basis in the three-dimensional EUCLIDEAN vector space in which the material body under consideration is postulated to move. Also, the notations $\mathbf{A}^D = \mathbf{A} - \frac{1}{3} (\operatorname{tr} \mathbf{A}) \mathbf{1}$ for the deviator of $\mathbf{A}$ and $\mathbf{A}^{T-1} = (\mathbf{A}^{-1})^T$, provided $\mathbf{A}^{-1}$ exists, are used.
Let $\boldsymbol{\mathcal{K}}$, $\boldsymbol{\mathcal{P}}$ be two fourth-order tensors, $\mathbf{A}$ a second-order tensor and $\mathbf{v}$ a vector. With respect to the orthonormal basis $\{\mathbf{e}_i\}$, the following applies. If $\boldsymbol{\mathcal{K}}$, $\boldsymbol{\mathcal{P}}$, $\mathbf{A}$ and $\mathbf{v}$ are represented by $\boldsymbol{\mathcal{K}} = \mathcal{K}_{ijkl} \mathbf{e}_i \otimes \mathbf{e}_j \otimes \mathbf{e}_k \otimes \mathbf{e}_l$, $\boldsymbol{\mathcal{P}} = \mathcal{P}_{ijkl} \mathbf{e}_i \otimes \mathbf{e}_j \otimes \mathbf{e}_k \otimes \mathbf{e}_l$, $\mathbf{A} = A_{ij} \mathbf{e}_i \otimes \mathbf{e}_j$ (often use is made of the notation $A_{ij} = (\mathbf{A})_{ij}$) and $\mathbf{v} = v_i \mathbf{e}_i$, respectively, then

$$\boldsymbol{\mathcal{K}}\boldsymbol{\mathcal{P}} = \mathcal{K}_{ijmn} \mathcal{P}_{mnkl} \, \mathbf{e}_i \otimes \mathbf{e}_j \otimes \mathbf{e}_k \otimes \mathbf{e}_l \quad , \tag{1.3}$$

$$\boldsymbol{\mathcal{K}}^T = \mathcal{K}_{ijkl} \, \mathbf{e}_k \otimes \mathbf{e}_l \otimes \mathbf{e}_i \otimes \mathbf{e}_j \quad , \tag{1.4}$$

$$\boldsymbol{\mathcal{K}}[\mathbf{A}] = \mathcal{K}_{ijmn} A_{mn} \, \mathbf{e}_i \otimes \mathbf{e}_j \quad , \tag{1.5}$$

$$\mathbf{A}^2 = \mathbf{A}\mathbf{A} = A_{ij} A_{jk} \, \mathbf{e}_i \otimes \mathbf{e}_k \quad , \quad \left(\mathbf{A}^{-2} = \mathbf{A}^{-1}\mathbf{A}^{-1}\right) \quad , \tag{1.6}$$

$$\mathbf{A}\mathbf{v} = A_{ij} v_j \, \mathbf{e}_i \quad . \tag{1.7}$$

Thus, for second-order tensors $\mathbf{A}$, $\mathbf{B}$,

$$\mathbf{A} \cdot \boldsymbol{\mathcal{K}}[\mathbf{B}] = \mathbf{B} \cdot \boldsymbol{\mathcal{K}}^T[\mathbf{A}] \quad . \tag{1.8}$$

In addition, $\boldsymbol{\mathcal{I}}$ is called the fourth-order identity tensor,

$$\boldsymbol{\mathcal{I}} = \delta_{im} \delta_{jn} \, \mathbf{e}_i \otimes \mathbf{e}_j \otimes \mathbf{e}_m \otimes \mathbf{e}_n \quad , \tag{1.9}$$

which satisfies the property

$$\boldsymbol{\mathcal{I}} = \boldsymbol{\mathcal{E}} + \boldsymbol{\mathcal{J}} \quad , \tag{1.10}$$

with

$$\boldsymbol{\mathcal{E}} = \mathcal{E}_{imjn} \, \mathbf{e}_i \otimes \mathbf{e}_m \otimes \mathbf{e}_j \otimes \mathbf{e}_n = \frac{1}{2} \left(\delta_{ij}\delta_{mn} + \delta_{in}\delta_{mj}\right) \, \mathbf{e}_i \otimes \mathbf{e}_m \otimes \mathbf{e}_j \otimes \mathbf{e}_n \quad , \tag{1.11}$$

$$\boldsymbol{\mathcal{J}} = \mathcal{J}_{imjn} \, \mathbf{e}_i \otimes \mathbf{e}_m \otimes \mathbf{e}_j \otimes \mathbf{e}_n = \frac{1}{2} \left(\delta_{ij}\delta_{mn} - \delta_{in}\delta_{mj}\right) \, \mathbf{e}_i \otimes \mathbf{e}_m \otimes \mathbf{e}_j \otimes \mathbf{e}_n \quad . \tag{1.12}$$

Hence, for the symmetric and the skew-symmetric part of an arbitrary second-order tensor $\mathbf{A}$, denoted by $\mathbf{A}_S$ and $\mathbf{A}_A$, respectively, follows

$$\mathbf{A}_S = \boldsymbol{\mathcal{E}}\,[\mathbf{A}] \quad , \quad \mathbf{A}_A = \boldsymbol{\mathcal{J}}\,[\mathbf{A}] \quad , \tag{1.13}$$

while

$$\boldsymbol{\mathcal{I}}\,[\mathbf{A}] = \mathbf{A} \quad . \tag{1.14}$$

The inner product between two fourth-order tensors $\boldsymbol{\mathcal{K}}$ and $\boldsymbol{\mathcal{P}}$ is given by

$$\boldsymbol{\mathcal{K}} \cdot \boldsymbol{\mathcal{P}} = \mathcal{K}_{ijkl}\mathcal{P}_{ijkl} \quad , \tag{1.15}$$

where $\mathcal{K}_{ijkl}$, $\mathcal{P}_{ijkl}$ are the components of $\boldsymbol{\mathcal{K}}$ and $\boldsymbol{\mathcal{P}}$, respectively, relative to the orthonormal basis $\{\mathbf{e}_i\}$.

1.4 Glossary of Symbols

Symbol	Name	Place of definition or first occurrence
Boldface arabic numbers		
$\mathbf{0}$	zero vector, zero tensor	(3.107)
$\mathbf{1}$	identity tensor	(1.2)
Boldface capital latin letters		
$\mathbf{A}$	ALMANSI strain tensor	(3.135)
$\mathbf{B}$	left CAUCHY-GREEN strain tensor	(2.12)
$\mathbf{C}$	right CAUCHY-GREEN strain tensor	(2.14)
$\mathbf{D}$	symmetric part of the velocity gradient tensor $\mathbf{L}$	(2.8)
$\mathbf{E}$	GREEN strain tensor	(2.14), (2.17)
$\mathbf{F}$	deformation gradient tensor	(2.3)
$\mathbf{L}$	velocity gradient tensor	(2.7)
$\mathbf{M}$	structural tensor	(3.113)
$\hat{\mathbf{N}}$	tensor defining the outward normal on the yield surface	(3.59)
$\hat{\mathbf{P}}$	MANDEL stress tensor	(2.24)
$\mathbf{P}_i$	Transformation matrix	(3.212)
$\overline{\mathbf{Q}}$	rigid body rotation	(3.21)
$\mathbf{R}$	proper orthogonal rotation tensor	(2.4)
$\mathbf{S}$	weighted CAUCHY stress tensor	(2.21)
$\mathbf{T}$	CAUCHY stress tensor	(2.21)
$\hat{\mathbf{T}}$	Second PIOLA-KIRCHHOFF stress tensor relative to the plastic intermediate configuration	(2.22)
$\tilde{\mathbf{T}}$	Second PIOLA-KIRCHHOFF stress tensor relative to the reference configuration	(2.23)
$\mathbf{U}$	symmetric positive definite stretch tensor	(2.4)
$\mathbf{V}$	symmetric positive definite stretch tensor	(2.4)
$\mathbf{W}$	skew-symmetric part of the velocity gradient tensor $\mathbf{L}$	(2.8)
$\mathbf{X}$	position vector in the reference configuration $\mathcal{R}_R$	(2.1)
$\bar{\mathbf{X}}$	configuration, inverse of $\bar{\mathbf{x}}$	(2.2)
$\mathbf{Y}$	internal, symmetric second-order strain tensor	(3.64)
$\mathbf{Z}$	internal, symmetric stress tensor, thermodynamical conjugate to $\mathbf{Y}$	(3.65)
Boldface small latin letters		
$\mathbf{e}_i$	orthonormal basis in EUCLIDEAN vector space	(1.2)
$\hat{\mathbf{h}}$	set of internal state variables in stress formulation	(3.36)
$\mathbf{m}_i$	unit vector, representing local axes of symmetry	(3.110)
$\boldsymbol{n}$	positive unit normal vector	(3.4)
$\boldsymbol{q}$	heat flux vector	(3.4)
$\mathbf{v}$	velocity vector in the current configuration $\mathcal{R}_t$	(2.7)
$\mathbf{x}$	position vector in the current configuration $\mathcal{R}_t$	(2.1)
$\bar{\mathbf{x}}$	configuration, one-to-one mapping	(2.1)

Capital latin letters

A	surface	(3.3)
$ABCD$	small strain cycle	Fig. 3.2
B_i	material parameters	(5.35)
$C_s\,[t_0, t_e]$	small strain cycle	(3.42)
D	diameter of steel ball in BRINELL hardness test	(4.1)
F	overstress / yield function	(5.9)
H	entropy	(3.1)
$I\,(t_0, t_e)$	integral over the stress power	(3.42)
L	loading factor	(3.39)
P	load in BRINELL hardness test	(4.1)
S	elastic compliance	(4.2)
V	volume	(3.2)
$W_p^{(ef)}$	effective inelastic stress power	(3.31)

Small latin letters

b_i	material parameters	(3.142), (5.34)
c_i	material parameters	(3.140), (5.22)
e	specific inner energy	(3.13)
f	yield function	(3.36), (5.10)
h	specific entropy	(3.2)
k_0	material parameter representing constant yield stress	(3.169), (5.9)
l_i	material parameters	(3.154)
m	viscosity parameter	(3.63), (5.19)
s	plastic arc length	(3.59), (5.18)
t	time	
v_i	material parameters	(3.169)

Boldface capital greek letters

$\boldsymbol{\Delta}$	rotation tensor in the kinematic hardening law	Fig. 3.1
$\boldsymbol{\Phi}$	rotation tensor in the elasticity law	Fig. 3.1
$\hat{\boldsymbol{\Gamma}}$	internal strain tensor	(2.11)
$\boldsymbol{\Lambda}$	deformation measure	(3.43)
$\boldsymbol{\Pi}$	rotation tensor in the flow rule	Fig. 3.1
$\boldsymbol{\Theta}$	proper orthogonal tensor, representing either $\boldsymbol{\Phi}$ or $\boldsymbol{\Delta}$ or $\boldsymbol{\Pi}$	(3.110)
$\hat{\boldsymbol{\Omega}}$	plastic spin	(3.26), (3.111)

Boldface small greek letters

$\boldsymbol{\sigma}$	effective stress	(3.166)
$\boldsymbol{\xi}$	backstress tensor	(3.66), (5.9)

Greek letters

Φ	surface density	(3.3)
Θ	absolute temperature	(3.4)
α_i	material parameters	(3.126) (5.25)
γ	specific entropy production	(3.5)
δ_{ij}	KRONECKER symbol	(1.2)
ζ	norming factor in the normality rule	(3.200), (5.17)

η	viscosity parameter	(3.63), (5.19)
χ	convex function	(3.107)
λ, μ	LAMÉ constants	(5.4)
ψ	specific free energy	(3.14), (5.2)
φ	constitutive function describing the evolution of backstress	(5.14)
$\varrho\,, \varrho_R$	mass density in the current and reference configuration	(3.2), (3.16)
ϕ	angle in BRINELL hardness test	(4.1)
ξ	volume density	(3.3)

Boldface calligraphic letters

$\boldsymbol{\mathcal{A}}$, $\boldsymbol{\mathcal{A}}_j$	fourth-order tensor(s) in yield function	(5.11), (5.26)
$\boldsymbol{\mathcal{B}}^{(k)}$	symmetric, positive definite fourth order tensor	(3.102)
$\boldsymbol{\mathcal{C}}^{(e)}$	fourth-order elasticity tensor	(3.128), (5.3)
$\boldsymbol{\mathcal{C}}^{(k)}$	fourth-order tensor in kinematic hardening rule	(3.83)
$\boldsymbol{\mathcal{D}}_j$	thermodynamical conjugate of $\boldsymbol{\mathcal{A}}_j$	(5.25)
$\boldsymbol{\mathcal{E}}$	symmetric part of $\boldsymbol{\mathcal{I}}$	(1.11)
$\boldsymbol{\mathcal{H}}$, $\boldsymbol{\mathcal{H}}_0$	fourth-order tensor in yield function	(5.9), (5.11)
$\boldsymbol{\mathcal{I}}$	fourth-order identity tensor	(1.9)
$\boldsymbol{\mathcal{J}}$	skew-symmetric part of $\boldsymbol{\mathcal{I}}$	(1.12)
$\boldsymbol{\mathcal{K}}$	fourth-order tensor in yield function	(3.169)
$\boldsymbol{\mathcal{L}}$	fourth-order tensor in kinematic hardening rule	(3.155)
$\boldsymbol{\mathcal{M}}^{(k)}$	fourth-order tensor, inverse of $\boldsymbol{\mathcal{C}}^{(k)}$	(3.90)

Calligraphic letters

$\mathcal{B}$	material body	
$\mathcal{D}_{int}$	internal dissipation	(3.29)
$\mathcal{R}_R$	actual configuration	Fig. 2.1
$\mathcal{R}_t$, $\mathcal{R}_t^\star$	actual configuration	Fig. 2.1
$\hat{\mathcal{R}}_t$, $\hat{\mathcal{R}}_t^\star$	actual configuration	Fig. 2.1

Operators

det	determinant
div	divergence operator with respect to the actual configuration
Div	divergence operator with respect to the reference configuration
grad	gradient operator with respect to the actual configuration
Grad	gradient operator with respect to the reference configuration
tr	trace

Indices

$\tilde{(\cdot)}$	quantity in the reference configuration
$\hat{(\cdot)}$	quantity in the actual configuration
$\dot{(\cdot)}$	material time derivative
$\overset{\triangle}{(\cdot)}$	OLDROYD time derivative
$(\cdot)^{-1}$	inverse of a tensor
$(\cdot)^{D}$	deviator of a tensor
$(\cdot)^{T}$	transpose of a tensor
$(\cdot)^{(e)}$	quantity related to elasticity

$(\cdot)^{(k)}$	quantity related to kinematic hardening
$(\cdot)^{(y)}$	quantity related to the yield function
$(\cdot)_S$	symmetric part of a tensor
$(\cdot)_A$	skew-symmetric part of a tensor
$(\cdot)_e$	elastic part of a tensor
$(\cdot)_p$	inelastic part of a tensor
$(\cdot)_R$	quantity in the reference configuration

Chapter 2

Basic kinematical relations

Let us consider a material body $\mathcal{B}$ in the three-dimensional EUCLIDEAN space E, that occupies at time $t = 0$ the spatial area $\mathcal{R}_R$, also called reference configuration. After choosing a fixed origin in E, every material point $P \in \mathcal{B}$ may be identified by a position vector (or referenced position) $\mathbf{X}$ of point X relative to the fixed origin. $\mathbf{x}$ describes the position vector (or current position) for an associated point x, occupied by the same material point P at time t in the actual configuration $\mathcal{R}_t$. A motion of the continuum body $\mathcal{B}$ in E is a one parameter family of configurations, where time t is the parameter,

$$\bar{\mathbf{x}} : (\mathbf{X}, t) \rightarrow \mathbf{x} = \bar{\mathbf{x}}(\mathbf{X}, t) \quad , \tag{2.1}$$

and which is uniquely invertible at fixed time t through

$$\mathbf{X} = \bar{\mathbf{X}}(\mathbf{x}, t) \quad . \tag{2.2}$$

Further, it is assumed that the motion possesses continuous derivatives with respect to space and time, as desired. The deformation gradient tensor connected to motion (2.1) is defined through

$$\mathbf{F} = \mathbf{F}(\mathbf{X}, t) = \frac{\partial \bar{\mathbf{x}}}{\partial \mathbf{X}} = \operatorname{Grad} \bar{\mathbf{x}} \quad . \tag{2.3}$$

Since $\det \mathbf{F} > 0$ is assumed, a unique polar decomposition

$$\mathbf{F} = \mathbf{R}\mathbf{U} = \mathbf{V}\mathbf{R} \tag{2.4}$$

exists, with the proper orthogonal tensor $\mathbf{R}$ and the symmetric, positive definite stretch tensors $\mathbf{U}$ and $\mathbf{V}$. The multiplicative decomposition of the deformation gradient tensor into an elastic and a plastic part,

$$\mathbf{F} = \mathbf{F}_e \mathbf{F}_p \quad , \tag{2.5}$$

is supposed to apply. Assuming plastic incompressibility,

$$\det \mathbf{F}_p = 1 \quad . \tag{2.6}$$

The material time derivative of the deformation gradient tensor defines the EULERIAN velocity gradient tensor $\mathbf{L}$:

$$\mathbf{L} = \frac{\partial \mathbf{v}}{\partial \mathbf{x}} = \frac{\partial \dot{\bar{\mathbf{x}}}(\mathbf{X}, t)}{\partial \mathbf{X}} \frac{\partial \mathbf{X}}{\partial \mathbf{x}} = \frac{\partial}{\partial t} \left(\frac{\partial \bar{\mathbf{x}}(\mathbf{X}, t)}{\partial \mathbf{X}} \right) \frac{\partial \mathbf{X}}{\partial \mathbf{x}} = \dot{\mathbf{F}} \mathbf{F}^{-1} \quad , \tag{2.7}$$

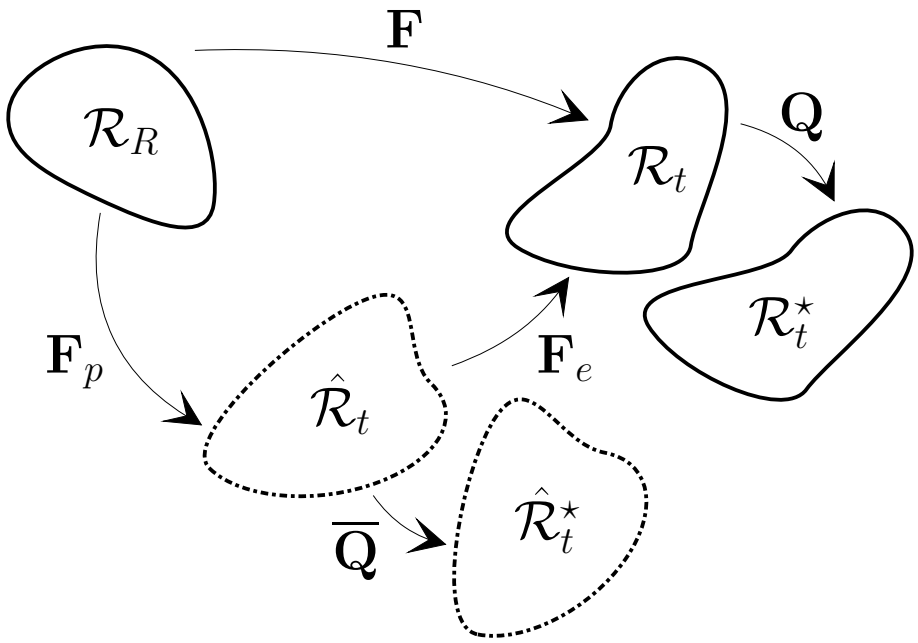

Figure 2.1: Decomposition of the deformation

where $\mathbf{v}(\mathbf{x},t) := \dot{\mathbf{x}}$ and

$$\mathbf{L} = \mathbf{D} + \mathbf{W}, \quad \mathbf{D} = \frac{1}{2}(\mathbf{L} + \mathbf{L}^T), \quad \mathbf{W} = \frac{1}{2}(\mathbf{L} - \mathbf{L}^T) \quad . \tag{2.8}$$

The multiplicative decomposition (2.5) introduces a so-called plastic intermediate configuration $\hat{\mathcal{R}}_t$ (cf. also Fig. 2.1), which in general is <u>not</u> compatible and therefore not an EUCLIDEAN one (for further references dealing with (2.5) see also LEE AND LIU [68], LUBLINER [74], MAUGIN [78]). Quantities referred to the plastic intermediate configuration will be denoted by a superposed $\hat{(\cdot)}$-symbol, while a superposed $\tilde{(\cdot)}$-symbol represents a quantity in the reference configuration $\mathcal{R}_R$. The plastic velocity gradient $\hat{\mathbf{L}}_p$ is given through

$$\hat{\mathbf{L}}_p = \dot{\mathbf{F}}_p \mathbf{F}_p^{-1} = \hat{\mathbf{D}}_p + \hat{\mathbf{W}}_p \quad , \tag{2.9}$$

with

$$\hat{\mathbf{D}}_p = \frac{1}{2}(\hat{\mathbf{L}}_p + \hat{\mathbf{L}}_p^T) \quad , \hat{\mathbf{W}}_p = \frac{1}{2}(\hat{\mathbf{L}}_p - \hat{\mathbf{L}}_p^T) \quad . \tag{2.10}$$

By using (2.5), the following kinematical relations can be obtained (see also Appendix A):

$$\hat{\boldsymbol{\Gamma}}_e = \frac{1}{2}\left(\hat{\mathbf{C}}_e - \mathbf{1}\right) \quad , \quad \hat{\mathbf{C}}_e = \mathbf{F}_e^T\mathbf{F}_e = \hat{\mathbf{U}}_e^2 \quad , \tag{2.11}$$

$$\hat{\boldsymbol{\Gamma}}_p = \frac{1}{2}\left(\mathbf{1} - \hat{\mathbf{B}}_p^{-1}\right) \quad , \quad \hat{\mathbf{B}}_p = \mathbf{F}_p\mathbf{F}_p^T = \hat{\mathbf{V}}_p^2 \quad , \tag{2.12}$$

$$\hat{\boldsymbol{\Gamma}} = \hat{\boldsymbol{\Gamma}}_e + \hat{\boldsymbol{\Gamma}}_p \quad , \tag{2.13}$$

$$\mathbf{E} = \frac{1}{2}\left(\mathbf{C} - \mathbf{1}\right) = \mathbf{F}_p^T\hat{\boldsymbol{\Gamma}}\mathbf{F}_p \quad , \quad \mathbf{C} = \mathbf{F}^T\mathbf{F} \quad , \tag{2.14}$$

$$\mathbf{E}_e = \mathbf{F}_p^T\hat{\boldsymbol{\Gamma}}_e\mathbf{F}_p \quad , \tag{2.15}$$

$$\mathbf{E}_p = \frac{1}{2}\left(\mathbf{C}_p - \mathbf{1}\right) = \mathbf{F}_p^T\hat{\boldsymbol{\Gamma}}_p\mathbf{F}_p \quad , \quad \mathbf{C}_p = \mathbf{F}_p^T\mathbf{F}_p \quad , \tag{2.16}$$

$$\mathbf{E} = \mathbf{E}_e + \mathbf{E}_p \quad . \tag{2.17}$$

Here, $\hat{\mathbf{C}}_e$ and $\hat{\mathbf{B}}_p$ are the elastic right CAUCHY-GREEN and the plastic left CAUCHY-GREEN tensors, respectively. Also, the tensors $\hat{\boldsymbol{\Gamma}}_e$ and $\hat{\boldsymbol{\Gamma}}_p$ are called the elastic GREEN and the plastic ALMANSI strain tensors with respect to the plastic intermediate configuration. On the basis of these relations it can be seen that

$$\hat{\mathbf{D}}_p = \overset{\triangle}{\hat{\boldsymbol{\Gamma}}}_p = \mathbf{F}_p^{T-1}\dot{\mathbf{E}}_p\mathbf{F}_p^{-1} \quad , \tag{2.18}$$

$$\overset{\triangle}{\hat{\boldsymbol{\Gamma}}} = \mathbf{F}_p^{T-1}\dot{\mathbf{E}}\mathbf{F}_p^{-1} = \mathbf{F}_e^T\mathbf{D}\mathbf{F}_e \quad , \tag{2.19}$$

with

$$\overset{\triangle}{\hat{\mathbf{X}}} = \dot{\hat{\mathbf{X}}} + \hat{\mathbf{L}}_p^T\hat{\mathbf{X}} + \hat{\mathbf{X}}\hat{\mathbf{L}}_p \tag{2.20}$$

for a second-order tensor $\hat{\mathbf{X}}$ relative to the plastic intermediate configuration. As (2.18) indicates, $\hat{\mathbf{D}}_p$ may be interpreted as a particular OLDROYD derivative of $\hat{\boldsymbol{\Gamma}}_p$ (see also TSAKMAKIS [100]).

We designate by $\mathbf{T}$ the CAUCHY stress tensor, by $\mathbf{S}$ the weighted CAUCHY stress tensor and by $\hat{\mathbf{T}}$, $\tilde{\mathbf{T}}$ the SECOND PIOLA-KIRCHHOFF stress tensor relative to the plastic intermediate and the reference configuration, respectively:

$$\mathbf{S} = (\det\mathbf{F})\,\mathbf{T} \quad , \tag{2.21}$$

$$\hat{\mathbf{T}} = \mathbf{F}_e^{-1}\mathbf{S}\mathbf{F}_e^{T-1} \quad , \tag{2.22}$$

$$\tilde{\mathbf{T}} = \mathbf{F}_p^{-1}\hat{\mathbf{T}}\mathbf{F}_p^{T-1} = \mathbf{F}^{-1}\mathbf{S}\mathbf{F}^{T-1} \quad . \tag{2.23}$$

Another stress tensor, related to the plastic dissipation, is the so-called MANDEL stress tensor (cf. LUBLINER [73])

$$\hat{\mathbf{P}} := \mathbf{F}_e^T\mathbf{S}\mathbf{F}_e^{T-1} = \hat{\mathbf{G}}\left(\hat{\boldsymbol{\Gamma}}_e, \hat{\mathbf{T}}\right) = \left(\mathbf{1} + 2\hat{\boldsymbol{\Gamma}}_e\right)\hat{\mathbf{T}} = \hat{\mathbf{C}}_e\hat{\mathbf{T}} \quad , \tag{2.24}$$

which is referred to the plastic intermediate configuration. The multiplicative decomposition of the deformation gradient is unique except for a rigid body rotation $\overline{\mathbf{Q}}$, superposed on the plastic intermediate configuration (see Fig. 2.1 and cf. CASEY AND NAGHDI [14], GREEN AND NAGHDI [39]). Under such rotations, the deformation and stress fields transform according to the equations given in Appendix A.

Chapter 3

Modelling of anisotropic (Visco-)Plasticity

In this chapter a thermodynamically consistent model for anisotropic (visco-)plasticity, derived from the second law of thermodynamics, is presented. It is based on recent publications by Häusler et al. [43] and Tsakmakis [106]. The model consists of an anisotropic elasticity law, nonlinear anisotropic kinematic hardening and an anisotropic flow rule. For the inner scalar- and tensor-valued state variables, describing hardening, constitutive equations are derived as sufficient conditions to fulfill the second law of thermodynamics in the form of the Clausius-Duhem inequality. To describe rotations of the axes of anisotropy in the elasticity law, the kinematic hardening and the flow rule, three rotation tensors, $\mathbf{\Phi}$, $\mathbf{\Delta}$ and $\mathbf{\Pi}$ are introduced, respectively (cf. Fig. 3.1).

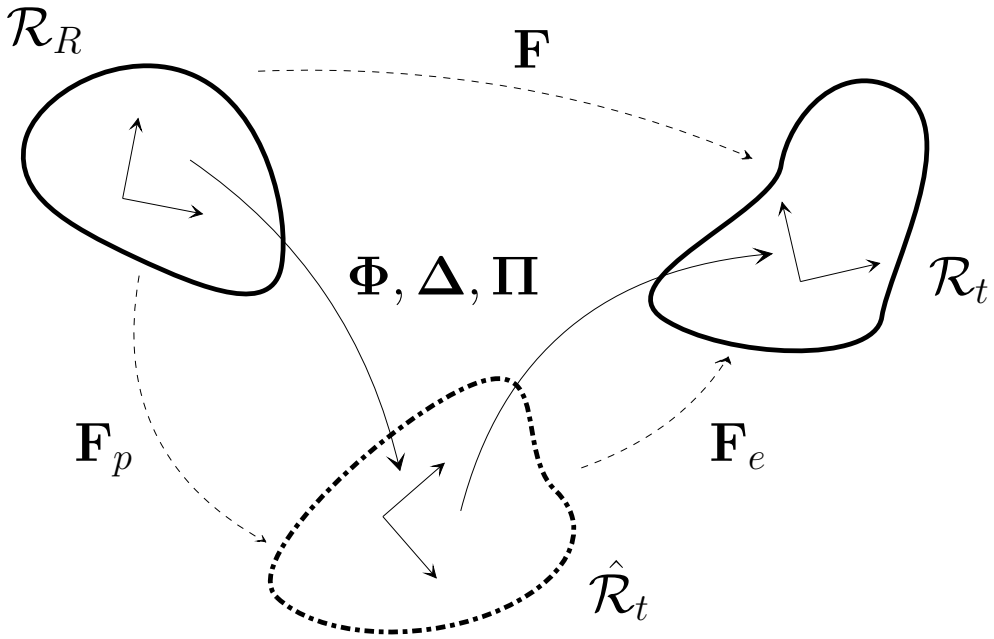

Figure 3.1: Representation of the axes of anisotropy

3.1 Second law of thermodynamics

Physical phenomena have often the tendency to "move" in one direction. For example, heat tends to flow from the "warmer" to the "colder" region of a body. These effects can be analyzed correctly through the introduction of a new quantity, the so-called entropy H. The entropy is supposed to be a scalar valued function,

$$H = H(\mathcal{R}_t, t) \quad . \tag{3.1}$$

Then a specific entropy $h = \hat{h}(\mathbf{x}, t)$ exists, with

$$H = \int_{\mathcal{R}_t} \varrho h \, dV \quad , \tag{3.2}$$

and for h applies a balance relation

$$\dot{H} = \int_{\partial\mathcal{R}_t} \Phi \, dA + \int_{\mathcal{R}_t} \xi \, dV \quad , \tag{3.3}$$

where Φ and ξ are surface- and volume-densities, respectively. In order to fulfill the required dissipation property (irreversible behavior), the assumption is made that $\dot{H}$ consists of two parts, one being responsible for the supply of entropy from the surrounding,

$$\int_{\partial\mathcal{R}_t} -\frac{\boldsymbol{q}}{\Theta} \cdot \boldsymbol{n} \, dA + \int_{\mathcal{R}_t} \frac{r}{\Theta} \, dV \ , \ \Theta : \text{absolute temperature} \ , \ r : \text{radiation term} \quad , \tag{3.4}$$

and

$$\int_{\mathcal{R}_t} \varrho\gamma \, dV \quad , \quad \gamma : \text{specific entropy production} \quad . \tag{3.5}$$

Here, $\boldsymbol{q}$ is the so-called heat flux vector and $\boldsymbol{n}$ is the positive unit outward normal on $\partial\mathcal{R}_t$. From (3.3), (3.4) and (3.5) follows that

$$\Phi = -\frac{\boldsymbol{q}}{\Theta} \cdot \boldsymbol{n} \quad , \tag{3.6}$$

$$\xi = \frac{r}{\Theta} + \varrho\gamma \quad , \tag{3.7}$$

and

$$\dot{H} = \int_{\partial\mathcal{R}_t} -\frac{\boldsymbol{q}}{\Theta} \cdot \boldsymbol{n} \, dA + \int_{\mathcal{R}_t} (\frac{r}{\Theta} + \varrho\gamma) \, dV \quad . \tag{3.8}$$

The irreversible character is taken into account by demanding that

$$\int_{\mathcal{R}_t} \varrho\gamma \, dV \geq 0 \quad . \tag{3.9}$$

This is also called the second law of thermodynamics in form of the Clausius-Duhem inequality.

3.1.1 Local form of the Clausius-Duhem inequality

From (3.2),

$$\dot{H} = \int_{\mathcal{R}_t} \varrho \dot{h}\, dV \quad . \tag{3.10}$$

On using (3.10), (3.9) can be rewritten as

$$\int_{\mathcal{R}_t} \left\{ (\dot{h} - \frac{r}{\Theta})\varrho + \mathrm{div}\frac{\boldsymbol{q}}{\Theta} \right\} dV \geq 0 \quad , \tag{3.11}$$

and on applying the localization theorem the local for of the Clausius-Duhem inequality reads as

$$\dot{h} - \frac{r}{\Theta} + \frac{1}{\varrho}\mathrm{div}\frac{\boldsymbol{q}}{\Theta} \geq 0 \quad . \tag{3.12}$$

Together with the first law of thermodynamics, which states

$$\frac{1}{\varrho}\mathrm{div}\boldsymbol{q} = r + \frac{1}{\varrho}\mathbf{T}\cdot\mathbf{D} - \dot{e} \quad , \tag{3.13}$$

where e is the specific internal energy, and the definition of the specific free energy ψ,

$$\psi := e - \Theta h \quad , \tag{3.14}$$

(3.12) can be recasted into

$$\frac{1}{\varrho_R}\mathbf{S}\cdot\mathbf{D} - \dot{\psi} - h\dot{\Theta} - \frac{1}{\varrho\Theta}\boldsymbol{q}\cdot\mathrm{grad}\Theta \geq 0 \quad . \tag{3.15}$$

In view of isothermal deformations with a uniform temperature distribution, assumed in this work, the Clausius-Duhem inequality reads (cf. Coleman and Gurtin [18], Haupt [41], Truesdell and Noll [99])

$$\mathbf{S}\cdot\mathbf{D} - \varrho_R\dot{\psi} \geq 0 \quad . \tag{3.16}$$

By virtue of (2.19) and (2.22), (3.16) can be rewritten in the form

$$\hat{\mathbf{T}}\cdot\overset{\triangle}{\hat{\mathbf{\Gamma}}} - \varrho_R\dot{\psi} \geq 0 \quad . \tag{3.17}$$

The specific free energy ψ is assumed to be additively decomposed into an elastic and a plastic part, ψ_e and ψ_p, respectively,

$$\psi(t) = \psi_e(t) + \psi_p(t) \quad . \tag{3.18}$$

Hence,

$$\hat{\mathbf{T}}\cdot\overset{\triangle}{\hat{\mathbf{\Gamma}}} - \varrho_R\dot{\psi}_e - \varrho_R\dot{\psi}_p \geq 0 \quad . \tag{3.19}$$

3.2 Elasticity law and dissipation inequality

In this work, the elastic response of a material is supposed to exhibit an orientational type of anisotropy. DAFALIAS [27], [32] assumes for such a kind of anisotropy, that some axes of anisotropy may rotate, the rate of rotation being specified by the plastic spin concept. The main concern of these works is the plastic spin governing the rate of rotation. However, these works are written in a purely mechanic context. In opposite, our work is embedded in a thermodynamical framework, as described in TSAKMAKIS [106]. According to this, the elastic part of the free energy function ψ_e is assumed to be a function, besides of $\mathbf{F}_e$, of $\mathbf{\Phi}(t)$, the rotation of the axes of anisotropy in the elasticity law:

$$\psi_e\left(t\right) = \overline{\psi}_e\left(\mathbf{F}_e\left(t\right), \mathbf{\Phi}\left(t\right)\right) \quad , \quad \mathbf{\Phi}^T = \mathbf{\Phi}^{-1} \quad . \tag{3.20}$$

The tensor $\mathbf{\Phi}$ is defined to rotate vectors from the reference configuration to the plastic intermediate configuration and to satisfy transformation properties under arbitrary rigid body rotations $\overline{\mathbf{Q}}$ superposed on the plastic intermediate configuration similar to those for $\mathbf{R}_p$ (see Appendix A):

$$\mathbf{\Phi} \rightarrow \mathbf{\Phi}^\star = \overline{\mathbf{Q}}\mathbf{\Phi} \quad . \tag{3.21}$$

From a more physical point of view, $\mathbf{\Phi}$ is assumed to rotate some axes characteristic for the elastic anisotropy of the underlying substructure. If no plastic flow occurs during a loading process, these axes have to remain fixed. So $\mathbf{\Phi}$ is a kinematical quantity, which in addition to $\mathbf{F}_p$ characterizes the plastic deformation process.
It should be remarked here, that in the terminology of DAFALIAS [32], the rate $\dot{\mathbf{\Phi}}\mathbf{\Phi}^T$ is the constitutive spin. It can be shown (see Appendix B), that requiring from the elastic free energy ψ_e to remain unaltered under arbitrary rigid body rotations superposed on both the current and the plastic intermediate configuration is equivalent to require from ψ_e to possess representations of the form

$$\psi_e = \overline{\overline{\psi}}_e\left(\hat{\mathbf{\Gamma}}_e, \mathbf{\Phi}\right) = \tilde{\psi}_e\left(\tilde{\mathbf{\Gamma}}_e\right) \quad , \quad \tilde{\mathbf{\Gamma}}_e := \mathbf{\Phi}^T\hat{\mathbf{\Gamma}}_e\mathbf{\Phi} \quad . \tag{3.22}$$

$\tilde{\mathbf{\Gamma}}_e$ denotes a strain measure in the reference configuration with

$$\mathbf{\Phi}\frac{\partial\tilde{\psi}_e}{\partial\tilde{\mathbf{\Gamma}}_e}\mathbf{\Phi}^T = \frac{\partial\overline{\overline{\psi}}_e}{\partial\hat{\mathbf{\Gamma}}_e} \quad , \quad \left(2\hat{\mathbf{\Gamma}}_e\mathbf{\Phi}\frac{\partial\tilde{\psi}_e}{\partial\tilde{\mathbf{\Gamma}}_e}\mathbf{\Phi}^T\right)_A = \left(\frac{\partial\overline{\overline{\psi}}_e}{\partial\mathbf{\Phi}}\mathbf{\Phi}^T\right)_A \quad . \tag{3.23}$$

From (3.22) follows

$$\begin{aligned}
\dot{\psi}_e &= \mathbf{\Phi}\frac{\partial\tilde{\psi}_e}{\partial\tilde{\mathbf{\Gamma}}_e}\mathbf{\Phi}^T \cdot \dot{\hat{\mathbf{\Gamma}}}_e + \operatorname{tr}\left[2\hat{\mathbf{\Gamma}}_e\mathbf{\Phi}\frac{\partial\tilde{\psi}_e}{\partial\tilde{\mathbf{\Gamma}}_e}\mathbf{\Phi}^T\left(\mathbf{\Phi}\dot{\mathbf{\Phi}}^T\right)\right] \\
&= \mathbf{\Phi}\frac{\partial\tilde{\psi}_e}{\partial\tilde{\mathbf{\Gamma}}_e}\mathbf{\Phi}^T \cdot \overset{\triangle}{\hat{\mathbf{\Gamma}}}_e - 2\mathbf{\Phi}\frac{\partial\tilde{\psi}_e}{\partial\tilde{\mathbf{\Gamma}}_e}\mathbf{\Phi}^T \cdot \hat{\mathbf{\Gamma}}_e\hat{\mathbf{L}}_p + \operatorname{tr}\left[2\hat{\mathbf{\Gamma}}_e\mathbf{\Phi}\frac{\partial\tilde{\psi}_e}{\partial\tilde{\mathbf{\Gamma}}_e}\mathbf{\Phi}^T\left(\mathbf{\Phi}\dot{\mathbf{\Phi}}^T\right)\right] \\
&= \mathbf{\Phi}\frac{\partial\tilde{\psi}_e}{\partial\tilde{\mathbf{\Gamma}}_e}\mathbf{\Phi}^T \cdot \overset{\triangle}{\hat{\mathbf{\Gamma}}}_e - 2\hat{\mathbf{\Gamma}}_e\mathbf{\Phi}\frac{\partial\tilde{\psi}_e}{\partial\tilde{\mathbf{\Gamma}}_e}\mathbf{\Phi}^T \cdot \hat{\mathbf{L}}_p + 2\hat{\mathbf{\Gamma}}_e\mathbf{\Phi}\frac{\partial\tilde{\psi}_e}{\partial\tilde{\mathbf{\Gamma}}_e}\mathbf{\Phi}^T \cdot \dot{\mathbf{\Phi}}\mathbf{\Phi}^T \\
&= \mathbf{\Phi}\frac{\partial\tilde{\psi}_e}{\partial\tilde{\mathbf{\Gamma}}_e}\mathbf{\Phi}^T \cdot \overset{\triangle}{\hat{\mathbf{\Gamma}}} - \mathbf{\Phi}\frac{\partial\tilde{\psi}_e}{\partial\tilde{\mathbf{\Gamma}}_e}\mathbf{\Phi}^T \cdot \hat{\mathbf{D}}_p - 2\hat{\mathbf{\Gamma}}_e\mathbf{\Phi}\frac{\partial\tilde{\psi}_e}{\partial\tilde{\mathbf{\Gamma}}_e}\mathbf{\Phi}^T \cdot \hat{\mathbf{L}}_p + 2\hat{\mathbf{\Gamma}}_e\mathbf{\Phi}\frac{\partial\tilde{\psi}_e}{\partial\tilde{\mathbf{\Gamma}}_e}\mathbf{\Phi}^T \cdot \dot{\mathbf{\Phi}}\mathbf{\Phi}^T \\
&= \mathbf{\Phi}\frac{\partial\tilde{\psi}_e}{\partial\tilde{\mathbf{\Gamma}}_e}\mathbf{\Phi}^T \cdot \overset{\triangle}{\hat{\mathbf{\Gamma}}} - \left(\mathbf{1} + 2\hat{\mathbf{\Gamma}}_e\right)\mathbf{\Phi}\frac{\partial\tilde{\psi}_e}{\partial\tilde{\mathbf{\Gamma}}_e}\mathbf{\Phi}^T \cdot \hat{\mathbf{D}}_p - 2\hat{\mathbf{\Gamma}}_e\mathbf{\Phi}\frac{\partial\tilde{\psi}_e}{\partial\tilde{\mathbf{\Gamma}}_e}\mathbf{\Phi}^T \cdot \left(\hat{\mathbf{W}}_p - \dot{\mathbf{\Phi}}\mathbf{\Phi}^T\right) \quad .
\end{aligned} \tag{3.24}$$

Here (2.9), (2.13) and (2.18) have been used. It is worth remarking that the tensor $\dfrac{\partial\tilde{\psi}_e}{\partial\tilde{\mathbf{\Gamma}}_e}$ (and therefore the tensor $\mathbf{\Phi}\dfrac{\partial\tilde{\psi}_e}{\partial\tilde{\mathbf{\Gamma}}_e}\mathbf{\Phi}^T$ too) is symmetric, while the tensor $\dot{\mathbf{\Phi}}\mathbf{\Phi}^T$ is skew-symmetric. On substituting (3.24) into (3.19),

$$\begin{aligned}\left(\hat{\mathbf{T}}-\varrho_R\mathbf{\Phi}\frac{\partial\tilde{\psi}_e}{\partial\tilde{\mathbf{\Gamma}}_e}\mathbf{\Phi}^T\right)\cdot\overset{\triangle}{\hat{\mathbf{\Gamma}}}+\left(\mathbf{1}+2\hat{\mathbf{\Gamma}}_e\right)\left(\varrho_R\mathbf{\Phi}\frac{\partial\tilde{\psi}_e}{\partial\tilde{\mathbf{\Gamma}}_e}\mathbf{\Phi}^T\right)\cdot\hat{\mathbf{D}}_p\\ +2\hat{\mathbf{\Gamma}}_e\left(\varrho_R\mathbf{\Phi}\frac{\partial\tilde{\psi}_e}{\partial\tilde{\mathbf{\Gamma}}_e}\mathbf{\Phi}^T\right)\cdot\left(\hat{\mathbf{W}}_p-\dot{\mathbf{\Phi}}\mathbf{\Phi}^T\right)-\varrho_R\dot{\psi}_p\geq 0\quad .\end{aligned}\tag{3.25}$$

In the terminology of Dafalias [32], $\hat{\mathbf{W}}_p$ is the plastic material spin, while

$$\hat{\mathbf{\Omega}}^{(e)}:=\hat{\mathbf{W}}_p-\dot{\mathbf{\Phi}}\mathbf{\Phi}^T\tag{3.26}$$

denotes the plastic spin associated with the elasticity law. Under rigid body rotations superposed on the plastic intermediate configuration the skew-symmetric tensor $\hat{\mathbf{\Omega}}^{(e)}$ transforms according to (see Appendix A, (3.21))

$$\hat{\mathbf{\Omega}}^{(e)}\to\left(\hat{\mathbf{\Omega}}^{(e)}\right)^*=\overline{\mathbf{Q}}\hat{\mathbf{\Omega}}^{(e)}\overline{\mathbf{Q}}^T\quad .\tag{3.27}$$

The plastic part of the free energy, ψ_p is assumed to depend on internal state variables describing the hardening response and the Cauchy stress $\hat{\mathbf{T}}$ in the plastic intermediate configuration is defined to be a function of state variables (but not of their rates). For the case of rate-dependent plasticity (also called viscoplasticity) the evolution of the internal state variables depends on state variables only, which means that $\hat{\mathbf{D}}_p$, $\hat{\mathbf{W}}_p-\dot{\mathbf{\Phi}}\mathbf{\Phi}^T$ and $\dot{\psi}_p$ are functions of state variables only. Thus, following similar arguments as used in Coleman and Gurtin [18], for viscoplasticity the relations (cf. (3.23))

$$\hat{\mathbf{T}}=\varrho_R\frac{\partial\overline{\overline{\psi}}_e}{\partial\hat{\mathbf{\Gamma}}_e}=\varrho_R\mathbf{\Phi}\frac{\partial\tilde{\psi}_e}{\partial\tilde{\mathbf{\Gamma}}_e}\mathbf{\Phi}^T\quad ,\tag{3.28}$$

$$\begin{aligned}\mathcal{D}_{int}:=&\left(\mathbf{1}+2\hat{\mathbf{\Gamma}}_e\right)\left(\varrho_R\mathbf{\Phi}\frac{\partial\tilde{\psi}_e}{\partial\tilde{\mathbf{\Gamma}}_e}\mathbf{\Phi}^T\right)\cdot\hat{\mathbf{D}}_p\\ &+2\hat{\mathbf{\Gamma}}_e\left(\varrho_R\mathbf{\Phi}\frac{\partial\tilde{\psi}_e}{\partial\tilde{\mathbf{\Gamma}}_e}\mathbf{\Phi}^T\right)\cdot\left(\hat{\mathbf{W}}_p-\dot{\mathbf{\Phi}}\mathbf{\Phi}^T\right)-\varrho_R\dot{\psi}_p\geq 0\end{aligned}\tag{3.29}$$

can be proven to be necessary and sufficient conditions in order for inequality (3.25) to be valid in every admissible process. So this theory of viscoplasticity falls in the general framework of Coleman and Gurtin's [18] thermodynamics with internal state variables (cf. also Kratochvil and Dillon [66]). Inequality (3.29) is known as the internal dissipation inequality. In the case of rate-independent plasticity (also just called plasticity) the evolution of internal state variables is defined to depend, besides on the state variables, on the deformation rate. As a consequence, the relations (3.28), (3.29) are necessary and sufficient for (3.25) to be valid in every purely elastic admissible process. If (3.28) and (3.29) are also assumed to apply along loading paths where inelastic flow is involved, then in the case of (rate-independent) plasticity laws these relations are generally only sufficient conditions for the validity of (3.25) in every admissible process.

For plasticity as well as viscoplasticity laws, it follows from (3.28), (3.29), together with (2.9), (2.24), that

$$\mathcal{D}_{int} = \hat{\mathbf{P}}_S \cdot \hat{\mathbf{D}}_p + \hat{\mathbf{P}}_A \cdot \left(\hat{\mathbf{W}}_p - \dot{\mathbf{\Phi}}\mathbf{\Phi}^T \right) - \varrho_R \dot{\psi}_p = \hat{\mathbf{P}} \cdot \left(\hat{\mathbf{L}}_p - \dot{\mathbf{\Phi}}\mathbf{\Phi}^T \right) - \varrho_R \dot{\psi}_p \geq 0 \quad . \tag{3.30}$$

Equation (3.28) represents a general elasticity law characterizing materials with anisotropy of orientational type. The term

$$W_p^{(ef)} := \hat{\mathbf{P}} \cdot \left(\hat{\mathbf{L}}_p - \dot{\mathbf{\Phi}}\mathbf{\Phi}^T \right) \tag{3.31}$$

is interpreted to describe an effective inelastic stress power. From (3.21),

$$\dot{\mathbf{\Phi}}^\star \mathbf{\Phi}^{\star T} = \overline{\mathbf{Q}} \dot{\mathbf{\Phi}} \mathbf{\Phi}^T \overline{\mathbf{Q}}^T + \dot{\overline{\mathbf{Q}}}\, \overline{\mathbf{Q}}^T \quad , \tag{3.32}$$

so that (cf. Appendix A)

$$\hat{\mathbf{L}}_p^\star - \dot{\mathbf{\Phi}}^\star \mathbf{\Phi}^{\star T} = \overline{\mathbf{Q}} \left(\hat{\mathbf{L}}_p - \dot{\mathbf{\Phi}}\mathbf{\Phi}^T \right) \overline{\mathbf{Q}}^T \quad , \tag{3.33}$$

$$W_p^{(ef)\star} = \hat{\mathbf{P}}^\star \cdot \left(\hat{\mathbf{L}}_p^\star - \dot{\mathbf{\Phi}}^\star \mathbf{\Phi}^{\star T} \right) = \hat{\mathbf{P}} \cdot \left(\hat{\mathbf{L}}_p - \dot{\mathbf{\Phi}}\mathbf{\Phi}^T \right) = W_p^{(ef)} \quad . \tag{3.34}$$

That means the effective plastic stress power $W_p^{(ef)}$ remains unaltered under arbitrary rigid body rotations superposed on the plastic intermediate configuration. The rate of the plastic part of the free energy, $\dot{\psi}_p$, is postulated to describe the power related to the energy stored in the material and is also required to be unaltered under arbitrary rigid body rotations superposed on the plastic intermediate configuration. Since $\varrho_R = \varrho_R^\star$ remains unchanged, it follows that the internal dissipation is unaltered under arbitrary rigid body rotations superposed on the plastic intermediate configuration as well:

$$\mathcal{D}_{int}^\star = \mathcal{D}_{int} \quad . \tag{3.35}$$

3.3 Flow rule for plasticity and the postulate of Il'iushin

The postulate of Il'iushin has been investigated in the context of rate-independent plasticity by many authors as e.g. Casey and Tseng [17], Dafalias [24], Fosdick and Volkmann [36], Hill [49], Hill and Rice [50], Lin and Naghdi [69], Lubliner [73], Lucchesi and Silhavy [75], Srinivasa [96], as well as Tsakmakis [103], [104]. Various aspects of the postulate have been discussed in Lubliner [73], where it has been shown that a unique normality rule for $\hat{\mathbf{L}}_p$ cannot be derived generally. However, in the case of an invertible isotropic elasticity law a proper normality rule for $\hat{\mathbf{D}}_p$ can be established (cf. Tsakmakis [103] and Tsakmakis and Willuweit [105]). This section will deal with rate-independent plasticity only. For this case and for elastic anisotropy of orientational type, as described in Sect. 3.2, a normality rule for the deformation rate $\hat{\mathbf{L}}_p - \dot{\mathbf{\Phi}}\mathbf{\Phi}^T$ will be derived as a sufficient condition for the postulate. Let assume the existence of a yield function in a stress space formulation with respect to the plastic intermediate configuration of the form

$$f(t) = \hat{f}\left(\hat{\mathbf{P}}, \hat{\mathbf{h}} \right) = \bar{f}\left(\hat{\mathbf{P}}_S, \hat{\mathbf{P}}_A, \hat{\mathbf{h}} \right) \quad . \tag{3.36}$$

Here, $\hat{\mathbf{h}}$ stands for a set of internal state variables $\hat{h}_i$, $1 \leq i \leq M$, which are scalars or components of tensors reflecting hardening properties. It is assumed that (3.36) may be rewritten in a strain space formulation with respect to the reference configuration in the form

$$f(t) = \tilde{g}\left(\mathbf{E}, \mathbf{E}_p, \mathbf{q} \right) \quad , \tag{3.37}$$

where $\mathbf{q}$ denotes a set of internal state variables q_j, $1 \leq j \leq N$, associated in some way with the hardening variables $\hat{h}_i$. The equation

$$f = \hat{f}\left(\hat{\mathbf{P}}, \hat{\mathbf{h}}\right) = \tilde{g}\left(\mathbf{E}, \mathbf{E}_p, \mathbf{q}\right) = 0 \tag{3.38}$$

is called yield condition. It describes for fixed values of $\hat{\mathbf{h}}$ a so-called yield surface in the space of the MANDEL stress tensors $\hat{\mathbf{P}}$, and for fixed values of $\mathbf{E}_p$ and $\mathbf{q}$ a yield surface in the space of the strain tensors $\mathbf{E}$. For simplicity, these yield surfaces are assumed to be smooth. (A discussion about yield surfaces in the strain and stress spaces, expressed in terms of $\mathbf{E}$ and $\tilde{\mathbf{T}}$, respectively, is given in CASEY AND NAGHDI [16]).
For rate-independent plasticity, loading processes involving plastic flow may be described by using, instead of time t, a scalar parameter s denoting a plastic arc length. It is postulated that for $s = const$ all internal state variables have to remain constant as well. Further, it is convenient to introduce a so-called loading factor $\mathsf{L}(t)$,

$$\mathsf{L} := \left[\dot{f}\right]_{s=const} \quad . \tag{3.39}$$

Then, the model response is characterized as follows (a discussion about loading conditions is given in TSAKMAKIS [101]):

$$f < 0 \quad \Leftrightarrow \quad \text{elastic range}, \tag{3.40}$$

$$f = 0 \quad \& \quad \mathsf{L}\begin{Bmatrix} < 0 \\ = 0 \\ > 0 \end{Bmatrix} \quad \Leftrightarrow \quad \begin{cases} \text{elastic unloading} \\ \text{neutral loading} \\ \text{plastic loading} \end{cases} \quad . \tag{3.41}$$

Plastic flow is defined to occur only when conditions for plastic loading are satisfied. It is important to remark that not every tensor $\hat{\mathbf{P}}$, satisfying the relation $\hat{f}\left(\hat{\mathbf{P}}, \hat{\mathbf{h}}\right) \leq 0$, must be an accessible MANDEL stress state. This follows from the fact that for given $\hat{\mathbf{P}}$ (2.24) represents a nonlinear system of equations for $\hat{\mathbf{\Gamma}}_e$ and it may happen that no solutions exist.
Now, cycles in the space of the GREEN strain tensors $\mathbf{E}$ are considered. Note that a cycle in the space of a strain measure implies a cycle in the space of any further strain measure and vice versa. Following LUCCHESI AND SILHAVY [75], strain cycles are denoted as small (but not necessarily infinitesimal small) ones if the following condition is satisfied. During the cyclic process, the initial strain state is always on or inside the yield surfaces $\tilde{g} = 0$ corresponding to the process. In other words, the initial strain state lies always in the intersection of all the elastic ranges surrounded by the yield surfaces $\tilde{g} = 0$ during the process. $C_s\left[t_0, t_e\right]$ is written for a small cycle, which begins at time t_0 and ends at time t_e. A material is defined to satisfy the postulate of IL'IUSHIN for small cycles, if for fixed material particle

$$I\left(t_0, t_e\right) := \int_{t_0}^{t_e} \mathbf{S}\left(t\right) \cdot \mathbf{D}\left(t\right)\, dt = \int_{t_0}^{t_e} \tilde{\mathbf{T}}\left(t\right) \cdot \dot{\mathbf{E}}\left(t\right)\, dt \geq 0 \quad \text{for every } C_s\left[t_0, t_e\right] \quad . \tag{3.42}$$

It is worth emphasizing that (3.42) is the isothermal version of a general dissipation postulate, which has been proposed by LUCCHESI AND SILHAVY [75] as a non-isothermal generalization of the classical postulate of IL'IUSHIN for arbitrary isothermal strain cycles. Inequality (3.42) has been also supposed by TSAKMAKIS [104] in discussing elastic-plastic materials with vanishing small pure elastic range. However, the condition that the cycles should be small is imposed in LUCCHESI AND SILHAVY [75] in order to make the postulate of IL'IUSHIN "derivable from

some sufficient conditions (the normality rule)", which is rather a mathematical point of view. On the other hand, the condition of small cycles was assumed in TSAKMAKIS [104] in order to obtain a "stability condition" for material response, which is not too restrictive when modeling the observed behavior of various materials. This is rather a physical point of view.
For deriving some consequences from inequality (3.42), it is convenient to express the stress tensor $\tilde{\mathbf{T}}$ in terms of the GREEN strain tensor. To this end the deformation measure $\mathbf{\Lambda}$ in the reference configuration is defined by

$$\mathbf{\Lambda} := \mathbf{F}_p^{-1}\mathbf{\Phi} \quad , \tag{3.43}$$

from which

$$\dot{\mathbf{\Lambda}} := -\mathbf{F}_p^{-1}\left(\hat{\mathbf{L}}_p - \dot{\mathbf{\Phi}}\mathbf{\Phi}^T\right)\mathbf{\Phi} \quad . \tag{3.44}$$

Thus, from $(3.22)_2$, (2.13)–(2.17),

$$\tilde{\mathbf{\Gamma}}_e = \mathbf{\Lambda}^T\mathbf{E}_e\mathbf{\Lambda} = \mathbf{\Lambda}^T\mathbf{E}\mathbf{\Lambda} - \mathbf{\Lambda}^T\mathbf{E}_p\mathbf{\Lambda} \quad , \tag{3.45}$$

so that, by virtue of $(3.22)_1$,

$$\psi_e = \tilde{\psi}_e\left(\mathbf{\Lambda}^T\mathbf{E}\mathbf{\Lambda} - \mathbf{\Lambda}^T\mathbf{E}_p\mathbf{\Lambda}\right) =: \tilde{\tilde{\psi}}_e\left(\mathbf{E}, \mathbf{E}_p, \mathbf{\Lambda}\right) \quad . \tag{3.46}$$

Hence

$$\begin{aligned}\dot{\psi}_e &= \frac{\partial\tilde{\tilde{\psi}}_e}{\partial\mathbf{E}}\cdot\dot{\mathbf{E}} + \frac{\partial\tilde{\tilde{\psi}}_e}{\partial\mathbf{E}_p}\cdot\dot{\mathbf{E}}_p + \frac{\partial\tilde{\tilde{\psi}}_e}{\partial\mathbf{\Lambda}}\cdot\dot{\mathbf{\Lambda}} \\ &= \mathbf{F}_p\frac{\partial\tilde{\tilde{\psi}}_e}{\partial\mathbf{E}}\mathbf{F}_p^T\cdot\overset{\triangle}{\hat{\mathbf{\Gamma}}} + \left(\mathbf{F}_p\frac{\partial\tilde{\tilde{\psi}}_e}{\partial\mathbf{E}_p}\mathbf{F}_p^T - \mathbf{F}_p^{T-1}\frac{\partial\tilde{\tilde{\psi}}_e}{\partial\mathbf{\Lambda}}\mathbf{\Phi}^T\right)\cdot\left(\hat{\mathbf{L}}_p - \dot{\mathbf{\Phi}}\mathbf{\Phi}^T\right) \quad .\end{aligned} \tag{3.47}$$

On the other hand, on taking the material time derivative of $(3.22)_1$, we get, after some rearrangement of terms,

$$\begin{aligned}\dot{\psi}_e &= \frac{\partial\tilde{\psi}_e}{\partial\tilde{\mathbf{\Gamma}}_e}\cdot\dot{\tilde{\mathbf{\Gamma}}}_e \\ &= \frac{\partial\tilde{\psi}_e}{\partial\tilde{\mathbf{\Gamma}}_e}\cdot\left(\mathbf{\Lambda}^T\mathbf{E}_e\mathbf{\Lambda}\right)^{\cdot} \\ &= \mathbf{\Lambda}\frac{\partial\tilde{\psi}_e}{\partial\tilde{\mathbf{\Gamma}}_e}\mathbf{\Lambda}^T\cdot\dot{\mathbf{E}} - \mathbf{\Lambda}\frac{\partial\tilde{\psi}_e}{\partial\tilde{\mathbf{\Gamma}}_e}\mathbf{\Lambda}^T\cdot\dot{\mathbf{E}}_p + 2\frac{\partial\tilde{\psi}_e}{\partial\tilde{\mathbf{\Gamma}}_e}\cdot\mathbf{\Lambda}^T\mathbf{E}_e\dot{\mathbf{\Lambda}} \\ &= \frac{1}{\varrho_R}\hat{\mathbf{T}}\cdot\overset{\triangle}{\hat{\mathbf{\Gamma}}} - \frac{1}{\varrho_R}\hat{\mathbf{T}}\cdot\hat{\mathbf{D}}_p - \frac{2}{\varrho_R}\hat{\mathbf{\Gamma}}_e\hat{\mathbf{T}}\cdot\left(\hat{\mathbf{L}}_p - \dot{\mathbf{\Phi}}\mathbf{\Phi}^T\right) \\ &= \frac{1}{\varrho_R}\hat{\mathbf{T}}\cdot\overset{\triangle}{\hat{\mathbf{\Gamma}}} - \frac{1}{\varrho_R}\hat{\mathbf{P}}\cdot\left(\hat{\mathbf{L}}_p - \dot{\mathbf{\Phi}}\mathbf{\Phi}^T\right) \quad .\end{aligned} \tag{3.48}$$

On comparing (3.47) with (3.48),

$$\hat{\mathbf{P}}\cdot\left(\hat{\mathbf{L}}_p - \dot{\mathbf{\Phi}}\mathbf{\Phi}^T\right) = -\varrho_R\left(\mathbf{F}_p\frac{\partial\tilde{\tilde{\psi}}_e}{\partial\mathbf{E}_p}\mathbf{F}_p^T - \mathbf{F}_p^{T-1}\frac{\partial\tilde{\tilde{\psi}}_e}{\partial\mathbf{\Lambda}}\mathbf{\Phi}^T\right)\cdot\left(\hat{\mathbf{L}}_p - \dot{\mathbf{\Phi}}\mathbf{\Phi}^T\right) \tag{3.49}$$

and

$$\hat{\mathbf{T}} = \varrho_R \mathbf{F}_p \frac{\partial \tilde{\tilde{\psi}}_e}{\partial \mathbf{E}} \mathbf{F}_p^T \quad , \tag{3.50}$$

from which

$$\tilde{\mathbf{T}} = \varrho_R \frac{\partial \tilde{\tilde{\psi}}_e}{\partial \mathbf{E}} \quad . \tag{3.51}$$

Now, (3.42) is asssumed to apply and a small strain cycle $ABCD$ (Fig. 3.2) is considered,

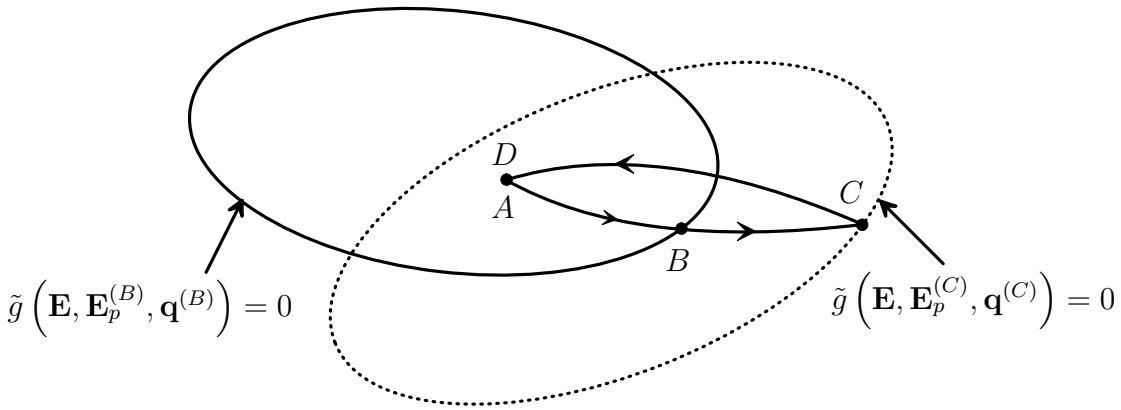

Figure 3.2: A small strain cycle with plastic flow occurring between B and C only.

which is parameterized by time t. We denote by $\mathbf{X}^{(P)}$ the value of some quantity $\mathbf{X}$ at the point P. Thus, the times associated with points A, B, C, D are $t^{(A)}$, $t^{(B)}$, $t^{(C)}$, $t^{(D)}$, respectively ($t^{(A)} < t^{(B)} < t^{(C)} < t^{(D)}$). The strain cycle begins and ends at $\mathbf{E} = \mathbf{E}^{(A)} = \mathbf{E}^{(D)}$, while plastic flow occurs between B and C only. Since (3.28), and therefore (3.51) too, is assumed to hold during plastic loading as well, it can be shown that (cf. (3.42))

$$\begin{aligned}
\frac{I\left(t^{(A)}, t^{(D)}\right)}{\varrho_R} &= \int_{t^{(A)}}^{t^{(D)}} \frac{1}{\varrho_R} \tilde{\mathbf{T}}(t) \cdot \dot{\mathbf{E}}(t)\, dt \\
&= \int_{t^{(A)}}^{t^{(D)}} \frac{\partial \tilde{\tilde{\psi}}_e\left(\mathbf{E}(t), \mathbf{E}_p(t), \mathbf{\Lambda}(t)\right)}{\partial \mathbf{E}(t)} \cdot \dot{\mathbf{E}}(t)\, dt \\
&= \tilde{\tilde{\psi}}_e\left(\mathbf{E}^{(A)}, \mathbf{E}_p^{(C)}, \mathbf{\Lambda}^{(C)}\right) - \tilde{\tilde{\psi}}_e\left(\mathbf{E}^{(A)}, \mathbf{E}_p^{(B)}, \mathbf{\Lambda}^{(B)}\right) \\
&\quad - \int_{t^{(B)}}^{t^{(C)}} \frac{\partial \tilde{\tilde{\psi}}_e\left(\mathbf{E}(t), \mathbf{E}_p(t), \mathbf{\Lambda}(t)\right)}{\partial \mathbf{E}_p(t)} \cdot \dot{\mathbf{E}}_p(t)\, dt \\
&\quad - \int_{t^{(B)}}^{t^{(C)}} \frac{\partial \tilde{\tilde{\psi}}_e\left(\mathbf{E}(t), \mathbf{E}_p(t), \mathbf{\Lambda}(t)\right)}{\partial \mathbf{\Lambda}(t)} \cdot \dot{\mathbf{\Lambda}}(t)\, dt
\end{aligned}$$

$$
\begin{aligned}
&= \int_{t^{(B)}}^{t^{(C)}} \left[\frac{\partial \tilde{\tilde{\psi}}_e \left(\mathbf{E}^{(A)}, \mathbf{E}_p(t), \mathbf{\Lambda}(t) \right)}{\partial \mathbf{E}_p(t)} \cdot \dot{\mathbf{E}}_p(t) \right. \\
&\qquad \left. + \frac{\partial \tilde{\tilde{\psi}}_e \left(\mathbf{E}^{(A)}, \mathbf{E}_p(t), \mathbf{\Lambda}(t) \right)}{\partial \mathbf{\Lambda}(t)} \cdot \dot{\mathbf{\Lambda}}(t) \right] dt \\
&\quad - \int_{t^{(B)}}^{t^{(C)}} \frac{\partial \tilde{\tilde{\psi}}_e \left(\mathbf{E}(t), \mathbf{E}_p(t), \mathbf{\Lambda}(t) \right)}{\partial \mathbf{E}_p(t)} \cdot \dot{\mathbf{E}}_p(t) \; dt \\
&\quad - \int_{t^{(B)}}^{t^{(C)}} \frac{\partial \tilde{\tilde{\psi}}_e \left(\mathbf{E}(t), \mathbf{E}_p(t), \mathbf{\Lambda}(t) \right)}{\partial \mathbf{\Lambda}(t)} \cdot \dot{\mathbf{\Lambda}}(t) \; dt \\
&= \int_{t^{(B)}}^{t^{(C)}} \left\{ \left[\frac{\partial \tilde{\tilde{\psi}}_e \left(\mathbf{E}^{(A)}, \mathbf{E}_p(t), \mathbf{\Lambda}(t) \right)}{\partial \mathbf{E}_p(t)} \right. \right. \\
&\qquad \left. - \frac{\partial \tilde{\tilde{\psi}}_e \left(\mathbf{E}(t), \mathbf{E}_p(t), \mathbf{\Lambda}(t) \right)}{\partial \mathbf{E}_p(t)} \right] \cdot \dot{\mathbf{E}}_p \\
&\quad + \left[\frac{\partial \tilde{\tilde{\psi}}_e \left(\mathbf{E}^{(A)}, \mathbf{E}_p(t), \mathbf{\Lambda}(t) \right)}{\partial \mathbf{\Lambda}(t)} \right. \\
&\qquad \left. \left. - \frac{\partial \tilde{\tilde{\psi}}_e \left(\mathbf{E}(t), \mathbf{E}_p(t), \mathbf{\Lambda}(t) \right)}{\partial \mathbf{\Lambda}(t)} \right] \cdot \dot{\mathbf{\Lambda}}(t) \right\} dt \geq 0 \quad .
\end{aligned}
\tag{3.52}
$$

By using Taylor's theorem,

$$
\begin{aligned}
&\lim_{t^{(C)} \to t^{(B)}} \frac{I\left(t^{(A)}, t^{(D)}\right)/\varrho_R}{t^{(C)} - t^{(B)}} = \\
&= \left[\frac{\partial \tilde{\tilde{\psi}}_e \left(\mathbf{E}^{(A)}, \mathbf{E}_p(t), \mathbf{\Lambda}(t) \right)}{\partial \mathbf{E}_p(t)} \cdot \dot{\mathbf{E}}_p(t) - \frac{\partial \tilde{\tilde{\psi}}_e \left(\mathbf{E}(t), \mathbf{E}_p(t), \mathbf{\Lambda}(t) \right)}{\partial \mathbf{E}_p(t)} \cdot \dot{\mathbf{E}}_p(t) \right]_{t=t^{(B)}} \\
&+ \left[\frac{\partial \tilde{\tilde{\psi}}_e \left(\mathbf{E}^{(A)}, \mathbf{E}_p(t), \mathbf{\Lambda}(t) \right)}{\partial \mathbf{\Lambda}(t)} \cdot \dot{\mathbf{\Lambda}}(t) - \frac{\partial \tilde{\tilde{\psi}}_e \left(\mathbf{E}(t), \mathbf{E}_p(t), \mathbf{\Lambda}(t) \right)}{\partial \mathbf{\Lambda}(t)} \cdot \dot{\mathbf{\Lambda}}(t) \right]_{t=t^{(B)}} \geq 0 \quad .
\end{aligned}
\tag{3.53}
$$

Since the point B can be chosen randomly on the yield surface, the index $t^{(B)}$ in (3.53) may be dropped to get, as a necessary condition for (3.42), the inequality

$$
\begin{aligned}
&- \frac{\partial \tilde{\tilde{\psi}}_e \left(\mathbf{E}, \mathbf{E}_p, \mathbf{\Lambda} \right)}{\partial \mathbf{E}_p} \cdot \dot{\mathbf{E}}_p - \frac{\partial \tilde{\tilde{\psi}}_e \left(\mathbf{E}, \mathbf{E}_p, \mathbf{\Lambda} \right)}{\partial \mathbf{\Lambda}} \cdot \dot{\mathbf{\Lambda}} \geq \\
&\quad - \frac{\partial \tilde{\tilde{\psi}}_e \left(\mathbf{E}^{(A)}, \mathbf{E}_p, \mathbf{\Lambda} \right)}{\partial \mathbf{E}_p} \cdot \dot{\mathbf{E}}_p - \frac{\partial \tilde{\tilde{\psi}}_e \left(\mathbf{E}^{(A)}, \mathbf{E}_p, \mathbf{\Lambda} \right)}{\partial \mathbf{\Lambda}} \cdot \dot{\mathbf{\Lambda}} \quad ,
\end{aligned}
\tag{3.54}
$$

where $\mathbf{E}$ denotes a strain state on the yield surface, the variables $\mathbf{E}_p$, $\mathbf{\Lambda}$ being associated with this state. $\mathbf{E}^{(A)}$ is a strain state on or inside the yield surface, i.e. $\tilde{g}\left(\mathbf{E}^{(A)}, \mathbf{E}_p, \mathbf{q}\right) \leq 0$, where the internal state variables $\mathbf{q}$ are associated with the strain state $\mathbf{E}$. Conversely, (3.54) is a sufficient condition for (3.42). This can be examined by taking the integral of (3.54) along a strain cycle as shown in Fig. 3.1. For (3.54) to remain valid during this strain cycle, $\mathbf{E}^{(A)}$ must always lie in the intersection of all the elastic ranges during the strain cycle, which in turn implies that the strain cycle $ABCD$ is small. Then, following steps similar to those in (3.52), it is a straightforward matter to arrive at (3.42).

Using (3.44), (3.49), it is readily seen that

$$\frac{\partial \tilde{\tilde{\psi}}_e}{\partial \mathbf{\Lambda}} \cdot \dot{\mathbf{\Lambda}} = -\frac{\partial \tilde{\tilde{\psi}}_e}{\partial \mathbf{E}_p} \cdot \dot{\mathbf{E}}_p - \frac{1}{\varrho_R} \hat{\mathbf{P}} \cdot \left(\hat{\mathbf{L}}_p - \dot{\mathbf{\Phi}} \mathbf{\Phi}^T \right) \quad . \tag{3.55}$$

By virtue of this result inequality (3.54) is equivalent to

$$\hat{\mathbf{P}} \cdot \left(\hat{\mathbf{L}}_p - \dot{\mathbf{\Phi}} \mathbf{\Phi}^T \right) \geq \hat{\mathbf{P}}^{(A)} \cdot \left(\hat{\mathbf{L}}_p - \dot{\mathbf{\Phi}} \mathbf{\Phi}^T \right) \quad , \tag{3.56}$$

or

$$\hat{\mathbf{P}}_S \cdot \hat{\mathbf{D}}_p + \hat{\mathbf{P}}_A \cdot \left(\hat{\mathbf{W}}_p - \dot{\mathbf{\Phi}} \mathbf{\Phi}^T \right) \geq \hat{\mathbf{P}}_S^{(A)} \cdot \hat{\mathbf{D}}_p + \hat{\mathbf{P}}_A^{(A)} \cdot \left(\hat{\mathbf{W}}_p - \dot{\mathbf{\Phi}} \mathbf{\Phi}^T \right) \quad . \tag{3.57}$$

Recall that (3.56) is equivalent to the inequality (3.54) and therefore to (3.42) as well. Inequality (3.56) expresses the so-called principle of maximum plastic stress power. Indeed, with respect to a purely mechanical formulation of the theory, according to (3.31), inequality (3.56) states that, for given effective plastic deformation rate $\hat{\mathbf{L}}_p - \dot{\mathbf{\Phi}} \mathbf{\Phi}^T$, among all admissible stress tensors $\hat{\mathbf{P}}^{(A)}$, the actual tensor $\hat{\mathbf{P}}$ maximizes the effective plastic stress power $W_p^{(ef)}$. The term admissible stress tensor denotes an accessible MANDEL stress tensor which is on or inside the yield surface $\hat{f} = 0$ (cf. (3.38)). In the case of isothermal deformations with a uniform temperature distribution, this work deals with, the internal dissipation is given by (cf. (3.30))

$$\mathcal{D}_{int} \left(\hat{\mathbf{P}}, \hat{\mathbf{L}}_p - \dot{\mathbf{\Phi}} \mathbf{\Phi}^T, \dot{\psi}_p \right) = \hat{\mathbf{P}} \cdot \left(\hat{\mathbf{L}}_p - \dot{\mathbf{\Phi}} \mathbf{\Phi}^T \right) - \varrho_R \dot{\psi}_p \quad . \tag{3.58}$$

Then, (3.56) states, that for given internal state variables and their rates, i.e. for given $\hat{\mathbf{L}}_p - \dot{\mathbf{\Phi}} \mathbf{\Phi}^T$ and $\dot{\psi}_p$, among all admissible stress tensors $\hat{\mathbf{P}}^{(A)}$, the actual one $\hat{\mathbf{P}}$ maximizes the plastic dissipation $\mathcal{D}_{int}$. It can be shown (see e.g. LUBLINER [74], Sect. 3.2.2) for a treatment in the context of small deformations), that convexity of the level set $\{\hat{\mathbf{P}} | \hat{f}(\hat{\mathbf{P}}, \hat{\mathbf{h}}) \leq 0, \hat{\mathbf{h}} = \textit{fixed}\}$ and a normality rule for $\hat{\mathbf{L}}_p - \dot{\mathbf{\Phi}} \mathbf{\Phi}^T$ are sufficient conditions for inequality (3.56). The term normality rule means that $\hat{\mathbf{L}}_p - \dot{\mathbf{\Phi}} \mathbf{\Phi}^T$ has to be directed along the outward normal on the yield surface, which has been assumed to be smooth:

$$\hat{\mathbf{L}}_p - \dot{\mathbf{\Phi}} \mathbf{\Phi}^T = \sqrt{\frac{3}{2}} \dot{s} \hat{\mathbf{N}} \quad , \quad \hat{\mathbf{N}} := \frac{\dfrac{\partial \hat{f}}{\partial \hat{\mathbf{P}}}}{\left\| \dfrac{\partial \hat{f}}{\partial \hat{\mathbf{P}}} \right\|} \quad , \tag{3.59}$$

where $\dot{s}$ is a positive scalar for plastic loading. Of course, $(3.59)_1$ can be decomposed into its symmetric and skew-symmetric part:

$$\hat{\mathbf{D}}_p = \sqrt{\frac{3}{2}} \dot{s} \hat{\mathbf{N}}_S = \sqrt{\frac{3}{2}} \dot{s} \frac{\dfrac{\partial \bar{f}}{\partial \hat{\mathbf{P}}_S}}{\left\| \dfrac{\partial \bar{f}}{\partial \hat{\mathbf{P}}} \right\|} = \sqrt{\frac{3}{2}} \dot{s} \frac{\left(\dfrac{\partial \hat{f}}{\partial \hat{\mathbf{P}}} \right)_S}{\left\| \left(\dfrac{\partial \hat{f}}{\partial \hat{\mathbf{P}}} \right) \right\|} \quad , \tag{3.60}$$

$$\hat{\mathbf{\Omega}}^{(e)} := \hat{\mathbf{W}}_p - \dot{\mathbf{\Phi}} \mathbf{\Phi}^T = \sqrt{\frac{3}{2}} \dot{s} \hat{\mathbf{N}}_A = \sqrt{\frac{3}{2}} \dot{s} \frac{\dfrac{\partial \bar{f}}{\partial \hat{\mathbf{P}}_A}}{\left\| \dfrac{\partial \bar{f}}{\partial \hat{\mathbf{P}}} \right\|} = \sqrt{\frac{3}{2}} \dot{s} \frac{\left(\dfrac{\partial \hat{f}}{\partial \hat{\mathbf{P}}} \right)_A}{\left\| \left(\dfrac{\partial \hat{f}}{\partial \hat{\mathbf{P}}} \right) \right\|} \quad , \tag{3.61}$$

with $\hat{\mathbf{N}}_S$ and $\hat{\mathbf{N}}_A$ being the symmetric and the skew-symmetric part of $\hat{\mathbf{N}}$, respectively. (3.59) (respectively (3.60), (3.61)) represents the flow rule for rate independent plasticity, where $\dot{s}$ has to be determined from the so-called consistency condition $\frac{d}{dt}\hat{f} = 0$. Moreover, it is readily seen that

$$\begin{aligned}\dot{s} &= \sqrt{\frac{2}{3}\left(\hat{\mathbf{L}}_p - \dot{\mathbf{\Phi}}\mathbf{\Phi}^T\right)\cdot\left(\hat{\mathbf{L}}_p - \dot{\mathbf{\Phi}}\mathbf{\Phi}^T\right)} \\ &= \sqrt{\frac{2}{3}\left(\hat{\mathbf{D}}_p\cdot\hat{\mathbf{D}}_p + \left(\hat{\mathbf{W}}_p - \dot{\mathbf{\Phi}}\mathbf{\Phi}^T\right)\cdot\left(\hat{\mathbf{W}}_p - \dot{\mathbf{\Phi}}\mathbf{\Phi}^T\right)\right)} \quad . \end{aligned} \tag{3.62}$$

It is perhaps of interest to remark that, on the basis of (3.61), the plastic spin related to the elasticity law vanishes identically if and only if the yield function is dependent on the symmetric part of $\hat{\mathbf{P}}$ only. Also, the approach in NAGHDI AND TRAPP [83] for discussing limiting cases like that of rigid bodies applies, practically, to the present theory as well.

3.4 Flow rule for viscoplasticity

For the purposes of this work it suffices to concentrate on viscoplasticity models which arise from the plasticity ones by adopting all the constitutive equations except from the evolution equation for s. This is now defined in terms of a so-called overstress. Note that whereas for rate-independent plasticity the yield function always satisfies the condition $f = \hat{f}\left(\hat{\mathbf{P}}, \hat{\mathbf{h}}\right) \leq 0$, in the case of viscoplasticity no such restrictions on f are imposed. However, for viscoplasticity only such functions f are admitted, for which the level set $\{\hat{\mathbf{P}} | \hat{f}(\hat{\mathbf{P}}, \hat{\mathbf{h}}) \leq 0, \hat{\mathbf{h}} = \textit{fixed}\}$ is convex. A positive value of f is called overstress, so that $\dot{s}$ is supposed to be given as a function of $\left\langle \hat{f} \right\rangle$. Especially, an evolution equation of the form

$$\dot{s} = \frac{\left\langle \hat{f} \right\rangle^m}{\eta} \geq 0 \tag{3.63}$$

is assumed to hold, where m and η are positive material parameters.

3.5 Kinematic hardening and yield function

For simplicity, in what follows isotropic hardening in the yield function is not regarded. So ψ_p is supposed to consist only of the contribution arising from kinematic hardening effects. In analogy to ψ_e (cf. (3.22)), ψ_p is assumed to be of the form

$$\psi_p = \overline{\overline{\psi}}_p\left(\hat{\mathbf{Y}}, \mathbf{\Delta}\right) = \tilde{\psi}_p\left(\tilde{\mathbf{Y}}\right) \quad , \quad \tilde{\mathbf{Y}} := \mathbf{\Delta}^T\hat{\mathbf{Y}}\mathbf{\Delta} \quad , \quad \mathbf{\Delta}^T = \mathbf{\Delta}^{-1} \quad . \tag{3.64}$$

Here, $\hat{\mathbf{Y}}$ is an internal symmetric second-order strain tensor, which operates in the plastic intermediate configuration, while the proper orthogonal tensor $\mathbf{\Delta}$ (two-point tensor field) is defined to rotate some symmetry axes, related to the kinematic hardening response, from the reference to the plastic intermediate configuration. Physically, plastic flow causes the plastic deformation gradient $\mathbf{F}_p$, the related plastic strain with respect to the plastic intermediate configuration and the related effective plastic stress power, $\hat{\mathbf{\Gamma}}_p$ and $W_p^{(ef)}$, respectively. However, only a part of $W_p^{(ef)}$ may be dissipated as heat, and the remainder will be stored in the material

mainly by changes in the density and arrangement of dislocations (measurements of energy storage in the material can be found e.g. in OLIFERUK ET AL. [86]). The strain $\hat{\mathbf{Y}}$ is a part of $\hat{\mathbf{\Gamma}}_p$ and is interpreted to represent the strain related to the stress power stored in the material, the later being $\varrho_R\dot{\psi}_p$ (further remarks about this topic can be found in TSAKMAKIS AND WILLUWEIT [105]). We denote by $\hat{\mathbf{Z}}$ the internal stress tensor, which is thermodynamically conjugate to $\hat{\mathbf{Y}}$. In analogy to (3.28)

$$\hat{\mathbf{Z}} := \varrho_R \frac{\partial \overline{\overline{\psi}}_p}{\partial \hat{\mathbf{Y}}} = \varrho_R \mathbf{\Delta} \frac{\partial \tilde{\psi}_p}{\partial \tilde{\mathbf{Y}}} \mathbf{\Delta}^T \tag{3.65}$$

is set. Evidently, the tensor $\hat{\mathbf{Z}}$ is symmetric and operates in the plastic intermediate configuration. Kinematic hardening is described by the back-stress tensor $\hat{\boldsymbol{\xi}}$, which is postulated to posses the structure of a MANDEL stress tensor. Formally, $\hat{\boldsymbol{\xi}}$ can be defined, in analogy to (2.24), through

$$\hat{\boldsymbol{\xi}} = \left(\mathbf{1} + 2\hat{\mathbf{Y}}\right)\hat{\mathbf{Z}} = \hat{\boldsymbol{\xi}}_S + \hat{\boldsymbol{\xi}}_A \quad , \tag{3.66}$$

where

$$\hat{\boldsymbol{\xi}}_S = \hat{\mathbf{Z}} + \hat{\mathbf{Y}}\hat{\mathbf{Z}} + \hat{\mathbf{Z}}\hat{\mathbf{Y}} \quad , \tag{3.67}$$

$$\hat{\boldsymbol{\xi}}_A = \hat{\mathbf{Y}}\hat{\mathbf{Z}} - \hat{\mathbf{Z}}\hat{\mathbf{Y}} \quad , \tag{3.68}$$

or

$$\hat{\boldsymbol{\xi}}_A = \varrho_R \mathbf{\Delta} \left(\tilde{\mathbf{Y}} \frac{\partial \tilde{\psi}_p}{\partial \tilde{\mathbf{Y}}} - \frac{\partial \tilde{\psi}_p}{\partial \tilde{\mathbf{Y}}} \tilde{\mathbf{Y}} \right) \mathbf{\Delta}^T \quad . \tag{3.69}$$

It can be shown, that under arbitrary rigid body rotations superposed on the plastic intermediate configuration $\hat{\boldsymbol{\xi}}$ transforms according to

$$\hat{\boldsymbol{\xi}}^* = \overline{\mathbf{Q}}\hat{\boldsymbol{\xi}}\overline{\mathbf{Q}}^T \quad . \tag{3.70}$$

Also the same is true for $\hat{\boldsymbol{\xi}}_S$ and $\hat{\boldsymbol{\xi}}_A$. Moreover, $\tilde{\mathbf{Y}}$ is referred to the reference configuration and satisfies the transformation property $\tilde{\mathbf{Y}}^* = \tilde{\mathbf{Y}}$, so that the invariance with respect to rigid body rotations superposed on the plastic intermediate configuration does not restrict $\tilde{\psi}_p$ to be an isotropic tensor function of $\tilde{\mathbf{Y}}$. Therefore,

$$\tilde{\mathbf{Y}} \frac{\partial \tilde{\psi}_p}{\partial \tilde{\mathbf{Y}}} \neq \frac{\partial \tilde{\psi}_p}{\partial \tilde{\mathbf{Y}}} \tilde{\mathbf{Y}} \tag{3.71}$$

and $\hat{\boldsymbol{\xi}}_A$ in (3.69) will not vanish generally.
The yield function is supposed to exhibit, besides kinematic, also orientational hardening:

$$f = \overline{\overline{f}}\left(\hat{\mathbf{P}}, \hat{\boldsymbol{\xi}}, \mathbf{\Pi}\right) \quad , \quad \mathbf{\Pi}^T = \mathbf{\Pi}^{-1} \quad , \tag{3.72}$$

where $\mathbf{\Pi}$, like $\mathbf{\Phi}$ and $\mathbf{\Delta}$, is an orthogonal tensor, which rotates some symmetry axes related to the yield condition. Inequality (3.30) will be inspected next, which now takes the form

$$\begin{aligned} \mathcal{D}_{int} &= \left(\hat{\mathbf{P}} - \hat{\boldsymbol{\xi}}\right) \cdot \left(\hat{\mathbf{L}}_p - \dot{\mathbf{\Phi}}\mathbf{\Phi}^T\right) + \hat{\boldsymbol{\xi}} \cdot \left(\hat{\mathbf{L}}_p - \dot{\mathbf{\Phi}}\mathbf{\Phi}^T\right) - \varrho_R\dot{\psi}_p \\ &= \sqrt{\frac{3}{2}}\dot{s}\left(\hat{\mathbf{P}} - \hat{\boldsymbol{\xi}}\right) \cdot \hat{\mathbf{N}} + \hat{\mathbf{Z}} \cdot \hat{\mathbf{D}}_p + 2\hat{\mathbf{Y}}\hat{\mathbf{Z}} \cdot \hat{\mathbf{D}}_p + \hat{\boldsymbol{\xi}}_A \cdot \hat{\mathbf{\Omega}}^{(e)} - \varrho_R\dot{\psi}_p \geq 0 \quad . \end{aligned} \tag{3.73}$$

Because of the convexity of the level set $\{\hat{\mathbf{P}}|\overline{\overline{f}}(\hat{\mathbf{P}},\hat{\boldsymbol{\xi}},\boldsymbol{\Pi}) = const,\ \hat{\boldsymbol{\xi}} = fixed,\ \boldsymbol{\Pi} = fixed\}$, it can be shown that $\left(\hat{\mathbf{P}} - \hat{\boldsymbol{\xi}}\right)\cdot\hat{\mathbf{N}} \geq 0$ and the inequality (3.73) is satisfied, provided the inequality

$$\hat{\mathbf{Z}}\cdot\hat{\mathbf{D}}_p + 2\hat{\mathbf{Y}}\hat{\mathbf{Z}}\cdot\hat{\mathbf{D}}_p + \hat{\boldsymbol{\xi}}_A\cdot\hat{\boldsymbol{\Omega}}^{(e)} - \varrho_R\dot{\psi}_p \geq 0 \tag{3.74}$$

holds. From (3.64), (3.65),

$$\dot{\psi}_p = \frac{\partial\tilde{\psi}_p}{\partial\tilde{\mathbf{Y}}}\cdot\left(\dot{\boldsymbol{\Delta}}^T\hat{\mathbf{Y}}\boldsymbol{\Delta} + \boldsymbol{\Delta}^T\dot{\hat{\mathbf{Y}}}\boldsymbol{\Delta} + \boldsymbol{\Delta}^T\hat{\mathbf{Y}}\dot{\boldsymbol{\Delta}}\right) = \frac{1}{\varrho_R}\hat{\mathbf{Z}}\cdot\dot{\hat{\mathbf{Y}}} + \frac{1}{\varrho_R}\hat{\boldsymbol{\xi}}_A\cdot\dot{\boldsymbol{\Delta}}\boldsymbol{\Delta}^T \quad , \tag{3.75}$$

where $\dot{\boldsymbol{\Delta}}\boldsymbol{\Delta}^T$ denotes a skew-symmetric tensor (the so-called constitutive spin). On substituting (3.75) in (3.74),

$$\hat{\mathbf{Z}}\cdot\hat{\mathbf{D}}_p + 2\hat{\mathbf{Y}}\hat{\mathbf{Z}}\cdot\hat{\mathbf{D}}_p + \hat{\boldsymbol{\xi}}_A\cdot\hat{\boldsymbol{\Omega}}^{(e)} - \hat{\mathbf{Z}}\cdot\dot{\hat{\mathbf{Y}}} - \hat{\boldsymbol{\xi}}_A\cdot\dot{\boldsymbol{\Delta}}\boldsymbol{\Delta}^T \geq 0 \quad . \tag{3.76}$$

Sufficient conditions for the validity of this inequality can be established appropriately by prescribing the rate of $\hat{\mathbf{Y}}$ (strain space formulation) or the rate of $\hat{\mathbf{Z}}$ (stress space formulation). This approach is demonstrated for the stress space formulation. To this end, $\tilde{\psi}_p\left(\tilde{\mathbf{Y}}\right)$ is assumed to be given by

$$\psi_p = \tilde{\psi}_p\left(\tilde{\mathbf{Y}}\right) = \frac{1}{2\varrho_R}\tilde{\mathbf{Y}}\cdot\tilde{\boldsymbol{\mathcal{C}}}^{(k)}\left[\tilde{\mathbf{Y}}\right] \quad , \tag{3.77}$$

where

$$\tilde{\boldsymbol{\mathcal{C}}}^{(k)} := \frac{\partial^2\tilde{\psi}_p}{\partial\tilde{\mathbf{Y}}\partial\tilde{\mathbf{Y}}} \tag{3.78}$$

denotes a time independent symmetric positive definite fourth-order tensor. The later satisfies the properties

$$\tilde{\mathcal{C}}^{(\mathrm{k})}_{ijkl} = \tilde{\mathcal{C}}^{(\mathrm{k})}_{jikl} = \tilde{\mathcal{C}}^{(\mathrm{k})}_{ijlk} = \tilde{\mathcal{C}}^{(\mathrm{k})}_{klij} \quad , \tag{3.79}$$

with respect to an orthonormal basis $\{\mathbf{e}_i\}$, and remains unaltered if arbitrary rigid body rotations $\overline{\mathbf{Q}}$ are superposed on the plastic intermediate configuration:

$$\tilde{\boldsymbol{\mathcal{C}}}^{(k)} \rightarrow \left(\tilde{\boldsymbol{\mathcal{C}}}^{(k)}\right)^* = \tilde{\boldsymbol{\mathcal{C}}}^{(k)} \quad . \tag{3.80}$$

From (3.64), (3.65) and (3.77),

$$\psi_p = \overline{\overline{\psi}}_p\left(\hat{\mathbf{Y}},\boldsymbol{\Delta}\right) = \frac{1}{2\varrho_R}\hat{\mathbf{Y}}\cdot\hat{\boldsymbol{\mathcal{C}}}^{(k)}(\boldsymbol{\Delta})\left[\hat{\mathbf{Y}}\right] \quad , \tag{3.81}$$

$$\hat{\mathbf{Z}} = \hat{\boldsymbol{\mathcal{C}}}^{(k)}\left[\hat{\mathbf{Y}}\right] \quad , \tag{3.82}$$

where the fourth-order tensor $\hat{\boldsymbol{\mathcal{C}}}^{(k)}$ is given by

$$\hat{\boldsymbol{\mathcal{C}}}^{(k)} := \frac{\partial^2\overline{\overline{\psi}}_p}{\partial\hat{\mathbf{Y}}\partial\hat{\mathbf{Y}}} \tag{3.83}$$

and satisfies, with respect to an orthonormal basis $\{\mathbf{e}_i\}$, properties of the form (3.79). The two tensors $\tilde{\boldsymbol{\mathcal{C}}}^{(k)}$ and $\hat{\boldsymbol{\mathcal{C}}}^{(k)}$ are related by

$$\hat{\boldsymbol{\mathcal{C}}}^{(k)}\left[\hat{\mathbf{X}}\right] = \boldsymbol{\Delta}\left(\tilde{\boldsymbol{\mathcal{C}}}^{(k)}\left[\boldsymbol{\Delta}^T\hat{\mathbf{X}}\boldsymbol{\Delta}\right]\right)\boldsymbol{\Delta}^T \quad , \tag{3.84}$$

$\hat{\mathbf{X}}$ being an arbitrary second-order symmetric tensor relative to the plastic intermediate configuration. With respect to an orthonormal basis $\{\mathbf{e}_i\}$, (3.84) yields

$$\hat{\mathcal{C}}^{(\mathrm{k})}_{ijmn} = \Delta_{\mathrm{ir}}\Delta_{\mathrm{js}}\Delta_{\mathrm{mp}}\Delta_{\mathrm{nq}}\tilde{\mathcal{C}}^{(\mathrm{k})}_{rspq} \quad . \tag{3.85}$$

Under arbitrary rigid body rotations $\overline{\mathbf{Q}}$ superposed on the plastic intermediate configuration, $\boldsymbol{\Delta}$ is defined to transform according to (cf. (3.21))

$$\boldsymbol{\Delta} \to \boldsymbol{\Delta}^* = \overline{\mathbf{Q}}\boldsymbol{\Delta} \quad , \tag{3.86}$$

from which, by virtue of (3.80) and (3.84)

$$\hat{\boldsymbol{\mathcal{C}}}^{(k)} \to \left(\hat{\boldsymbol{\mathcal{C}}}^{(k)}\right)^* \quad , \tag{3.87}$$

with

$$\overline{\mathbf{Q}}^T \left\{ \left(\hat{\boldsymbol{\mathcal{C}}}^{(k)}\right)^* \left[\overline{\mathbf{Q}}\hat{\mathbf{X}}\overline{\mathbf{Q}}^T\right] \right\} \overline{\mathbf{Q}} = \hat{\boldsymbol{\mathcal{C}}}^{(k)} \left[\hat{\mathbf{X}}\right] \quad . \tag{3.88}$$

Here $\hat{\mathbf{X}}$ is given as in (3.84) and is defined to transform according to

$$\hat{\mathbf{X}} \to \hat{\mathbf{X}}^* = \overline{\mathbf{Q}}\hat{\mathbf{X}}\overline{\mathbf{Q}}^T \quad . \tag{3.89}$$

Let $\tilde{\boldsymbol{\mathcal{M}}}^{(k)}$ be a fourth-order tensor with

$$\tilde{\boldsymbol{\mathcal{M}}}^{(k)}\tilde{\boldsymbol{\mathcal{C}}}^{(k)} = \tilde{\boldsymbol{\mathcal{C}}}^{(k)}\tilde{\boldsymbol{\mathcal{M}}}^{(k)} = \boldsymbol{\mathcal{E}} \quad . \tag{3.90}$$

Note in passing that the existence of $\tilde{\boldsymbol{\mathcal{M}}}^{(k)}$ implies the existence of $\hat{\boldsymbol{\mathcal{M}}}^{(k)}$ with

$$\hat{\boldsymbol{\mathcal{M}}}^{(k)}\hat{\boldsymbol{\mathcal{C}}}^{(k)} = \hat{\boldsymbol{\mathcal{C}}}^{(k)}\hat{\boldsymbol{\mathcal{M}}}^{(k)} = \boldsymbol{\mathcal{E}} \quad . \tag{3.91}$$

Of course, $\tilde{\boldsymbol{\mathcal{M}}}^{(k)}$ and $\hat{\boldsymbol{\mathcal{M}}}^{(k)}$ satisfy properties of the form (3.79). In addition, $\tilde{\boldsymbol{\mathcal{M}}}^{(k)}$ and $\hat{\boldsymbol{\mathcal{M}}}^{(k)}$ obey transformation rules of the forms (3.80) and (3.88), respectively.
Now, in view of (3.77),

$$\varrho_R \frac{\partial \tilde{\psi}_p}{\partial \tilde{\mathbf{Y}}} = \tilde{\boldsymbol{\mathcal{C}}}^{(k)} \left[\tilde{\mathbf{Y}}\right] \quad , \tag{3.92}$$

or (cf. (3.65))

$$\tilde{\mathbf{Y}} = \tilde{\boldsymbol{\mathcal{M}}}^{(k)} \left[\varrho_R \frac{\partial \tilde{\psi}_p}{\partial \tilde{\mathbf{Y}}}\right] = \tilde{\boldsymbol{\mathcal{M}}}^{(k)} \left[\boldsymbol{\Delta}^T\hat{\mathbf{Z}}\boldsymbol{\Delta}\right] \quad . \tag{3.93}$$

Using the above relations it can be seen, after some algebraic manipulations, that

$$\hat{\mathbf{Z}} \cdot \dot{\hat{\mathbf{Y}}} = \hat{\mathbf{Y}} \cdot \dot{\hat{\mathbf{Z}}} - 2\hat{\boldsymbol{\xi}}_A \cdot \left(\dot{\boldsymbol{\Delta}}\boldsymbol{\Delta}^T\right) \quad . \tag{3.94}$$

On the other hand,

$$\hat{\mathbf{Y}} \cdot \dot{\hat{\mathbf{Z}}} = \tilde{\boldsymbol{\mathcal{M}}}^{(k)} \left[\boldsymbol{\Delta}^T\hat{\mathbf{Z}}\boldsymbol{\Delta}\right] \cdot \boldsymbol{\Delta}^T\overset{\triangledown}{\hat{\mathbf{Z}}}\boldsymbol{\Delta} + 2\hat{\mathbf{Y}}\hat{\mathbf{Z}} \cdot \hat{\mathbf{D}}_p + \hat{\boldsymbol{\xi}}_A \cdot \hat{\mathbf{W}}_p \quad , \tag{3.95}$$

where

$$\overset{\triangledown}{\hat{\mathbf{Z}}} := \dot{\hat{\mathbf{Z}}} - \hat{\mathbf{L}}_p\hat{\mathbf{Z}} - \hat{\mathbf{Z}}\hat{\mathbf{L}}_p^T \quad . \tag{3.96}$$

On inserting (3.95), (3.96) in (3.76), after some rearrangement of terms,

$$\boldsymbol{\Delta}^T\hat{\mathbf{Z}}\boldsymbol{\Delta}\cdot\left\{\boldsymbol{\Delta}^T\hat{\mathbf{D}}_p\boldsymbol{\Delta} - \tilde{\boldsymbol{\mathcal{M}}}^{(k)}\left[\boldsymbol{\Delta}^T\overset{\triangledown}{\hat{\mathbf{Z}}}\boldsymbol{\Delta}\right]\right\} + \hat{\boldsymbol{\xi}}_A\cdot\left(\hat{\boldsymbol{\Omega}}^{(e)} - \hat{\boldsymbol{\Omega}}^{(k)}\right) \geq 0 \quad , \tag{3.97}$$

where the skew-symmetric tensor $\hat{\boldsymbol{\Omega}}^{(k)}$ is given by

$$\hat{\boldsymbol{\Omega}}^{(k)} := \hat{\mathbf{W}}_p - \dot{\boldsymbol{\Delta}}\boldsymbol{\Delta}^T \quad . \tag{3.98}$$

$\dot{\boldsymbol{\Delta}}\boldsymbol{\Delta}^T$ is the constitutive spin related to the kinematic hardening and $\hat{\boldsymbol{\Omega}}^{(k)}$ the corresponding plastic spin. From (3.86) and Appendix A it can be deduced that

$$\hat{\boldsymbol{\Omega}}^{(k)} \rightarrow \left(\hat{\boldsymbol{\Omega}}^{(k)}\right)^* = \overline{\mathbf{Q}}\hat{\boldsymbol{\Omega}}^{(k)}\overline{\mathbf{Q}}^T \quad . \tag{3.99}$$

Clearly,

$$\boldsymbol{\Delta}^T\hat{\mathbf{Z}}\boldsymbol{\Delta}\cdot\left\{\boldsymbol{\Delta}^T\hat{\mathbf{D}}_p\boldsymbol{\Delta} - \tilde{\boldsymbol{\mathcal{M}}}^{(k)}\left[\boldsymbol{\Delta}^T\overset{\triangledown}{\hat{\mathbf{Z}}}\boldsymbol{\Delta}\right]\right\} \geq 0 \quad , \tag{3.100}$$

$$\hat{\boldsymbol{\xi}}_A\cdot\left(\hat{\boldsymbol{\Omega}}^{(e)} - \hat{\boldsymbol{\Omega}}^{(k)}\right) \geq 0 \tag{3.101}$$

are sufficient conditions for (3.97). Since $\overset{\triangledown}{\hat{\mathbf{Z}}}^\star = \overline{\mathbf{Q}}\overset{\triangledown}{\hat{\mathbf{Z}}}\overline{\mathbf{Q}}^T$, it follows that inequalities (3.100) and (3.101) remain unaltered if arbitrary rigid body rotations are superposed on the plastic intermediate configuration.

In order to fulfill (3.100), $\left(\boldsymbol{\Delta}^T\hat{\mathbf{D}}_p\boldsymbol{\Delta} - \tilde{\boldsymbol{\mathcal{M}}}^{(k)}\left[\boldsymbol{\Delta}^T\overset{\triangledown}{\hat{\mathbf{Z}}}\boldsymbol{\Delta}\right]\right)$ is assumed to be given by

$$\left(\boldsymbol{\Delta}^T\hat{\mathbf{D}}_p\boldsymbol{\Delta} - \tilde{\boldsymbol{\mathcal{M}}}^{(k)}\left[\boldsymbol{\Delta}^T\overset{\triangledown}{\hat{\mathbf{Z}}}\boldsymbol{\Delta}\right]\right) = \dot{s}\left(\tilde{\boldsymbol{\mathcal{M}}}^{(k)}\tilde{\boldsymbol{\mathcal{B}}}^{(\mathrm{k})}\right)\left[\boldsymbol{\Delta}^T\hat{\mathbf{Z}}\boldsymbol{\Delta}\right] \quad , \tag{3.102}$$

where $\tilde{\boldsymbol{\mathcal{B}}}^{(\mathrm{k})}$ represents a symmetric, positive semi-definite fourth-order tensor, which under rigid body rotations superposed on the plastic intermediate configuration obeys a transformation rule of the form (3.80).

From (3.102),

$$\overset{\triangledown}{\hat{\mathbf{Z}}} = \boldsymbol{\Delta}\left(\tilde{\boldsymbol{\mathcal{C}}}^{(k)}\left[\boldsymbol{\Delta}^T\hat{\mathbf{D}}_p\boldsymbol{\Delta}\right]\right)\boldsymbol{\Delta}^T - \dot{s}\boldsymbol{\Delta}\left(\tilde{\boldsymbol{\mathcal{B}}}^{(\mathrm{k})}\left[\boldsymbol{\Delta}^T\hat{\mathbf{Z}}\boldsymbol{\Delta}\right]\right)\boldsymbol{\Delta}^T \quad , \tag{3.103}$$

or

$$\overset{\triangledown}{\hat{\mathbf{Z}}} = \hat{\boldsymbol{\mathcal{C}}}^{(k)}\left[\hat{\mathbf{D}}_p\right] - \dot{s}\hat{\boldsymbol{\mathcal{B}}}^{(\mathrm{k})}\left[\hat{\mathbf{Z}}\right] \quad . \tag{3.104}$$

Here, the symmetric positive semi-definite fourth-order tensor $\hat{\boldsymbol{\mathcal{B}}}^{(\mathrm{k})} = \hat{\boldsymbol{\mathcal{B}}}^{(\mathrm{k})}(\boldsymbol{\Delta})$ is defined by

$$\hat{\boldsymbol{\mathcal{B}}}^{(\mathrm{k})}\left[\hat{\mathbf{X}}\right] := \boldsymbol{\Delta}\left(\tilde{\boldsymbol{\mathcal{B}}}^{(\mathrm{k})}\left[\boldsymbol{\Delta}^T\hat{\mathbf{X}}\boldsymbol{\Delta}\right]\right)\boldsymbol{\Delta}^T \quad , \tag{3.105}$$

where $\hat{\mathbf{X}}$ denotes a tensor as in (3.84).
It is readily shown that under arbitrary rigid body rotations superposed on the plastic intermediate configuration, the tensor $\hat{\boldsymbol{\mathcal{B}}}^{(\mathrm{k})}$ transforms according to

$$\overline{\mathbf{Q}}^T\left(\left(\hat{\boldsymbol{\mathcal{B}}}^{(\mathrm{k})}\right)^{\star}\left[\overline{\mathbf{Q}}\hat{\mathbf{X}}\overline{\mathbf{Q}}^T\right]\right)\overline{\mathbf{Q}} = \hat{\boldsymbol{\mathcal{B}}}^{(\mathrm{k})}\left[\hat{\mathbf{X}}\right] \quad , \tag{3.106}$$

with $\hat{\mathbf{X}}$ obeying the transformation (3.89).
A simple sufficient condition for (3.101) may be constructed by assuming the existence of a function

$$\chi = \hat{\chi}(\hat{\boldsymbol{\xi}}_A, \ldots) \geq 0 \quad , \tag{3.107}$$

which is convex with respect to $\hat{\boldsymbol{\xi}}_A$, remains unaltered if rigid body rotations $\overline{\mathbf{Q}}$ are superposed on the plastic intermediate configuration and satisfies the property $\hat{\chi}(\mathbf{0}, \ldots) = 0$. Then, the condition

$$\hat{\boldsymbol{\Omega}}^{(e)} - \hat{\boldsymbol{\Omega}}^{(k)} = \dot{s}\frac{\partial\hat{\chi}}{\partial\hat{\boldsymbol{\xi}}_A} \tag{3.108}$$

is sufficient for (3.101).
From (3.108) and (3.61),

$$\hat{\boldsymbol{\Omega}}^{(k)} = \sqrt{\frac{3}{2}}\dot{s}\hat{\mathbf{N}}_A - \dot{s}\frac{\partial\hat{\chi}}{\partial\hat{\boldsymbol{\xi}}_A} \quad . \tag{3.109}$$

Here (3.104) and (3.109) represent the evolution equations governing the response of kinematic hardening and (3.108) indicates that the plastic spin related to the elasticity law is always equal to the plastic spin related to the kinematical hardening rule provided the tensor $\dfrac{\partial\hat{\chi}}{\partial\hat{\boldsymbol{\xi}}_A}$ vanishes identically.

3.6 Constitutive model for orthotropic anisotropy

3.6.1 Plastic Spins

Before any inelastic deformation has occurred, the material is supposed to exhibit orthotropic anisotropy in the elasticity law, the kinematic hardening rule and the yield function. We denote by $\tilde{\mathbf{m}}_i^{(e)}$, $\tilde{\mathbf{m}}_i^{(k)}$ and $\tilde{\mathbf{m}}_i^{(y)}$, $i = 1, 2, 3$, the temporarily constant unit vectors in the reference configuration, representing the three local axes of symmetry in the elasticity law, the kinematic hardening rule and the yield function, respectively. With evolving plastic deformation the constitutive properties are assumed to remain orthotropic, with $\hat{\mathbf{m}}_i^{(e)}$, $\hat{\mathbf{m}}_i^{(k)}$ and $\hat{\mathbf{m}}_i^{(y)}$, $i = 1, 2, 3$, denoting the corresponding axes of symmetry in the plastic intermediate configuration. The vectors $\hat{\mathbf{m}}_i^{(e)}$, $\hat{\mathbf{m}}_i^{(k)}$ and $\hat{\mathbf{m}}_i^{(y)}$ are assumed to emerge by rotation from $\tilde{\mathbf{m}}_i^{(e)}$, $\tilde{\mathbf{m}}_i^{(k)}$ and $\tilde{\mathbf{m}}_i^{(y)}$, respectively, the corresponding rotations being $\boldsymbol{\Phi}$, $\boldsymbol{\Delta}$ and $\boldsymbol{\Pi}$. In the following the notation $\tilde{\mathbf{m}}_i$

is adopted for any one of the vectors $\tilde{\mathbf{m}}_i^{(e)}$, $\tilde{\mathbf{m}}_i^{(k)}$ and $\tilde{\mathbf{m}}_i^{(y)}$ and $\hat{\mathbf{m}}_i$ denotes the counterpart of $\tilde{\mathbf{m}}_i$ in the plastic intermediate configuration. Thus

$$\hat{\mathbf{m}}_i = \boldsymbol{\Theta}\tilde{\mathbf{m}}_i \quad , \tag{3.110}$$

with $\boldsymbol{\Theta}$ being either $\boldsymbol{\Phi}$ or $\boldsymbol{\Delta}$ or $\boldsymbol{\Pi}$, depending on wether the elasticity law or the kinematic hardening rule or the yield function is regarded, respectively. In the same sense $\hat{\boldsymbol{\Omega}}$ is written for any one of the plastic spins $\hat{\boldsymbol{\Omega}}^{(e)}$, $\hat{\boldsymbol{\Omega}}^{(k)}$ and $\hat{\boldsymbol{\Omega}}^{(y)}$:

$$\hat{\boldsymbol{\Omega}} := \hat{\mathbf{W}}_p - \dot{\boldsymbol{\Theta}}\boldsymbol{\Theta}^T \quad . \tag{3.111}$$

The counterpart of $\tilde{\mathbf{m}}_i$ in the actual configuration is assumed to be

$$\mathbf{m}_i = \mathbf{R}_e\hat{\mathbf{m}}_i = \mathbf{R}_e\boldsymbol{\Theta}\tilde{\mathbf{m}}_i \quad . \tag{3.112}$$

The vectors $\tilde{\mathbf{m}}_i$, $\hat{\mathbf{m}}_i$ and $\mathbf{m}_i$ are used to introduce the structural tensors $\tilde{\mathbf{M}}_i$, $\hat{\mathbf{M}}_i$ and $\mathbf{M}_i$:

$$\tilde{\mathbf{M}}_i := \tilde{\mathbf{m}}_i \otimes \tilde{\mathbf{m}}_i \quad , \quad \hat{\mathbf{M}}_i := \hat{\mathbf{m}}_i \otimes \hat{\mathbf{m}}_i = \boldsymbol{\Theta}\tilde{\mathbf{M}}_i\boldsymbol{\Theta}^T \quad , \quad \mathbf{M}_i := \mathbf{m}_i \otimes \mathbf{m}_i = \mathbf{R}_e\hat{\mathbf{M}}_i\mathbf{R}_e^T \quad . \tag{3.113}$$

Clearly,

$$\tilde{\mathbf{M}}_i\tilde{\mathbf{M}}_i = \tilde{\mathbf{M}}_i \quad , \quad \operatorname{tr}\tilde{\mathbf{M}}_i = 1 \tag{3.114}$$

and, because $\boldsymbol{\Theta}$ is a proper orthogonal tensor,

$$\hat{\mathbf{M}}_i\hat{\mathbf{M}}_i = \hat{\mathbf{M}}_i \quad , \quad \operatorname{tr}\hat{\mathbf{M}}_i = 1 \quad . \tag{3.115}$$

It is worth noting that $\mathbf{M}_i$ satisfies properties of the form (3.114) or (3.115), this being the motivation for the definition $(3.113)_3$. The vector $\tilde{\mathbf{m}}_i$ is assumed to remain unaltered whenever rigid body rotations $\overline{\mathbf{Q}}$ are superposed on the plastic intermediate configuration. This, as well as the transformation rule $\boldsymbol{\Theta} \to \boldsymbol{\Theta}^* = \overline{\mathbf{Q}}\boldsymbol{\Theta}$ (see TSAKMAKIS [106]), render $\tilde{\mathbf{M}}_i$ and $\hat{\mathbf{M}}_i$ to transform according to

$$\tilde{\mathbf{M}}_i \to \tilde{\mathbf{M}}_i^* = \tilde{\mathbf{M}}_i \quad , \quad \hat{\mathbf{M}}_i \to \hat{\mathbf{M}}_i^* = \overline{\mathbf{Q}}\hat{\mathbf{M}}_i\overline{\mathbf{Q}}^T \quad . \tag{3.116}$$

By taking the material time derivative of $(3.113)_2$ and since $\tilde{\mathbf{M}}_i$ are constant,

$$\dot{\hat{\mathbf{M}}}_i = \dot{\boldsymbol{\Theta}}\boldsymbol{\Theta}^T\hat{\mathbf{M}}_i - \hat{\mathbf{M}}_i\dot{\boldsymbol{\Theta}}\boldsymbol{\Theta}^T \tag{3.117}$$

or

$$\dot{\hat{\mathbf{M}}}_i = \hat{\mathbf{W}}_p\hat{\mathbf{M}}_i - \hat{\mathbf{M}}_i\hat{\mathbf{W}}_p - \hat{\boldsymbol{\Omega}}\hat{\mathbf{M}}_i + \hat{\mathbf{M}}_i\hat{\boldsymbol{\Omega}} \quad , \tag{3.118}$$

or

$$\begin{aligned}\overset{\triangle}{\mathbf{M}}_i &:= \dot{\mathbf{M}}_i + \mathbf{L}^T\mathbf{M}_i + \mathbf{M}_i\mathbf{L} \\ &= \mathbf{D}\mathbf{M}_i + \mathbf{M}_i\mathbf{D} - (\mathbf{W} - \dot{\mathbf{R}}_e\mathbf{R}_e^T - \mathbf{R}_e\hat{\mathbf{W}}_p\mathbf{R}_e^T + \mathbf{R}_e\hat{\boldsymbol{\Omega}}\mathbf{R}_e^T)\mathbf{M}_i \\ &\quad + \mathbf{M}_i(\mathbf{W} - \dot{\mathbf{R}}_e\mathbf{R}_e^T - \mathbf{R}_e\hat{\mathbf{W}}_p\mathbf{R}_e^T + \mathbf{R}_e\hat{\boldsymbol{\Omega}}\mathbf{R}_e^T) \quad .\end{aligned} \tag{3.119}$$

A useful relation between $\mathbf{L}$ and $\dot{\mathbf{R}}_e\mathbf{R}_e^T$ can be derived from (2.4), (2.5) and (2.8):

$$\mathbf{L} = \dot{\mathbf{V}}_e\mathbf{V}_e^{-1} + \mathbf{V}_e\dot{\mathbf{R}}_e\mathbf{R}_e^T\mathbf{V}_e^{-1} + \mathbf{V}_e\mathbf{R}_e\hat{\mathbf{L}}_p\mathbf{R}_e^T\mathbf{V}_e^{-1} \tag{3.120}$$

or

$$\dot{\mathbf{R}}_e\mathbf{R}_e^T = (\mathbf{V}_e^{-1}\mathbf{L}\mathbf{V}_e)_A + (\dot{\mathbf{V}}_e\mathbf{V}_e^{-1})_A - \mathbf{R}_e\hat{\mathbf{W}}_p\mathbf{R}_e^T \quad . \tag{3.121}$$

On substituting (3.121) and the definition

$$\mathbf{\Omega} := \mathbf{R}_e\hat{\mathbf{\Omega}}\mathbf{R}_e^T \tag{3.122}$$

in (3.119), one finds

$$\begin{aligned}\overset{\triangle}{\mathbf{M}}_i &= \mathbf{D}\mathbf{M}_i + \mathbf{M}_i\mathbf{D} - \{\mathbf{W} - (\mathbf{V}_e^{-1}\mathbf{L}\mathbf{V}_e)_A - (\dot{\mathbf{V}}_e\mathbf{V}_e^{-1})_A + \mathbf{\Omega}\}\mathbf{M}_i \\ &\quad + \mathbf{M}_i\{\mathbf{W} - (\mathbf{V}_e^{-1}\mathbf{L}\mathbf{V}_e)_A - (\dot{\mathbf{V}}_e\mathbf{V}_e^{-1})_A + \mathbf{\Omega}\} \quad ,\end{aligned} \tag{3.123}$$

with $\mathbf{\Omega}$ denoting an EULERIAN counterpart of the plastic spin $\hat{\mathbf{\Omega}}$. (3.123) represents the evolution equation governing the response of $\mathbf{M}_i$. The sum of the three structural tensors equals identity

$$\tilde{\mathbf{M}}_1 + \tilde{\mathbf{M}}_2 + \tilde{\mathbf{M}}_3 = \mathbf{1} \quad , \tag{3.124}$$

so only two out of the three structural tensors are necessary to describe orthotropy and in the following the index $i = 3$ will be dropped and only $\tilde{\mathbf{M}}_1$, $\tilde{\mathbf{M}}_2$ (respectively $\hat{\mathbf{M}}_1$, $\hat{\mathbf{M}}_2$ or $\mathbf{M}_1$, $\mathbf{M}_2$) will be used.

3.6.2 Elasticity law

Second-order structural tensors may be used to describe anisotropic constitutive properties (see e.g. BOEHLER [12], HÄUSLER [42], LIU [70]). If $\mathbf{\Phi}$ is assumed to enter into the elastic part of the free energy in the form $\mathbf{\Phi}\tilde{\mathbf{M}}^{(e)}\mathbf{\Phi}^T$, then

$$\psi_e = \overline{\overline{\psi}}_e(\hat{\mathbf{\Gamma}}_e, \mathbf{\Phi}) = \hat{\psi}_e(\hat{\mathbf{\Gamma}}_e, \hat{\mathbf{M}}^{(e)}) \tag{3.125}$$

with respect to $(3.113)_2$. Since ψ_e is required to be unaltered under rigid body rotations superposed on the plastic intermediate configuration, it follows, from $(3.115)_2$ and Appendix A, that $\hat{\psi}_e$ is an isotropic tensor function of $\hat{\mathbf{\Gamma}}_e$, $\hat{\mathbf{M}}_1^{(e)}$ and $\hat{\mathbf{M}}_2^{(e)}$. Hence, $\hat{\psi}_e$ may be represented by using the theorems on isotropic tensor functions outlined in SPENCER [95], ZHENG [114]. To derive a linear elasticity law, ψ_e is represented (cf. ARAVAS [4], as well as SPENCER [94], Chapter 6 and [95]) in the form

$$\begin{aligned}&\varrho_R\hat{\psi}_e(\hat{\mathbf{\Gamma}}_e, \hat{\mathbf{M}}_1^{(e)}, \hat{\mathbf{M}}_2^{(e)}) = \alpha_1 \operatorname{tr}\hat{\mathbf{\Gamma}}_e^2 + \alpha_2 \operatorname{tr}(\hat{\mathbf{\Gamma}}_e^2\hat{\mathbf{M}}_1^{(e)}) + \alpha_3 \operatorname{tr}(\hat{\mathbf{\Gamma}}_e^2\hat{\mathbf{M}}_2^{(e)}) \\ &+ \alpha_4\{\operatorname{tr}\hat{\mathbf{\Gamma}}_e\}^2 + \alpha_5\{\operatorname{tr}(\hat{\mathbf{\Gamma}}_e\hat{\mathbf{M}}_1^{(e)})\}^2 + \alpha_6\{\operatorname{tr}(\hat{\mathbf{\Gamma}}_e\hat{\mathbf{M}}_2^{(e)})\}^2 \\ &+ \alpha_7(\operatorname{tr}\hat{\mathbf{\Gamma}}_e)\operatorname{tr}(\hat{\mathbf{\Gamma}}_e\hat{\mathbf{M}}_1^{(e)}) + \alpha_8(\operatorname{tr}\hat{\mathbf{\Gamma}}_e)\operatorname{tr}(\hat{\mathbf{\Gamma}}_e\hat{\mathbf{M}}_2^{(e)}) + \alpha_9(\operatorname{tr}\hat{\mathbf{\Gamma}}_e\hat{\mathbf{M}}_1^{(e)})\operatorname{tr}(\hat{\mathbf{\Gamma}}_e\hat{\mathbf{M}}_2^{(e)}) \quad ,\end{aligned} \tag{3.126}$$

with α_i, $i = 1, \ldots, 9$ being material parameters. $(3.28)_2$, (3.125) and (3.126) then yield

$$\begin{aligned}\hat{\mathbf{T}} &= \varrho_R\frac{\partial\hat{\psi}_e(\hat{\mathbf{\Gamma}}_e, \hat{\mathbf{M}}_1^{(e)}, \hat{\mathbf{M}}_2^{(e)})}{\partial\hat{\mathbf{\Gamma}}_e} \\ &= \{2\alpha_1\hat{\mathbf{\Gamma}}_e + \alpha_2(\hat{\mathbf{\Gamma}}_e\hat{\mathbf{M}}_1^{(e)} + \hat{\mathbf{M}}_1^{(e)}\hat{\mathbf{\Gamma}}_e) + \alpha_3(\hat{\mathbf{\Gamma}}_e\hat{\mathbf{M}}_2^{(e)} + \hat{\mathbf{M}}_2^{(e)}\hat{\mathbf{\Gamma}}_e) \\ &+ \{2\alpha_4\operatorname{tr}\hat{\mathbf{\Gamma}}_e + \alpha_7\operatorname{tr}(\hat{\mathbf{\Gamma}}_e\hat{\mathbf{M}}_1^{(e)}) + \alpha_8\operatorname{tr}(\hat{\mathbf{\Gamma}}_e\hat{\mathbf{M}}_2^{(e)})\}\mathbf{1} \\ &+ \{\alpha_7\operatorname{tr}\hat{\mathbf{\Gamma}}_e + 2\alpha_5\operatorname{tr}(\hat{\mathbf{\Gamma}}_e\hat{\mathbf{M}}_1^{(e)}) + \alpha_9\operatorname{tr}(\hat{\mathbf{\Gamma}}_e\hat{\mathbf{M}}_2^{(e)})\}\hat{\mathbf{M}}_1^{(e)} \\ &+ \{\alpha_8\operatorname{tr}\hat{\mathbf{\Gamma}}_e + \alpha_9\operatorname{tr}(\hat{\mathbf{\Gamma}}_e\hat{\mathbf{M}}_1^{(e)}) + 2\alpha_6\operatorname{tr}(\hat{\mathbf{\Gamma}}_e\hat{\mathbf{M}}_2^{(e)})\}\hat{\mathbf{M}}_2^{(e)} \quad .\end{aligned} \tag{3.127}$$

This represents a linear orthotropic elasticity law relative to the plastic intermediate configuration,

$$\hat{\mathbf{T}} = \hat{\boldsymbol{\mathcal{C}}}^{(e)}[\hat{\boldsymbol{\Gamma}}_e] \quad , \tag{3.128}$$

or, with respect to an orthonormal basis system,

$$\hat{T}_{ij} = \hat{\mathcal{C}}^{(e)}_{ijkl}(\hat{\boldsymbol{\Gamma}}_e)_{kl} \quad . \tag{3.129}$$

The notation is usually simplified by using an orthonormal basis system $\{\mathbf{e}_i\}$, $i = 1, 2, 3$, with $\mathbf{e}_1 = \hat{\mathbf{m}}^{(e)}_1$ and $\mathbf{e}_2 = \hat{\mathbf{m}}^{(e)}_2$ being the two necessary axes to describe orthotropic anisotropy. With respect to this basis system the following abbreviation (VOIGHT notation) may be used

$$\hat{T}_{ij} \to \hat{T}_i \hat{=} \begin{pmatrix} \hat{T}_{11} \\ \hat{T}_{22} \\ \hat{T}_{33} \\ \hat{T}_{12} \\ \hat{T}_{13} \\ \hat{T}_{23} \end{pmatrix} \to \begin{pmatrix} \hat{T}_1 \\ \hat{T}_2 \\ \hat{T}_3 \\ \hat{T}_4 \\ \hat{T}_5 \\ \hat{T}_6 \end{pmatrix} \quad , \tag{3.130}$$

and analogous

$$(\hat{\Gamma}_e)_{ij} \to (\hat{\Gamma}_e)_i \hat{=} \begin{pmatrix} (\hat{\Gamma}_e)_{11} \\ (\hat{\Gamma}_e)_{22} \\ (\hat{\Gamma}_e)_{33} \\ (\hat{\Gamma}_e)_{12} \\ (\hat{\Gamma}_e)_{13} \\ (\hat{\Gamma}_e)_{23} \end{pmatrix} \to \begin{pmatrix} (\hat{\Gamma}_e)_1 \\ (\hat{\Gamma}_e)_2 \\ (\hat{\Gamma}_e)_3 \\ (\hat{\Gamma}_e)_4 \\ (\hat{\Gamma}_e)_5 \\ (\hat{\Gamma}_e)_6 \end{pmatrix} \quad , \tag{3.131}$$

so that (3.129) takes the form

$$\hat{T}_i = (\hat{\mathcal{C}}^{(e)})_{ij}(\hat{\Gamma}_e)_j \quad . \tag{3.132}$$

The components $(\hat{\mathcal{C}}^{(e)})_{ij}$ are given by

$$(\hat{\mathcal{C}}^{(e)})_{ij} \hat{=} \begin{pmatrix} c_{11} & c_{12} & c_{13} & 0 & 0 & 0 \\ c_{12} & c_{22} & c_{23} & 0 & 0 & 0 \\ c_{13} & c_{23} & c_{33} & 0 & 0 & 0 \\ 0 & 0 & 0 & c_{44} & 0 & 0 \\ 0 & 0 & 0 & 0 & c_{55} & 0 \\ 0 & 0 & 0 & 0 & 0 & c_{66} \end{pmatrix} \quad , \tag{3.133}$$

where

$$\begin{aligned} c_{11} &= 2(\alpha_1 + \alpha_2 + \alpha_4 + \alpha_5 + \alpha_7) \quad , \\ c_{22} &= 2(\alpha_1 + \alpha_3 + \alpha_4 + \alpha_6 + \alpha_8) \quad , \\ c_{33} &= 2(\alpha_1 + \alpha_4) \quad , \\ c_{12} &= 2\alpha_4 + \alpha_7 + \alpha_8 + \alpha_9 \quad , \\ c_{13} &= 2\alpha_4 + \alpha_7 \quad , \\ c_{23} &= 2\alpha_4 + \alpha_8 \quad , \\ c_{44} &= 2\alpha_1 + \alpha_2 + \alpha_3 \quad , \\ c_{55} &= 2\alpha_1 + \alpha_2 \quad , \\ c_{66} &= 2\alpha_1 + \alpha_3 \quad . \end{aligned} \tag{3.134}$$

To evaluate the elasticity law numerically it is necessary to transform (3.127) from the plastic intermediate to the actual configuration. Therefore the ALMANSI strain tensors in the current configuration

$$\mathbf{A} = \frac{1}{2}(\mathbf{1} - \mathbf{F}^{T-1}\mathbf{F}^{-1}) \quad , \tag{3.135}$$

$$\mathbf{A}_e = \frac{1}{2}(\mathbf{1} - \mathbf{F}_e^{T-1}\mathbf{F}_e^{-1}) = \frac{1}{2}(\mathbf{1} - \mathbf{B}_e^{-1}) = \mathbf{F}_e^{T-1}\hat{\mathbf{\Gamma}}_e\mathbf{F}_e^{-1} \quad , \tag{3.136}$$

$$\mathbf{A}_p = \mathbf{A} - \mathbf{A}_e = \frac{1}{2}(\mathbf{F}_e^{T-1}\mathbf{F}_e^{-1} - \mathbf{F}^{T-1}\mathbf{F}^{-1}) = \mathbf{F}_e^{T-1}\hat{\mathbf{\Gamma}}_p\mathbf{F}_e^{-1} \tag{3.137}$$

are introduced (cf. (2.17)). Then, observing the transformation $(3.113)_3$, (3.127) can be rewritten as

$$\begin{aligned}
\mathbf{S} &= 2\alpha_1(\mathbf{V}_e^2\mathbf{A}_e\mathbf{V}_e^2) + \alpha_2(\mathbf{V}_e^2\mathbf{A}_e\mathbf{V}_e\mathbf{M}_1^{(e)}\mathbf{V}_e + \mathbf{V}_e\mathbf{M}_1^{(e)}\mathbf{V}_e\mathbf{A}_e\mathbf{V}_e^2) \\
&\quad + \alpha_3(\mathbf{V}_e^2\mathbf{A}_e\mathbf{V}_e\mathbf{M}_2^{(e)}\mathbf{V}_e + \mathbf{V}_e\mathbf{M}_2^{(e)}\mathbf{V}_e\mathbf{A}_e\mathbf{V}_e^2) \\
&\quad + \{2\alpha_4\,\mathrm{tr}(\mathbf{V}_e^2\hat{\mathbf{\Gamma}}_e) + \alpha_7\,\mathrm{tr}(\mathbf{V}_e\hat{\mathbf{\Gamma}}_e\mathbf{V}_e\hat{\mathbf{M}}_1^{(e)}) + \alpha_8\,\mathrm{tr}(\mathbf{V}_e\hat{\mathbf{\Gamma}}_e\mathbf{V}_e\hat{\mathbf{M}}_2^{(e)})\}\mathbf{V}_e^2 \\
&\quad + \{\alpha_7\,\mathrm{tr}(\mathbf{V}_e^2\hat{\mathbf{\Gamma}}_e) + 2\alpha_5\,\mathrm{tr}(\mathbf{V}_e\hat{\mathbf{\Gamma}}_e\mathbf{V}_e\hat{\mathbf{M}}_1^{(e)}) + \alpha_9\,\mathrm{tr}(\mathbf{V}_e\hat{\mathbf{\Gamma}}_e\mathbf{V}_e\hat{\mathbf{M}}_2^{(e)})\}\mathbf{V}_e\mathbf{M}_1^{(e)}\mathbf{V}_e \\
&\quad + \{\alpha_8\,\mathrm{tr}(\mathbf{V}_e^2\hat{\mathbf{\Gamma}}_e) + \alpha_9\,\mathrm{tr}(\mathbf{V}_e\hat{\mathbf{\Gamma}}_e\mathbf{V}_e\hat{\mathbf{M}}_1^{(e)}) + 2\alpha_6\,\mathrm{tr}(\mathbf{V}_e\hat{\mathbf{\Gamma}}_e\mathbf{V}_e\hat{\mathbf{M}}_2^{(e)})\}\mathbf{V}_e\mathbf{M}_2^{(e)}\mathbf{V}_e \\
&=: \boldsymbol{\mathcal{C}}^{(e)}[\mathbf{A}_e] \quad .
\end{aligned} \tag{3.138}$$

3.6.3 Kinematic hardening rule

Following steps quite similar to those in the last section we arrive at

$$\psi_p = \overline{\overline{\psi}}_p(\hat{\mathbf{Y}}, \mathbf{\Delta}) = \hat{\psi}_p(\hat{\mathbf{Y}}, \hat{\mathbf{M}}_1^{(k)}, \hat{\mathbf{M}}_2^{(k)}) = \frac{1}{2\varrho_R}\hat{\mathbf{Y}} \cdot \hat{\boldsymbol{\mathcal{C}}}^{(k)}[\hat{\mathbf{Y}}] \quad , \tag{3.139}$$

$$\begin{aligned}
\varrho_R\hat{\psi}_p(\hat{\mathbf{Y}}, \hat{\mathbf{M}}_1^{(k)}, \hat{\mathbf{M}}_2^{(k)}) &= c_1\,\mathrm{tr}\,\hat{\mathbf{Y}}^2 + c_2\,\mathrm{tr}(\hat{\mathbf{Y}}^2\hat{\mathbf{M}}_1^{(k)}) + c_3\,\mathrm{tr}(\hat{\mathbf{Y}}^2\hat{\mathbf{M}}_2^{(k)}) \\
&\quad + c_4\{\mathrm{tr}\,\hat{\mathbf{Y}}\}^2 + c_5\{\mathrm{tr}(\hat{\mathbf{Y}}\hat{\mathbf{M}}_1^{(k)})\}^2 + c_6\{\mathrm{tr}(\hat{\mathbf{Y}}\hat{\mathbf{M}}_2^{(k)})\}^2 \\
&\quad + c_7(\mathrm{tr}\,\hat{\mathbf{Y}})\,\mathrm{tr}(\hat{\mathbf{Y}}\hat{\mathbf{M}}_1^{(k)}) + c_8(\mathrm{tr}\,\hat{\mathbf{Y}})\,\mathrm{tr}(\hat{\mathbf{Y}}\hat{\mathbf{M}}_2^{(k)}) + c_9(\mathrm{tr}\,\hat{\mathbf{Y}}\hat{\mathbf{M}}_1^{(k)})\,\mathrm{tr}(\hat{\mathbf{Y}}\hat{\mathbf{M}}_2^{(k)}) \quad ,
\end{aligned} \tag{3.140}$$

$$\begin{aligned}
\hat{\mathbf{Z}} &= \varrho_R\frac{\partial\hat{\psi}_p(\hat{\mathbf{Y}}, \hat{\mathbf{M}}_1^{(k)}, \hat{\mathbf{M}}_2^{(k)})}{\partial\hat{\mathbf{Y}}} = \hat{\boldsymbol{\mathcal{C}}}^{(k)}[\hat{\mathbf{Y}}] \\
&= 2c_1\hat{\mathbf{Y}} + c_2(\hat{\mathbf{Y}}\hat{\mathbf{M}}_1^{(k)} + \hat{\mathbf{M}}_1^{(k)}\hat{\mathbf{Y}}) + c_3(\hat{\mathbf{Y}}\hat{\mathbf{M}}_2^{(k)} + \hat{\mathbf{M}}_2^{(k)}\hat{\mathbf{Y}}) \\
&\quad + \{2c_4\,\mathrm{tr}\,\hat{\mathbf{Y}} + c_7\,\mathrm{tr}(\hat{\mathbf{Y}}\hat{\mathbf{M}}_1^{(k)}) + c_8\,\mathrm{tr}(\hat{\mathbf{Y}}\hat{\mathbf{M}}_2^{(k)})\}\mathbf{1} \\
&\quad + \{c_7\,\mathrm{tr}\,\hat{\mathbf{Y}} + 2c_5\,\mathrm{tr}(\hat{\mathbf{Y}}\hat{\mathbf{M}}_1^{(k)}) + c_9\,\mathrm{tr}(\hat{\mathbf{Y}}\hat{\mathbf{M}}_2^{(k)})\}\hat{\mathbf{M}}_1^{(k)} \\
&\quad + \{c_8\,\mathrm{tr}\,\hat{\mathbf{Y}} + c_9\,\mathrm{tr}(\hat{\mathbf{Y}}\hat{\mathbf{M}}_1^{(k)}) + 2c_6\,\mathrm{tr}(\hat{\mathbf{Y}}\hat{\mathbf{M}}_2^{(k)})\}\hat{\mathbf{M}}_2^{(k)} \quad ,
\end{aligned} \tag{3.141}$$

where c_i, $i = 1, \ldots, 9$ are material parameters.
For the tensor $\hat{\boldsymbol{\mathcal{B}}}^{(\mathrm{k})}$ in (3.104) it is natural to set, in analogy to (3.141),

$$\begin{aligned}
\hat{\boldsymbol{\mathcal{B}}}^{(\mathrm{k})}[\hat{\mathbf{Z}}] &= 2b_1\hat{\mathbf{Z}} + b_2(\hat{\mathbf{Z}}\hat{\mathbf{M}}_1^{(k)} + \hat{\mathbf{M}}_1^{(k)}\hat{\mathbf{Z}}) + b_3(\hat{\mathbf{Z}}\hat{\mathbf{M}}_2^{(k)} + \hat{\mathbf{M}}_2^{(k)}\hat{\mathbf{Z}}) \\
&\quad + \{2b_4\,\mathrm{tr}\,\hat{\mathbf{Z}} + b_7\,\mathrm{tr}(\hat{\mathbf{Z}}\hat{\mathbf{M}}_1^{(k)}) + b_8\,\mathrm{tr}(\hat{\mathbf{Z}}\hat{\mathbf{M}}_2^{(k)})\}\mathbf{1} \\
&\quad + \{b_7\,\mathrm{tr}\,\hat{\mathbf{Z}} + 2b_5\,\mathrm{tr}(\hat{\mathbf{Z}}\hat{\mathbf{M}}_1^{(k)}) + b_9\,\mathrm{tr}(\hat{\mathbf{Z}}\hat{\mathbf{M}}_2^{(k)})\}\hat{\mathbf{M}}_1^{(k)} \\
&\quad + \{b_8\,\mathrm{tr}\,\hat{\mathbf{Z}} + b_9\,\mathrm{tr}(\hat{\mathbf{Z}}\hat{\mathbf{M}}_1^{(k)}) + 2b_6\,\mathrm{tr}(\hat{\mathbf{Z}}\hat{\mathbf{M}}_2^{(k)})\}\hat{\mathbf{M}}_2^{(k)} \quad ,
\end{aligned} \tag{3.142}$$

b_i, $i = 1, \ldots, 9$ being material parameters. Of course, the tensors $\hat{\boldsymbol{\mathcal{C}}}^{(k)}$ and $\hat{\boldsymbol{\mathcal{B}}}^{(k)}$ satisfy, with respect to an orthonormal basis system $\{\mathbf{e}_i\}$, $i = 1, 2, 3$ with $\mathbf{e}_1 = \hat{\mathbf{m}}_1^{(k)}$ and $\mathbf{e}_2 = \hat{\mathbf{m}}_2^{(k)}$, properties of the form (3.133), (3.134). To obtain EULERIAN counterparts of (3.82) and (3.104), the stress tensor $\mathbf{Z}$ and the strain tensor $\mathbf{Y}$ are introduced, with

$$\mathbf{Z} := \mathbf{F}_e \hat{\mathbf{Z}} \mathbf{F}_e^T \quad , \tag{3.143}$$

$$\mathbf{Y} = \mathbf{F}_e^{T-1} \hat{\mathbf{Y}} \mathbf{F}_e^{-1} \quad . \tag{3.144}$$

Note that (cf. TSAKMAKIS [103])

$$\overset{\triangledown}{\mathbf{Z}} := \dot{\mathbf{Z}} - \mathbf{L}\mathbf{Z} - \mathbf{Z}\mathbf{L}^T = \mathbf{F}_e \overset{\triangledown}{\hat{\mathbf{Z}}} \mathbf{F}_e^T \tag{3.145}$$

and

$$\overset{\triangle}{\hat{\mathbf{\Gamma}}}_p := \dot{\hat{\mathbf{\Gamma}}}_p + \hat{\mathbf{L}}_p^T \hat{\mathbf{\Gamma}}_p + \hat{\mathbf{\Gamma}}_p \hat{\mathbf{L}}_p = \hat{\mathbf{D}}_p \quad , \tag{3.146}$$

$$\overset{\triangle}{\mathbf{A}}_p := \dot{\mathbf{A}} + \mathbf{L}^T \mathbf{A}_p + \mathbf{A}_p \mathbf{L} = \mathbf{F}_e^{T-1} \hat{\mathbf{D}}_p \mathbf{F}_e^{-1} \quad , \tag{3.147}$$

$$\overset{\triangle}{\mathbf{A}} := \dot{\mathbf{A}} + \mathbf{L}^T \mathbf{A} + \mathbf{A}\mathbf{L} = \mathbf{D} \quad . \tag{3.148}$$

Hence, (3.141) leads to (cf. also (3.138))

$$\mathbf{Z} = \boldsymbol{\mathcal{C}}^{(k)}[\mathbf{Y}] := \mathbf{F}_e(\hat{\boldsymbol{\mathcal{C}}}^{(k)}[\mathbf{F}_e^T \mathbf{Y} \mathbf{F}_e])\mathbf{F}_e^T \tag{3.149}$$

with

$$\begin{aligned}
\boldsymbol{\mathcal{C}}^{(k)}[\mathbf{Y}] = {} & 2c_1 \mathbf{V}_e^2 \mathbf{Y} \mathbf{V}_e^2 + c_2(\mathbf{V}_e^2 \mathbf{Y} \mathbf{V}_e \mathbf{M}_1^{(k)} \mathbf{V}_e + \mathbf{V}_e \mathbf{M}_1^{(k)} \mathbf{V}_e \mathbf{Y} \mathbf{V}_e^2) \\
& + c_3(\mathbf{V}_e^2 \mathbf{Y} \mathbf{V}_e \mathbf{M}_2^{(k)} \mathbf{V}_e + \mathbf{V}_e \mathbf{M}_2^{(k)} \mathbf{V}_e \mathbf{Y} \mathbf{V}_e^2) \\
& + \{2c_4 \operatorname{tr}(\mathbf{V}_e^2 \mathbf{Y}) + c_7 \operatorname{tr}(\mathbf{V}_e \mathbf{Y} \mathbf{V}_e \mathbf{M}_1^{(k)}) + c_8 \operatorname{tr}(\mathbf{V}_e \mathbf{Y} \mathbf{V}_e \mathbf{M}_2^{(k)})\} \mathbf{V}_e^2 \\
& + \{c_7 \operatorname{tr}(\mathbf{V}_e^2 \mathbf{Y}) + 2c_5 \operatorname{tr}(\mathbf{V}_e \mathbf{Y} \mathbf{V}_e \mathbf{M}_1^{(k)}) + c_9 \operatorname{tr}(\mathbf{V}_e \mathbf{Y} \mathbf{V}_e \mathbf{M}_2^{(k)})\} \mathbf{V}_e \mathbf{M}_1^{(k)} \mathbf{V}_e \\
& + \{c_8 \operatorname{tr}(\mathbf{V}_e^2 \mathbf{Y}) + c_9 \operatorname{tr}(\mathbf{V}_e \mathbf{Y} \mathbf{V}_e \mathbf{M}_1^{(k)}) + 2c_6 \operatorname{tr}(\mathbf{V}_e \mathbf{Y} \mathbf{V}_e \mathbf{M}_2^{(k)})\} \mathbf{V}_e \mathbf{M}_2^{(k)} \mathbf{V}_e \quad ,
\end{aligned} \tag{3.150}$$

which may be solved for $\mathbf{Y}$:

$$\mathbf{Y} = \boldsymbol{\mathcal{M}}^{(k)}[\mathbf{Z}] \quad , \quad \boldsymbol{\mathcal{M}}^{(k)} \boldsymbol{\mathcal{C}}^{(k)} = \boldsymbol{\mathcal{C}}^{(k)} \boldsymbol{\mathcal{M}}^{(k)} = \boldsymbol{\mathcal{E}} \quad . \tag{3.151}$$

Eqs. (3.149), (3.150) are EULERIAN counterparts of (3.82), the corresponding counterpart for (3.104) being

$$\overset{\triangledown}{\mathbf{Z}} = \boldsymbol{\mathcal{C}}^{(k)}[\overset{\triangle}{\mathbf{A}}_p] - \dot{s}\, \boldsymbol{\mathcal{B}}^{(k)}[\mathbf{Z}] \quad , \tag{3.152}$$

where $\boldsymbol{\mathcal{B}}^{(k)}$ is given by

$$\begin{aligned}
\boldsymbol{\mathcal{B}}^{(k)}[\mathbf{Z}] = {} & 2b_1 \mathbf{Z} + b_2(\mathbf{Z} \mathbf{V}_e^{-1} \mathbf{M}_1^{(k)} \mathbf{V}_e + \mathbf{V}_e \mathbf{M}_1^{(k)} \mathbf{V}_e^{-1} \mathbf{Z}) \\
& + b_3(\mathbf{Z} \mathbf{V}_e^{-1} \mathbf{M}_2^{(k)} \mathbf{V}_e + \mathbf{V}_e \mathbf{M}_2^{(k)} \mathbf{V}_e^{-1} \mathbf{Z}) \\
& + \{2b_4 \operatorname{tr}(\mathbf{V}_e^{-2} \mathbf{Z}) + b_7 \operatorname{tr}(\mathbf{V}_e^{-1} \mathbf{Z} \mathbf{V}_e^{-1} \mathbf{M}_1^{(k)}) + b_8 \operatorname{tr}(\mathbf{V}_e^{-1} \mathbf{Z} \mathbf{V}_e^{-1} \mathbf{M}_2^{(k)})\} \mathbf{V}_e^2 \\
& + \{b_7 \operatorname{tr}(\mathbf{V}_e^{-2} \mathbf{Z}) + 2b_5 \operatorname{tr}(\mathbf{V}_e^{-1} \mathbf{Z} \mathbf{V}_e^{-1} \mathbf{M}_1^{(k)}) + b_9 \operatorname{tr}(\mathbf{V}_e^{-1} \mathbf{Z} \mathbf{V}_e^{-1} \mathbf{M}_2^{(k)})\} \mathbf{V}_e \mathbf{M}_1^{(k)} \mathbf{V}_e \\
& + \{b_8 \operatorname{tr}(\mathbf{V}_e^{-2} \mathbf{Z}) + b_9 \operatorname{tr}(\mathbf{V}_e^{-1} \mathbf{Z} \mathbf{V}_e^{-1} \mathbf{M}_1^{(k)}) + 2b_6 \operatorname{tr}(\mathbf{V}_e^{-1} \mathbf{Z} \mathbf{V}_e^{-1} \mathbf{M}_2^{(k)})\} \mathbf{V}_e \mathbf{M}_2^{(k)} \mathbf{V}_e \quad .
\end{aligned} \tag{3.153}$$

To accomplish the kinematic hardening rule it remains to precise (3.109). It is convenient to assume $\chi = \hat{\chi}(\hat{\boldsymbol{\xi}}_A, \hat{\mathbf{M}}_1^{(k)}, \hat{\mathbf{M}}_2^{(k)})$. The function $\hat{\chi}$ is quadratic in the stresses and, on applying the theorems for isotropic tensor functions and taking into account (3.116),

$$\chi = \hat{\chi}(\hat{\boldsymbol{\xi}}_A, \hat{\mathbf{M}}_1^{(k)}, \hat{\mathbf{M}}_2^{(k)}) = -\frac{l_1}{2}\,\mathrm{tr}\,\hat{\boldsymbol{\xi}}_A^2 - \frac{l_2}{2}\,\mathrm{tr}(\hat{\boldsymbol{\xi}}_A^2\hat{\mathbf{M}}_1^{(k)}) - \frac{l_3}{2}\,\mathrm{tr}(\hat{\boldsymbol{\xi}}_A{}^2\hat{\mathbf{M}}_2^{(k)}) := \frac{1}{2}\hat{\boldsymbol{\xi}}_A \cdot \hat{\boldsymbol{\mathcal{L}}}[\hat{\boldsymbol{\xi}}_A] \quad , \tag{3.154}$$

where l_i, $i = 1, 2, 3$ are material parameters. The fourth-order tensor $\hat{\boldsymbol{\mathcal{L}}}$ is given by

$$\hat{\boldsymbol{\mathcal{L}}} = \frac{\partial^2 \hat{\chi}}{\partial \hat{\boldsymbol{\xi}}_A \partial \hat{\boldsymbol{\xi}}_A} \quad , \tag{3.155}$$

$$\frac{\partial \hat{\chi}}{\partial \hat{\boldsymbol{\xi}}_A} = \hat{\boldsymbol{\mathcal{L}}}[\hat{\boldsymbol{\xi}}_A] = l_1\hat{\boldsymbol{\xi}}_A + \frac{l_2}{2}(\hat{\boldsymbol{\xi}}_A\hat{\mathbf{M}}_1^{(k)} + \hat{\mathbf{M}}_1^{(k)}\hat{\boldsymbol{\xi}}_A) + \frac{l_3}{2}(\hat{\boldsymbol{\xi}}_A\hat{\mathbf{M}}_2^{(k)} + \hat{\mathbf{M}}_2^{(k)}\hat{\boldsymbol{\xi}}_A) \tag{3.156}$$

and transforms, under rigid body rotations $\overline{\mathbf{Q}}$ superposed on the plastic intermediate configuration, according to

$$\overline{\mathbf{Q}}^T(\hat{\boldsymbol{\mathcal{L}}}^*[\overline{\mathbf{Q}}\hat{\boldsymbol{\xi}}_A\overline{\mathbf{Q}}^T])\overline{\mathbf{Q}} = \hat{\boldsymbol{\mathcal{L}}}[\hat{\boldsymbol{\xi}}_A] \quad . \tag{3.157}$$

With respect to an orthonormal basis system $\{\mathbf{e}_i\}$, $i = 1, 2, 3$ with $\mathbf{e}_1 = \hat{\mathbf{m}}_1^{(k)}$ and $\mathbf{e}_2 = \hat{\mathbf{m}}_2^{(k)}$ the relations

$$\hat{\mathcal{L}}_{ijkl} = -\hat{\mathcal{L}}_{jikl} = -\hat{\mathcal{L}}_{ijlk} = \hat{\mathcal{L}}_{klij} \quad , \tag{3.158}$$

$$\begin{aligned}\hat{\mathcal{L}}_{ijkl} = {} & l_1\boldsymbol{\mathcal{I}}_{ijkl} + \frac{l_2}{4}\{\delta_{ik}\hat{M}_{1_{jl}} - \delta_{il}\hat{M}_{1_{jk}} + \hat{M}_{1_{ik}}\delta_{jl} - \hat{M}_{1_{il}}\delta_{jk}\} \\ & + \frac{l_3}{4}\{\delta_{ik}\hat{M}_{2_{jl}} - \delta_{il}\hat{M}_{2_{jk}} + \hat{M}_{2_{ik}}\delta_{jl} - \hat{M}_{2_{il}}\delta_{jk}\}\end{aligned} \tag{3.159}$$

apply and keeping in mind that $\hat{\boldsymbol{\xi}}_A$ is a deviator,

$$\chi = \left(l_1 + \frac{l_2}{2} + \frac{l_3}{2}\right)(\hat{\boldsymbol{\xi}}_A)_{12}^2 + \left(l_1 + \frac{l_2}{2}\right)(\hat{\boldsymbol{\xi}}_A)_{13}^2 + \left(l_1 + \frac{l_3}{2}\right)(\hat{\boldsymbol{\xi}}_A)_{23}^2 \quad . \tag{3.160}$$

The latter implies $\chi \geq 0$ provided $l_1 + \frac{l_2}{2} + \frac{l_3}{2} \geq 0$, $l_1 + \frac{l_2}{2} \geq 0$ and $l_1 + \frac{l_3}{2} \geq 0$. After inserting (3.156) in (3.109),

$$\hat{\boldsymbol{\Omega}}^{(k)} = \hat{\boldsymbol{\Omega}}^{(e)} - \dot{s}\left\{l_1\hat{\boldsymbol{\xi}}_A + \frac{l_2}{2}(\hat{\boldsymbol{\xi}}_A\hat{\mathbf{M}}_1^{(k)} + \hat{\mathbf{M}}_1^{(k)}\hat{\boldsymbol{\xi}}_A) + \frac{l_3}{2}(\hat{\boldsymbol{\xi}}_A\hat{\mathbf{M}}_2^{(k)} + \hat{\mathbf{M}}_2^{(k)}\hat{\boldsymbol{\xi}}_A)\right\} \quad . \tag{3.161}$$

With respect to the actual configuration, (3.161) takes the form (cf. (3.122)):

$$\boldsymbol{\Omega}^{(k)} = \boldsymbol{\Omega}^{(e)} - \dot{s}\mathbf{R}_e\left\{l_1\hat{\boldsymbol{\xi}}_A + \frac{l_2}{2}(\hat{\boldsymbol{\xi}}_A\hat{\mathbf{M}}_1^{(k)} + \hat{\mathbf{M}}_1^{(k)}\hat{\boldsymbol{\xi}}_A) + \frac{l_3}{2}(\hat{\boldsymbol{\xi}}_A\hat{\mathbf{M}}_2^{(k)} + \hat{\mathbf{M}}_2^{(k)}\hat{\boldsymbol{\xi}}_A)\right\}\mathbf{R}_e^T \quad . \tag{3.162}$$

It is assumed that, in view of (3.68),

$$\mathbf{R}_e\hat{\boldsymbol{\xi}}_A\mathbf{R}_e^T = \mathbf{V}_e\mathbf{Y}\mathbf{Z}\mathbf{V}_e^{-1} - \mathbf{V}_e^{-1}\mathbf{Z}\mathbf{Y}\mathbf{V}_e \quad , \tag{3.163}$$

so that (cf. Eqs. $(3.113)_3$, (3.122))

$$\boldsymbol{\Omega}^{(k)} = \boldsymbol{\Omega}^{(e)} - \dot{s}\mathbf{N}_A^{(k)} \quad , \tag{3.164}$$

with

$$\begin{aligned}\mathbf{N}_A^{(k)} := {} & l_1(\mathbf{V}_e\mathbf{Y}\mathbf{Z}\mathbf{V}_e^{-1} - \mathbf{V}_e^{-1}\mathbf{Z}\mathbf{Y}\mathbf{V}_e) \\ & + \frac{l_2}{2}\{(\mathbf{V}_e\mathbf{Y}\mathbf{Z}\mathbf{V}_e^{-1} - \mathbf{V}_e^{-1}\mathbf{Z}\mathbf{Y}\mathbf{V}_e)\mathbf{M}_1^{(k)} + \mathbf{M}_1^{(k)}(\mathbf{V}_e\mathbf{Y}\mathbf{Z}\mathbf{V}_e^{-1} - \mathbf{V}_e^{-1}\mathbf{Z}\mathbf{Y}\mathbf{V}_e)\} \\ & + \frac{l_3}{2}\{(\mathbf{V}_e\mathbf{Y}\mathbf{Z}\mathbf{V}_e^{-1} - \mathbf{V}_e^{-1}\mathbf{Z}\mathbf{Y}\mathbf{V}_e)\mathbf{M}_2^{(k)} + \mathbf{M}_2^{(k)}(\mathbf{V}_e\mathbf{Y}\mathbf{Z}\mathbf{V}_e^{-1} - \mathbf{V}_e^{-1}\mathbf{Z}\mathbf{Y}\mathbf{V}_e)\} \quad .\end{aligned} \tag{3.165}$$

3.6.4 Yield function – flow rule

The rotation $\mathbf{\Pi}$ in $(3.72)_1$ can be replaced by the structural tensors $\hat{\mathbf{M}}_1^{(y)}$ and $\hat{\mathbf{M}}_2^{(y)}$, using similar arguments as in Sect. 3.6.2. Further, $\hat{\mathbf{P}}$ and $\hat{\boldsymbol{\xi}}$ is assumed to enter into the yield function in terms of a effective stress $\hat{\boldsymbol{\sigma}}$,

$$\hat{\boldsymbol{\sigma}} := (\hat{\mathbf{P}} - \hat{\boldsymbol{\xi}})^D \quad . \tag{3.166}$$

Thus, from $(3.72)_1$ (cf. ARAVAS [4])

$$f = \overline{\overline{f}}(\hat{\mathbf{P}}, \hat{\boldsymbol{\xi}}, \mathbf{\Pi}) = \hat{f}(\hat{\boldsymbol{\sigma}}_S, \hat{\boldsymbol{\sigma}}_A, \hat{\mathbf{M}}_1^{(y)}, \hat{\mathbf{M}}_2^{(y)}) \tag{3.167}$$

where

$$\hat{\boldsymbol{\sigma}}_S = (\hat{\mathbf{P}}_S - \hat{\boldsymbol{\xi}}_S)^D \quad , \quad \hat{\boldsymbol{\sigma}}_A = \hat{\mathbf{P}}_A - \hat{\boldsymbol{\xi}}_A \tag{3.168}$$

denote the symmetric and skew-symmetric part of the effecive stress $\hat{\boldsymbol{\sigma}}$, respectively. In the ensuing analysis, the yield function is assumed to be quadratic in the stresses. Then, on applying the representation theorems for isotropic tensor functions (see SPENCER [95]),

$$\begin{aligned} f &= \hat{f}(\hat{\boldsymbol{\sigma}}_S, \hat{\boldsymbol{\sigma}}_A, \hat{\mathbf{M}}_1^{(y)}, \hat{\mathbf{M}}_2^{(y)}) \\ &= \{v_1 \operatorname{tr} \hat{\boldsymbol{\sigma}}_S^2 + v_2 \operatorname{tr}(\hat{\boldsymbol{\sigma}}_S \hat{\mathbf{M}}_1^{(y)} \hat{\boldsymbol{\sigma}}_S) + v_3 \operatorname{tr}(\hat{\boldsymbol{\sigma}}_S \hat{\mathbf{M}}_2^{(y)} \hat{\boldsymbol{\sigma}}_S) \\ &+ v_4 (\operatorname{tr}(\hat{\boldsymbol{\sigma}}_S \hat{\mathbf{M}}_1^{(y)}))^2 + v_5 (\operatorname{tr}(\hat{\boldsymbol{\sigma}}_S \hat{\mathbf{M}}_2^{(y)}))^2 + v_6 \operatorname{tr}(\hat{\boldsymbol{\sigma}}_S \hat{\mathbf{M}}_1^{(y)}) \operatorname{tr}(\hat{\boldsymbol{\sigma}}_S \hat{\mathbf{M}}_2^{(y)}) \\ &+ v_7 \operatorname{tr} \hat{\boldsymbol{\sigma}}_A^2 + v_8 \operatorname{tr}(\hat{\boldsymbol{\sigma}}_A \hat{\mathbf{M}}_1^{(y)} \hat{\boldsymbol{\sigma}}_A) + v_9 \operatorname{tr}(\hat{\boldsymbol{\sigma}}_A \hat{\mathbf{M}}_2^{(y)} \hat{\boldsymbol{\sigma}}_A) \\ &+ v_{10} \operatorname{tr}(\hat{\boldsymbol{\sigma}}_A \hat{\mathbf{M}}_1^{(y)} \hat{\boldsymbol{\sigma}}_S) + v_{11} \operatorname{tr}(\hat{\boldsymbol{\sigma}}_A \hat{\mathbf{M}}_2^{(y)} \hat{\boldsymbol{\sigma}}_S) + v_{12} \operatorname{tr}(\hat{\boldsymbol{\sigma}}_A \hat{\mathbf{M}}_1^{(y)} \hat{\boldsymbol{\sigma}}_S \hat{\mathbf{M}}_2^{(y)})\}^{\frac{1}{2}} - k_0 \\ &=: \sqrt{\hat{\boldsymbol{\sigma}} \cdot \hat{\boldsymbol{\mathcal{K}}}[\hat{\boldsymbol{\sigma}}]} - k_0 \quad , \end{aligned} \tag{3.169}$$

where k_0, v_i, $i = 1, \ldots, 12$ are material parameters. With respect to an orthonormal basis system $\{\mathbf{e}_i\}$, $i = 1, 2, 3$ with $\mathbf{e}_1 = \hat{\mathbf{m}}_1^{(y)}$ and $\mathbf{e}_2 = \hat{\mathbf{m}}_2^{(y)}$, (3.169) takes the form

$$f = \sqrt{\hat{\sigma}_m \hat{\mathcal{K}}_{mn} \hat{\sigma}_n} - k_0 \tag{3.170}$$

with

$$\hat{\sigma}_{ij} \to \hat{\sigma}_m \hat{=} \begin{pmatrix} \hat{\sigma}_{11} \\ \hat{\sigma}_{12} \\ \hat{\sigma}_{13} \\ \hat{\sigma}_{21} \\ \hat{\sigma}_{22} \\ \hat{\sigma}_{23} \\ \hat{\sigma}_{31} \\ \hat{\sigma}_{32} \\ \hat{\sigma}_{33} \end{pmatrix} \quad , \tag{3.171}$$

and keeping in mind that the effective stress tensor is a deviator,

$$\hat{\mathcal{K}}_{ijkl} \to \hat{\mathcal{K}}_{mn} \quad \hat{=} \begin{pmatrix} K_{1111} & 0 & 0 & 0 & K_{1122} & 0 & 0 & 0 & K_{1133} \\ 0 & K_{1212} & 0 & K_{1221} & 0 & 0 & 0 & 0 & 0 \\ 0 & 0 & K_{1313} & 0 & 0 & 0 & K_{1331} & 0 & 0 \\ 0 & K_{1221} & 0 & K_{2121} & 0 & 0 & 0 & 0 & 0 \\ K_{1122} & 0 & 0 & 0 & K_{2222} & 0 & 0 & 0 & K_{2233} \\ 0 & 0 & 0 & 0 & 0 & K_{2323} & 0 & K_{2332} & 0 \\ 0 & 0 & K_{1331} & 0 & 0 & 0 & K_{3131} & 0 & 0 \\ 0 & 0 & 0 & 0 & 0 & K_{2332} & 0 & K_{3232} & 0 \\ K_{1133} & 0 & 0 & 0 & K_{2233} & 0 & 0 & 0 & K_{3333} \end{pmatrix} \quad , \tag{3.172}$$

where

$$K_{1212} = \frac{1}{2}v_1 + \frac{1}{4}v_2 + \frac{1}{4}v_3 - \frac{1}{2}v_7 - \frac{1}{4}v_8 - \frac{1}{4}v_9 - \frac{1}{4}v_{10} + \frac{1}{4}v_{11} - \frac{1}{4}v_{12} \quad , \tag{3.173}$$

$$K_{1221} = 2v_1 + v_2 + v_3 + 2v_7 + v_8 + v_9 \quad , \tag{3.174}$$

$$K_{1313} = \frac{1}{2}v_1 + \frac{1}{4}v_2 - \frac{1}{2}v_7 - \frac{1}{4}v_8 - \frac{1}{4}v_{10} \quad , \tag{3.175}$$

$$K_{1331} = 2v_1 + v_2 + 2v_7 + v_8 \quad , \tag{3.176}$$

$$K_{2121} = \frac{1}{2}v_1 + \frac{1}{4}v_2 + \frac{1}{4}v_3 - \frac{1}{2}v_7 - \frac{1}{4}v_8 - \frac{1}{4}v_9 + \frac{1}{4}v_{10} - \frac{1}{4}v_{11} + \frac{1}{4}v_{12} \quad , \tag{3.177}$$

$$K_{2323} = \frac{1}{2}v_1 + \frac{1}{4}v_3 - \frac{1}{2}v_7 - \frac{1}{4}v_9 - \frac{1}{4}v_{11} \quad , \tag{3.178}$$

$$K_{2332} = 2v_1 + v_3 + 2v_7 + v_9 \quad , \tag{3.179}$$

$$K_{3131} = \frac{1}{2}v_1 + \frac{1}{4}v_2 - \frac{1}{2}v_7 - \frac{1}{4}v_8 + \frac{1}{4}v_{10} \quad , \tag{3.180}$$

$$K_{3232} = \frac{1}{2}v_1 + \frac{1}{4}v_3 - \frac{1}{2}v_7 - \frac{1}{4}v_9 + \frac{1}{4}v_{11} \quad , \tag{3.181}$$

$$\begin{aligned} &4K_{1111} - 4K_{1122} - 4K_{1133} + K_{2222} + 2K_{2233} + K_{3333} \\ &\quad = 6v_1 + 4v_2 + v_3 + 4v_4 + v_5 - 2v_6 \quad , \end{aligned} \tag{3.182}$$

$$\begin{aligned} &-4K_{1111} + 10K_{1122} - 2K_{1133} - 4K_{2222} - 2K_{2233} + 2K_{3333} \\ &\quad = -6v_1 - 4v_2 - 4v_3 - 4v_4 - 4v_5 + 5v_6 \quad , \end{aligned} \tag{3.183}$$

$$\begin{aligned} &-4K_{1111} - 2K_{1122} + 10K_{1133} + 2K_{2222} - 2K_{2233} - 4K_{3333} \\ &\quad = -6v_1 - 4v_2 + 2v_3 - 4v_4 + 2v_5 - v_6 \quad , \end{aligned} \tag{3.184}$$

$$\begin{aligned} &K_{1111} - 4K_{1122} + 2K_{1133} + 4K_{2222} - 4K_{2233} + K_{3333} \\ &\quad = 6v_1 + v_2 + 4v_3 + v_4 + 4v_5 - 2v_6 \quad , \end{aligned} \tag{3.185}$$

$$\begin{aligned} &2K_{1111} - 2K_{1122} - 2K_{1133} - 4K_{2222} + 10K_{2233} - 4K_{3333} \\ &\quad = -6v_1 + 2v_2 - 4v_3 + 2v_4 - 4v_5 - v_6 \quad , \end{aligned} \tag{3.186}$$

$$\begin{aligned} &K_{1111} + 2K_{1122} - 4K_{1133} + K_{2222} - 4K_{2233} + 4K_{3333} \\ &\quad = 6v_1 + v_2 + v_3 + v_4 + v_5 + v_6 \quad . \end{aligned} \tag{3.187}$$

For given $v_1, \ldots, v_{12}$ this is an inhomogeneous linear system consisting of 15 equations with 15 unknowns $K_{1111}, \ldots, K_{3333}$. From (3.182)-(3.187), it can be seen that the rank of the coefficient matrix $\mathbf{K}$ and the augmented matrix $\mathbf{KV}$ are equal, so that this system has solutions.

$$(\mathbf{K}) := \begin{pmatrix} 4 & -4 & -4 & 1 & 2 & 1 \\ -4 & 10 & -2 & -4 & -2 & 2 \\ -4 & -2 & 10 & 2 & -2 & -4 \\ 1 & -4 & 2 & 4 & -4 & 1 \\ 2 & -2 & -2 & -4 & 10 & -4 \\ 1 & 2 & -4 & 1 & -4 & 4 \end{pmatrix} \hat{=} \begin{pmatrix} 1 & 0 & -2 & 0 & 0 & 1 \\ 0 & 1 & -1 & 0 & -1 & 1 \\ 0 & 0 & 0 & 1 & -2 & 1 \\ 0 & 0 & 0 & 0 & 0 & 0 \\ 0 & 0 & 0 & 0 & 0 & 0 \\ 0 & 0 & 0 & 0 & 0 & 0 \end{pmatrix} \tag{3.188}$$

$$(\mathbf{KV}) := \begin{pmatrix} 4 & -4 & -4 & 1 & 2 & 1 & 6v_1 + 4v_2 + v_3 + 4v_4 + v_5 - 2v_6 \\ -4 & 10 & -2 & -4 & -2 & 2 & -6v_1 - 4v_2 - 4v_3 - 4v_4 - 4v_5 + 5v_6 \\ -4 & -2 & 10 & 2 & -2 & -4 & -6v_1 - 4v_2 + 2v_3 - 4v_4 + 2v_5 - v_6 \\ 1 & -4 & 2 & 4 & -4 & 1 & 6v_1 + v_2 + 4v_3 + v_4 + 4v_5 - 2v_6 \\ 2 & -2 & -2 & -4 & 10 & -4 & -6v_1 + 2v_2 - 4v_3 + 2v_4 - 4v_5 - v_6 \\ 1 & 2 & -4 & 1 & -4 & 4 & 6v_1 + v_2 + v_3 + v_4 + v_5 + v_6 \end{pmatrix}$$

$$\hat{=} \begin{pmatrix} 1 & 0 & -2 & 0 & 0 & 1 & 2v_1 + v_2 + v_4 \\ 0 & 1 & -1 & 0 & -1 & 1 & v_1 + \frac{1}{2}v_6 \\ 0 & 0 & 0 & 1 & -2 & 1 & 2v_1 + v_3 + v_5 \\ 0 & 0 & 0 & 0 & 0 & 0 & 0 \\ 0 & 0 & 0 & 0 & 0 & 0 & 0 \\ 0 & 0 & 0 & 0 & 0 & 0 & 0 \end{pmatrix} \tag{3.189}$$

However, since the rank is 3, three out of the six equations are linear dependent and (3.182)-(3.187) reduce to

$$K_{1111} - 2K_{1133} + K_{3333} = 2v_1 + v_2 + v_4 \quad , \tag{3.190}$$

$$K_{1122} - K_{1133} - K_{2233} + K_{3333} = v_1 + \frac{1}{2}v_6 \quad , \tag{3.191}$$

$$K_{2222} - 2K_{2233} + K_{3333} = 2v_1 + v_3 + v_5 \quad . \tag{3.192}$$

Therefore three of the coefficients K_{1111}, K_{1122}, K_{1133}, K_{2222}, K_{2233} and K_{3333} can be chosen freely and the remaining coefficients will be determined by solving (3.173)-(3.181), (3.190)-(3.192). On the other hand, if $\hat{\mathcal{K}}_{mn}$ are given, then $v_1, \ldots, v_{12}$ may be determined uniquely by solving (3.173)-(3.181), (3.190)-(3.192). In order to ensure the convexity properties the yield function f has to satisfy, it must be noted that the level set $\{\hat{\sigma}_m | \sqrt{\hat{\sigma}_m \hat{\mathcal{K}}_{mn} \hat{\sigma}_n} \leq k_0\}$ is identical to the level set $\{\hat{\sigma}_m | \hat{\sigma}_m \hat{\mathcal{K}}_{mn} \hat{\sigma}_n \leq k_0^2\}$. The later represents a convex set if the matrix $\hat{\mathcal{K}}_{mn}$ is positive semi-definite. By using some standard algebraic solver it can be proven that the

eigenvalues of $\hat{\mathcal{K}}_{mn}$ are nonnegative provided the following inequalities hold:

$$0 \leq v_1 + v_2 + v_4 - \frac{1}{2}v_6 \quad , \tag{3.193}$$

$$0 \leq v_1 + v_3 + v_5 - \frac{1}{2}v_6 \quad , \tag{3.194}$$

$$0 \leq v_1 + \frac{1}{2}v_6 \quad , \tag{3.195}$$

$$\begin{aligned} 0 \leq{}& \frac{1}{2}v_1 + \frac{1}{4}v_2 + \frac{1}{4}v_3 - \frac{1}{2}v_7 - \frac{1}{4}v_8 - \frac{1}{4}v_9 \\ &+ \frac{1}{4}\{v_{10}^2 + v_{11}^2 + v_{12}^2 + 2(-v_{10}v_{11} + v_{10}v_{12} - v_{11}v_{12}) + 16(v_2^2 + v_3^2 + v_8^2 + v_9^2) \\ &+ 32(v_8v_9 + v_2v_3 + v_2v_8 + v_2v_9 + v_3v_8 + v_3v_9) + 128v_1v_7 \\ &+ 64(v_1^2 + v_1v_2 + v_1v_3 + v_1v_8 + v_1v_9 + v_2v_7 + v_3v_7 + v_7^2 + v_7v_8 + v_7v_9)\}^{\frac{1}{2}} \quad , \end{aligned} \tag{3.196}$$

$$\begin{aligned} 0 \leq{}& \frac{1}{2}v_1 + \frac{1}{4}v_3 - \frac{1}{2}v_7 - \frac{1}{4}v_9 + \frac{1}{4}\{v_{11}^2 + 16(v_3^2 + v_9^2) + 32v_3v_9 \\ &+ 64(v_1^2 + v_1v_3 + v_1v_9 + v_3v_7 + v_7^2 + v_7v_9) + 128v_1v_7\}^{\frac{1}{2}} \quad , \end{aligned} \tag{3.197}$$

$$\begin{aligned} 0 \leq{}& \frac{1}{2}v_1 + \frac{1}{4}v_2 - \frac{1}{2}v_7 - \frac{1}{4}v_8 + \frac{1}{4}\{v_{10}^2 + 16(v_2^2 + v_8^2) + 32v_2v_8 \\ &+ 64(v_1^2 + v_1v_2 + v_1v_8 + v_2v_7 + v_7^2 + v_7v_8) + 128v_1v_7\}^{\frac{1}{2}} \quad . \end{aligned} \tag{3.198}$$

The flow rule (3.60) and (3.61) can be rewritten as

$$\hat{\mathbf{D}}_p = \frac{\dot{s}}{\zeta}\frac{\partial \hat{f}}{\partial \hat{\mathbf{P}}_S} \quad , \quad \hat{\boldsymbol{\Omega}}^{(e)} = \frac{\dot{s}}{\zeta}\frac{\partial \hat{f}}{\partial \hat{\mathbf{P}}_A} \quad , \tag{3.199}$$

with

$$\zeta = \sqrt{\frac{2}{3}}\left\|\frac{\partial \overline{\overline{f}}}{\partial \hat{\mathbf{P}}}\right\| \quad , \tag{3.200}$$

and

$$\begin{aligned} \frac{\partial \hat{f}}{\partial \hat{\mathbf{P}}_S} = \frac{1}{2(f+k_0)}\Big\{& 2v_1\hat{\boldsymbol{\sigma}}_S + v_2(\hat{\boldsymbol{\sigma}}_S\hat{\mathbf{M}}_1^{(y)} + \hat{\mathbf{M}}_1^{(y)}\hat{\boldsymbol{\sigma}}_S) + v_3(\hat{\boldsymbol{\sigma}}_S\hat{\mathbf{M}}_2^{(y)} + \hat{\mathbf{M}}_2^{(y)}\hat{\boldsymbol{\sigma}}_S) \\ &+ \frac{1}{2}v_{10}\left(\hat{\boldsymbol{\sigma}}_A\hat{\mathbf{M}}_1^{(y)} - \hat{\mathbf{M}}_1^{(y)}\hat{\boldsymbol{\sigma}}_A\right) + \frac{1}{2}v_{11}\left(\hat{\boldsymbol{\sigma}}_A\hat{\mathbf{M}}_2^{(y)} - \hat{\mathbf{M}}_2^{(y)}\hat{\boldsymbol{\sigma}}_A\right) \\ &+ \frac{1}{2}v_{12}\left(\hat{\mathbf{M}}_2^{(y)}\hat{\boldsymbol{\sigma}}_A\hat{\mathbf{M}}_1^{(y)} - \hat{\mathbf{M}}_1^{(y)}\hat{\boldsymbol{\sigma}}_A\hat{\mathbf{M}}_2^{(y)}\right) \\ &- \frac{1}{3}\left[(2v_2 + 2v_4 + v_6)\,\mathrm{tr}(\hat{\mathbf{M}}_1^{(y)}\hat{\boldsymbol{\sigma}}_S)(2v_3 + 2v_5 + v_6)\,\mathrm{tr}(\hat{\mathbf{M}}_2^{(y)}\hat{\boldsymbol{\sigma}}_S)\right]\mathbf{1} \\ &+ \frac{1}{3}\left[2v_4\,\mathrm{tr}(\hat{\mathbf{M}}_1^{(y)}\hat{\boldsymbol{\sigma}}_S) + v_6\,\mathrm{tr}(\hat{\mathbf{M}}_2^{(y)}\hat{\boldsymbol{\sigma}}_S)\right]\hat{\mathbf{M}}_1^{(y)} \\ &+ \frac{1}{3}\left[2v_5\,\mathrm{tr}(\hat{\mathbf{M}}_2^{(y)}\hat{\boldsymbol{\sigma}}_S) + v_6\,\mathrm{tr}(\hat{\mathbf{M}}_1^{(y)}\hat{\boldsymbol{\sigma}}_S)\right]\hat{\mathbf{M}}_2^{(y)}\Big\} \quad , \end{aligned} \tag{3.201}$$

$$\begin{aligned} \frac{\partial \hat{f}}{\partial \hat{\mathbf{P}}_A} = \frac{1}{2(f+k_0)}\Big\{& -2v_7\hat{\boldsymbol{\sigma}}_A - v_8(\hat{\boldsymbol{\sigma}}_A\hat{\mathbf{M}}_1^{(y)} + \hat{\mathbf{M}}_1^{(y)}\hat{\boldsymbol{\sigma}}_A) - v_9(\hat{\boldsymbol{\sigma}}_A\hat{\mathbf{M}}_2^{(y)} + \hat{\mathbf{M}}_2^{(y)}\hat{\boldsymbol{\sigma}}_A) \\ &+ \frac{1}{2}v_{10}(\hat{\boldsymbol{\sigma}}_S\hat{\mathbf{M}}_1^{(y)} - \hat{\mathbf{M}}_1^{(y)}\hat{\boldsymbol{\sigma}}_S) + \frac{1}{2}v_{11}(\hat{\boldsymbol{\sigma}}_S\hat{\mathbf{M}}_2^{(y)} - \hat{\mathbf{M}}_2^{(y)}\hat{\boldsymbol{\sigma}}_S) \\ &+ \frac{1}{2}v_{12}(\hat{\mathbf{M}}_2^{(y)}\hat{\boldsymbol{\sigma}}_S\hat{\mathbf{M}}_1^{(y)} - \hat{\mathbf{M}}_1^{(y)}\hat{\boldsymbol{\sigma}}_S\hat{\mathbf{M}}_2^{(y)})\Big\} \quad . \end{aligned} \tag{3.202}$$

In order to rewrite the yield function with respect to the actual configuration the effective stress tensor $\boldsymbol{\sigma}$ and its symmetric and skew-symmetric parts, $\boldsymbol{\sigma}_S$, $\boldsymbol{\sigma}_A$, respectively, are defined by

$$\boldsymbol{\sigma} := \mathbf{R}_e \hat{\boldsymbol{\sigma}} \mathbf{R}_e^T \quad , \quad \boldsymbol{\sigma}_S = \mathbf{R}_e \hat{\boldsymbol{\sigma}}_S \mathbf{R}_e^T \quad , \quad \boldsymbol{\sigma}_A = \mathbf{R}_e \hat{\boldsymbol{\sigma}}_A \mathbf{R}_e^T \quad . \tag{3.203}$$

Using (3.66), (3.135), (3.138), (3.143), (3.144) and (3.166)

$$\boldsymbol{\sigma} = \mathbf{R}_e (\hat{\mathbf{P}} - \hat{\boldsymbol{\xi}})^D \mathbf{R}_e^T = \{\mathbf{V}_e^{-1}(\mathbf{S} - \mathbf{Z})\mathbf{V}_e^{-1} + 2\mathbf{V}_e(\mathbf{A}_e\mathbf{S} - \mathbf{Y}\mathbf{Z})\mathbf{V}_e^{-1}\}^D \quad . \tag{3.204}$$

As a consequence of $(3.113)_3$, $(3.203)_2$ and $(3.203)_3$, the yield function (3.169) can be rewritten in the actual configuration as follows:

$$\begin{aligned} f = \{ & v_1 \operatorname{tr} \boldsymbol{\sigma}_S^2 + v_2 \operatorname{tr}(\boldsymbol{\sigma}_S \mathbf{M}_1^{(y)} \boldsymbol{\sigma}_S) + v_3 \operatorname{tr}(\boldsymbol{\sigma}_S \mathbf{M}_2^{(y)} \boldsymbol{\sigma}_S) \\ & + v_4 (\operatorname{tr}(\boldsymbol{\sigma}_S \mathbf{M}_1^{(y)}))^2 + v_5 (\operatorname{tr}(\boldsymbol{\sigma}_S \mathbf{M}_2^{(y)}))^2 + v_6 \operatorname{tr}(\boldsymbol{\sigma}_S \mathbf{M}_1^{(y)}) \operatorname{tr}(\boldsymbol{\sigma}_S \mathbf{M}_2^{(y)}) \\ & + v_7 \operatorname{tr} \boldsymbol{\sigma}_A^2 + v_8 \operatorname{tr}(\boldsymbol{\sigma}_A \mathbf{M}_1^{(y)} \boldsymbol{\sigma}_A) + v_9 \operatorname{tr}(\boldsymbol{\sigma}_A \mathbf{M}_2^{(y)} \boldsymbol{\sigma}_A) \\ & + v_{10} \operatorname{tr}(\boldsymbol{\sigma}_A \mathbf{M}_1^{(y)} \boldsymbol{\sigma}_S) + v_{11} \operatorname{tr}(\boldsymbol{\sigma}_A \mathbf{M}_2^{(y)} \boldsymbol{\sigma}_S) + v_{12} \operatorname{tr}(\boldsymbol{\sigma}_A \mathbf{M}_1^{(y)} \boldsymbol{\sigma}_S \mathbf{M}_2^{(y)}) \}^{\frac{1}{2}} - k_0 \\ =: & \sqrt{\boldsymbol{\sigma} \cdot \boldsymbol{\mathcal{K}}[\boldsymbol{\sigma}]} - k_0 \quad . \end{aligned} \tag{3.205}$$

In a similar fashion it can be shown, by using among others (3.122), (3.147) and (3.200), that an EULERIAN format of $(3.199)_{1,2}$ could be

$$\overset{\triangle}{\mathbf{A}}_p = \frac{\dot{s}}{\zeta} \mathbf{N}_S^{(y)} \quad , \tag{3.206}$$

$$\boldsymbol{\Omega}^{(e)} = \frac{\dot{s}}{\zeta} \mathbf{N}_A^{(y)} \quad , \tag{3.207}$$

with

$$\begin{aligned} \mathbf{N}_S^{(y)} := & \mathbf{F}_e^{T-1} \frac{\partial \hat{f}}{\partial \hat{\mathbf{P}}_S} \mathbf{F}_e^{-1} \\ = & \frac{1}{2(f + k_0)} \mathbf{V}_e^{-1} \Big\{ 2v_1 \boldsymbol{\sigma}_S + v_2 (\boldsymbol{\sigma}_S \mathbf{M}_1^{(y)} + \mathbf{M}_1^{(y)} \boldsymbol{\sigma}_S) + v_3 (\boldsymbol{\sigma}_S \mathbf{M}_2^{(y)} + \mathbf{M}_2^{(y)} \boldsymbol{\sigma}_S) \\ & + \frac{1}{2} v_{10} \left(\boldsymbol{\sigma}_A \mathbf{M}_1^{(y)} - \mathbf{M}_1^{(y)} \boldsymbol{\sigma}_A \right) + \frac{1}{2} v_{11} \left(\boldsymbol{\sigma}_A \mathbf{M}_2^{(y)} - \mathbf{M}_2^{(y)} \boldsymbol{\sigma}_A \right) \\ & + \frac{1}{2} v_{12} \left(\mathbf{M}_2^{(y)} \boldsymbol{\sigma}_A \mathbf{M}_1^{(y)} - \mathbf{M}_1^{(y)} \boldsymbol{\sigma}_A \mathbf{M}_2^{(y)} \right) \\ & - \frac{1}{3} \Big[(2v_2 + 2v_4 + v_6) \operatorname{tr}(\mathbf{M}_1^{(y)} \boldsymbol{\sigma}_S) (2v_3 + 2v_5 + v_6) \operatorname{tr}(\mathbf{M}_2^{(y)} \boldsymbol{\sigma}_S) \Big] \mathbf{1} \\ & + \frac{1}{3} \Big[2v_4 \operatorname{tr}(\mathbf{M}_1^{(y)} \boldsymbol{\sigma}_S) + v_6 \operatorname{tr}(\mathbf{M}_2^{(y)} \boldsymbol{\sigma}_S) \Big] \mathbf{M}_1^{(y)} \\ & + \frac{1}{3} \Big[2v_5 \operatorname{tr}(\mathbf{M}_2^{(y)} \boldsymbol{\sigma}_S) + v_6 \operatorname{tr}(\mathbf{M}_1^{(y)} \boldsymbol{\sigma}_S) \Big] \mathbf{M}_2^{(y)} \Big\} \mathbf{V}_e^{-1} \quad , \end{aligned} \tag{3.208}$$

$$\begin{aligned} \mathbf{N}_A^{(y)} := & \mathbf{R}_e \frac{\partial \hat{f}}{\partial \hat{\mathbf{P}}_A} \mathbf{R}_e^T \\ = & \frac{1}{2(f + k_0)} \Big\{ - 2v_7 \boldsymbol{\sigma}_A - v_8 (\boldsymbol{\sigma}_A \mathbf{M}_1^{(y)} + \mathbf{M}_1^{(y)} \boldsymbol{\sigma}_A) - v_9 (\boldsymbol{\sigma}_A \mathbf{M}_2^{(y)} + \mathbf{M}_2^{(y)} \boldsymbol{\sigma}_A) \\ & + \frac{1}{2} v_{10} (\boldsymbol{\sigma}_S \mathbf{M}_1^{(y)} - \mathbf{M}_1^{(y)} \boldsymbol{\sigma}_S) + \frac{1}{2} v_{11} (\boldsymbol{\sigma}_S \mathbf{M}_2^{(y)} - \mathbf{M}_2^{(y)} \boldsymbol{\sigma}_S) \\ & + \frac{1}{2} v_{12} (\mathbf{M}_2^{(y)} \boldsymbol{\sigma}_S \mathbf{M}_1^{(y)} - \mathbf{M}_1^{(y)} \boldsymbol{\sigma}_S \mathbf{M}_2^{(y)}) \Big\} \quad , \end{aligned} \tag{3.209}$$

and

$$\zeta = \sqrt{\frac{2}{3}\left(\frac{\partial \hat{f}}{\partial \hat{\mathbf{P}}_S} \cdot \frac{\partial \hat{f}}{\partial \hat{\mathbf{P}}_S} + \frac{\partial \hat{f}}{\partial \hat{\mathbf{P}}_A} \cdot \frac{\partial \hat{f}}{\partial \hat{\mathbf{P}}_A}\right)} = \sqrt{\frac{2}{3}(\mathbf{V}_e^2 \mathbf{N}_S^{(y)} \mathbf{V}_e^2 \cdot \mathbf{N}_S^{(y)} + \mathbf{N}_A^{(y)} \cdot \mathbf{N}_A^{(y)})} \quad . \tag{3.210}$$

It remains to specify the evolution of $\mathbf{M}_1^{(y)}$ and $\mathbf{M}_2^{(y)}$, or, which is the same (cf. (3.122)), the equation governing the response of $\mathbf{\Omega}^{(y)}$. However, since no experimental evidence is available yet, the following ansatz will be used:

$$\mathbf{\Omega}^{(y)} = \mathbf{\Omega}^{(e)} \quad . \tag{3.211}$$

3.7 Constitutive model for cubic anisotropy

In this section a constitutive model exhibiting cubic symmetry is proposed, which has been derived from the constitutive model for viscoplasticity with kinematic hardening for orthotropic materials, introduced above. Cubic symmetry represents a special case of orthotropic symmetry, with three orthogonal planes of symmetry and additionally three extra axes of symmetry which can be taken as rotations through 90° about the X_1, X_2 and X_3 axis of orthotropy, respectively (cf. Billington and Tate [11]). A fourth-order tensor $\boldsymbol{\mathcal{K}}$ then must be invariant under the transformations

$$\mathbf{P}_1 := \begin{pmatrix} 1 & 0 & 0 \\ 0 & 0 & 1 \\ 0 & -1 & 0 \end{pmatrix} \quad , \quad \mathbf{P}_2 := \begin{pmatrix} 0 & 0 & 1 \\ 0 & 1 & 0 \\ -1 & 0 & 0 \end{pmatrix} \quad , \quad \mathbf{P}_3 := \begin{pmatrix} 0 & 1 & 0 \\ -1 & 0 & 0 \\ 0 & 0 & 1 \end{pmatrix} \quad . \tag{3.212}$$

All relations of the previous section still hold, with additional restrictions outlined in the following.

3.7.1 Elasticity law for cubic anisotropy

The components $(\hat{\mathcal{C}}^{(e)})_{ij}$ of the tensor $\hat{\boldsymbol{\mathcal{C}}}^{(e)}$ in the elasticity law for cubic anisotropy are given by (cf. Billington and Tate [11])

$$(\hat{\mathcal{C}}^{(e)})_{ij} \hat{=} \begin{pmatrix} c_{11} & c_{12} & c_{12} & 0 & 0 & 0 \\ c_{12} & c_{11} & c_{12} & 0 & 0 & 0 \\ c_{12} & c_{12} & c_{11} & 0 & 0 & 0 \\ 0 & 0 & 0 & c_{44} & 0 & 0 \\ 0 & 0 & 0 & 0 & c_{44} & 0 \\ 0 & 0 & 0 & 0 & 0 & c_{44} \end{pmatrix} \quad , \tag{3.213}$$

where $c_{11} = c_{22} = c_{33}$, $c_{12} = c_{13} = c_{23}$, $c_{44} = c_{55} = c_{66}$ and the three remaining independent constants are (cf. (3.134))

$$\begin{aligned} c_{11} &= 2(\alpha_1 + \alpha_2 + \alpha_4 + \alpha_5 + \alpha_7) = 2(\alpha_1 + \alpha_3 + \alpha_4 + \alpha_6 + \alpha_8) = 2(\alpha_1 + \alpha_4) \quad , \\ c_{12} &= 2\alpha_4 + \alpha_7 + \alpha_8 + \alpha_9 = 2\alpha_4 + \alpha_7 = 2\alpha_4 + \alpha_8 \quad , \\ c_{44} &= 2\alpha_1 + \alpha_2 + \alpha_3 = 2\alpha_1 + \alpha_2 = 2\alpha_1 + \alpha_3 \quad . \end{aligned} \tag{3.214}$$

Resolving $(3.214)_{1-3}$ leads to the additional relations

$$\alpha_2 = \alpha_3 = 0 \quad , \quad \alpha_5 = \alpha_6 = -\alpha_7 = -\alpha_8 = \alpha_9 \quad , \tag{3.215}$$

with α_1, α_4 and α_9 being the three independent material parameters for cubic anisotropy. Then (3.138) can be rewritten as

$$\begin{aligned}\mathbf{S} &= 2\alpha_1(\mathbf{V}_e^2\mathbf{A}_e\mathbf{V}_e^2)\\ &+ \{2\alpha_4\,\mathrm{tr}(\mathbf{V}_e^2\mathbf{A}_e) - \alpha_9\,\mathrm{tr}(\mathbf{V}_e\mathbf{A}_e\mathbf{V}_e\hat{\mathbf{M}}_1^{(e)}) - \alpha_9\,\mathrm{tr}(\mathbf{V}_e\mathbf{A}_e\mathbf{V}_e\hat{\mathbf{M}}_2^{(e)})\}\mathbf{V}_e^2\\ &+ \{-\alpha_9\,\mathrm{tr}(\mathbf{V}_e^2\mathbf{A}_e) + 2\alpha_9\,\mathrm{tr}(\mathbf{V}_e\mathbf{A}_e\mathbf{V}_e\hat{\mathbf{M}}_1^{(e)}) + \alpha_9\,\mathrm{tr}(\mathbf{V}_e\mathbf{A}_e\mathbf{V}_e\hat{\mathbf{M}}_2^{(e)})\}\mathbf{V}_e\mathbf{M}_1^{(e)}\mathbf{V}_e\\ &+ \{-\alpha_9\,\mathrm{tr}(\mathbf{V}_e^2\mathbf{A}_e) + \alpha_9\,\mathrm{tr}(\mathbf{V}_e\mathbf{A}_e\mathbf{V}_e\hat{\mathbf{M}}_1^{(e)}) + 2\alpha_9\,\mathrm{tr}(\mathbf{V}_e\mathbf{A}_e\mathbf{V}_e\hat{\mathbf{M}}_2^{(e)})\}\mathbf{V}_e\mathbf{M}_2^{(e)}\mathbf{V}_e\\ &=: \boldsymbol{\mathcal{C}}^{(e)}[\mathbf{A}_e] \quad . \end{aligned} \tag{3.216}$$

3.7.2 Kinematic hardening rule for cubic anisotropy

The tensors $\hat{\boldsymbol{\mathcal{C}}}^{(k)}$ and $\hat{\boldsymbol{\mathcal{B}}}^{(\mathrm{k})}$ satisfy, with respect to an orthonormal basis system $\{\mathbf{e}_i\}$, $i = 1, 2, 3$ with $\mathbf{e}_1 = \hat{\mathbf{m}}_1^{(k)}$ and $\mathbf{e}_2 = \hat{\mathbf{m}}_2^{(k)}$, properties of the form (3.213)-(3.215), so (3.150) and (3.153) now read

$$\begin{aligned}\boldsymbol{\mathcal{C}}^{(k)}[\mathbf{Y}] &= 2c_1\mathbf{V}_e^2\mathbf{Y}\mathbf{V}_e^2\\ &+ \{2c_4\,\mathrm{tr}(\mathbf{V}_e^2\mathbf{Y}) - c_9\,\mathrm{tr}(\mathbf{V}_e\mathbf{Y}\mathbf{V}_e\mathbf{M}_1^{(k)}) - c_9\,\mathrm{tr}(\mathbf{V}_e\mathbf{Y}\mathbf{V}_e\mathbf{M}_2^{(k)})\}\mathbf{V}_e^2\\ &+ \{-c_9\,\mathrm{tr}(\mathbf{V}_e^2\mathbf{Y}) + 2c_9\,\mathrm{tr}(\mathbf{V}_e\mathbf{Y}\mathbf{V}_e\mathbf{M}_1^{(k)}) + c_9\,\mathrm{tr}(\mathbf{V}_e\mathbf{Y}\mathbf{V}_e\mathbf{M}_2^{(k)})\}\mathbf{V}_e\mathbf{M}_1^{(k)}\mathbf{V}_e\\ &+ \{-c_9\,\mathrm{tr}(\mathbf{V}_e^2\mathbf{Y}) + c_9\,\mathrm{tr}(\mathbf{V}_e\mathbf{Y}\mathbf{V}_e\mathbf{M}_1^{(k)}) + 2c_9\,\mathrm{tr}(\mathbf{V}_e\mathbf{Y}\mathbf{V}_e\mathbf{M}_2^{(k)})\}\mathbf{V}_e\mathbf{M}_2^{(k)}\mathbf{V}_e \quad , \end{aligned} \tag{3.217}$$

and

$$\begin{aligned}\boldsymbol{\mathcal{B}}^{(k)}[\mathbf{Z}] &= 2b_1\mathbf{Z}\\ &+ \{2b_4\,\mathrm{tr}(\mathbf{V}_e^{-2}\mathbf{Z}) - b_9\,\mathrm{tr}(\mathbf{V}_e^{-1}\mathbf{Z}\mathbf{V}_e^{-1}\mathbf{M}_1^{(k)}) - b_9\,\mathrm{tr}(\mathbf{V}_e^{-1}\mathbf{Z}\mathbf{V}_e^{-1}\mathbf{M}_2^{(k)})\}\mathbf{V}_e^2\\ &+ \{-b_9\,\mathrm{tr}(\mathbf{V}_e^{-2}\mathbf{Z}) + 2b_9\,\mathrm{tr}(\mathbf{V}_e^{-1}\mathbf{Z}\mathbf{V}_e^{-1}\mathbf{M}_1^{(k)}) + b_9\,\mathrm{tr}(\mathbf{V}_e^{-1}\mathbf{Z}\mathbf{V}_e^{-1}\mathbf{M}_2^{(k)})\}\mathbf{V}_e\mathbf{M}_1^{(k)}\mathbf{V}_e\\ &+ \{-b_9\,\mathrm{tr}(\mathbf{V}_e^{-2}\mathbf{Z}) + b_9\,\mathrm{tr}(\mathbf{V}_e^{-1}\mathbf{Z}\mathbf{V}_e^{-1}\mathbf{M}_1^{(k)}) + 2b_9\,\mathrm{tr}(\mathbf{V}_e^{-1}\mathbf{Z}\mathbf{V}_e^{-1}\mathbf{M}_2^{(k)})\}\mathbf{V}_e\mathbf{M}_2^{(k)}\mathbf{V}_e \quad . \end{aligned} \tag{3.218}$$

3.7.3 Yield function and flow rule for cubic anisotropy

By making use of $(3.212)_{1-3}$, the fourth-order tensor $\hat{\boldsymbol{\mathcal{K}}}$ in (3.172) now becomes

$$\hat{\mathcal{K}}_{mn} \;\hat{=}\; \begin{pmatrix} K_{1111} & 0 & 0 & 0 & K_{1122} & 0 & 0 & 0 & K_{1122} \\ 0 & K_{1212} & 0 & K_{1221} & 0 & 0 & 0 & 0 & 0 \\ 0 & 0 & K_{1313} & 0 & 0 & 0 & K_{1221} & 0 & 0 \\ 0 & K_{1221} & 0 & K_{1313} & 0 & 0 & 0 & 0 & 0 \\ K_{1122} & 0 & 0 & 0 & K_{1111} & 0 & 0 & 0 & K_{1122} \\ 0 & 0 & 0 & 0 & 0 & K_{1212} & 0 & K_{1221} & 0 \\ 0 & 0 & K_{1221} & 0 & 0 & 0 & K_{1212} & 0 & 0 \\ 0 & 0 & 0 & 0 & 0 & K_{1221} & 0 & K_{1313} & 0 \\ K_{1122} & 0 & 0 & 0 & K_{1122} & 0 & 0 & 0 & K_{1111} \end{pmatrix} \quad , \tag{3.219}$$

where

$$K_{1212} = \frac{1}{2}v_1 + \frac{1}{4}v_2 + \frac{1}{4}v_3 - \frac{1}{2}v_7 - \frac{1}{4}v_8 - \frac{1}{4}v_9 - \frac{1}{4}v_{10} + \frac{1}{4}v_{11} - \frac{1}{4}v_{12} \quad , \tag{3.220}$$

$$K_{1212} = \frac{1}{2}v_1 + \frac{1}{4}v_3 - \frac{1}{2}v_7 - \frac{1}{4}v_9 - \frac{1}{4}v_{11} \quad , \tag{3.221}$$

$$K_{1212} = \frac{1}{2}v_1 + \frac{1}{4}v_2 - \frac{1}{2}v_7 - \frac{1}{4}v_8 + \frac{1}{4}v_{10} \quad , \tag{3.222}$$

$$K_{1221} = 2v_1 + v_2 + 2v_7 + v_8 \quad , \tag{3.223}$$

$$K_{1221} = 2v_1 + v_2 + v_3 + 2v_7 + v_8 + v_9 \quad , \tag{3.224}$$

$$K_{1221} = 2v_1 + v_3 + 2v_7 + v_9 \quad , \tag{3.225}$$

$$K_{1313} = \frac{1}{2}v_1 + \frac{1}{4}v_2 + \frac{1}{4}v_3 - \frac{1}{2}v_7 - \frac{1}{4}v_8 - \frac{1}{4}v_9 + \frac{1}{4}v_{10} - \frac{1}{4}v_{11} + \frac{1}{4}v_{12} \quad , \tag{3.226}$$

$$K_{1313} = \frac{1}{2}v_1 + \frac{1}{4}v_2 - \frac{1}{2}v_7 - \frac{1}{4}v_8 - \frac{1}{4}v_{10} \quad , \tag{3.227}$$

$$K_{1313} = \frac{1}{2}v_1 + \frac{1}{4}v_3 - \frac{1}{2}v_7 - \frac{1}{4}v_9 + \frac{1}{4}v_{11} \quad , \tag{3.228}$$

$$6K_{1111} - 6K_{1122} = 6v_1 + 4v_2 + v_3 + 4v_4 + v_5 - 2v_6 \quad , \tag{3.229}$$

$$-6K_{1111} + 6K_{1122} = -6v_1 - 4v_2 - 4v_3 - 4v_4 - 4v_5 + 5v_6 \quad , \tag{3.230}$$

$$-6K_{1111} + 6K_{1122} = -6v_1 - 4v_2 + 2v_3 - 4v_4 + 2v_5 - v_6 \quad , \tag{3.231}$$

$$6K_{1111} - 6K_{1122} = 6v_1 + v_2 + 4v_3 + v_4 + 4v_5 - 2v_6 \quad , \tag{3.232}$$

$$-6K_{1111} + 6K_{1122} = -6v_1 + 2v_2 - 4v_3 + 2v_4 - 4v_5 - v_6 \quad , \tag{3.233}$$

$$6K_{1111} - 6K_{1122} = 6v_1 + v_2 + v_3 + v_4 + v_5 + v_6 \quad . \tag{3.234}$$

From these relations it can be seen that cubic symmetry implies the following conditions for the material parameters:

$$\begin{aligned}
&v_2 = 0 \quad , \\
&v_3 = 0 \quad , \\
&v_4 = v_5 = v_6 \quad , \\
&v_8 = 0 \quad , \\
&v_9 = 0 \quad , \\
&v_{11} = -v_{10} \quad , \\
&v_{12} = -3v_{10} \quad .
\end{aligned} \tag{3.235}$$

Chapter 4

Finite element simulation of a Brinell hardness indentation test of a single-crystal Ni-base superalloy (CMSX4), oriented in [001]-direction

The indentation test with a sphere, first proposed by J.A. Brinell in 1900, is often used to determine the mechanical properties of metallic materials, whenever the standard methods like the tension- and torsion-test are not feasible. Due to the local restriction of the deformation also very small volumes of material can be examined (cf. Dieter [13]). Basic investigations, showing that the spherical form of the indenter enables the identification of a large part of the stress-strain-response through the depth-load response of the indentation test have been performed for elastic-plastic materials by Huber [57] (see also the literature cited herein).
The aim of this and further material testing procedures like e.g. the nano-indenter is generally to identify material parameters. For a constitutive model with linear isotropic hardening this is shown in Huber et al. [52], for viscoplasticity with nonlinear hardening in Mahnken and Stein [76] and for plasticity with nonlinear isotropic and kinematic hardening in Huber [57], Huber et al. [53], [54], [55], [56].
In this work, the expensive procedure of determining material parameters will not be further debated. Rather, we will address qualitative properties of spherical indentation when the testing material exhibits cubic anisotropy.

4.1 Experimental procedure - Material parameters

In the Brinell hardness test the surface of a specimen is indented with a ball at a certain load. The load is applied for a standard time and the diameter of the indentation is measured with a low power microscope after removal of the load. The average of two readings of the diameter of the impression at right angles should be made. The surface on which the indentation is made should be smooth and free from dirt or scale. The Brinell hardness number (BHN) is expressed as

$$\mathrm{BHN} = \frac{P}{(\pi/2)D^2(1-\cos\phi)} \quad , \tag{4.1}$$

where P is the applied load, D the diameter of the ball and 2Φ the angle included by the indentation and the center of the ball. Fig. 4.1 shows a sketch of the basic parameters used

to describe the BRINELL hardness indentation test and it can be seen that the diameter of the indentation d is given by $d = D \sin \phi$.

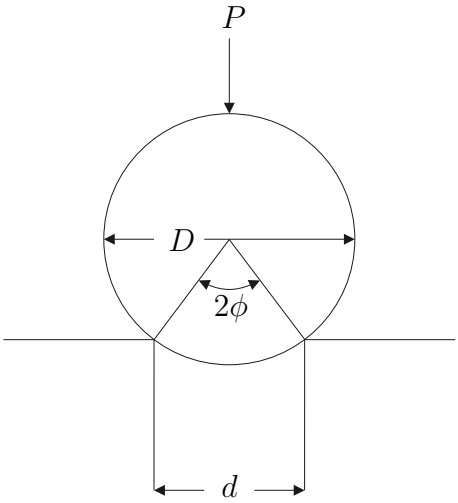

Figure 4.1: Basic parameters in Brinell test

The experimental data of a Brinell hardness indentation test of a nickel-based single-crystal superalloy (CMSX4), that displays cubic symmetry were supplied by Dipl.-Ing. K. Wintrich of the Materials Research Institute at Darmstadt University of Technology, Germany and are shown in Table 4.1.

applied force P	490.35 [N] (50 [kg])
elastic modulus of the steel ball	210 [GPa]
diameter D of the ball	1.25 [mm]
duration of the indentation test	10 [s]
average diameter d of indentation	4.95×10^{-1} [mm]
calculated depth of indentation	5.11×10^{-2} [mm]

Table 4.1: Parameters of the indenting experiment (courtesy of K. Wintrich, TU-Darmstadt)

Advanced industrial gas turbines must operated at increasing high temperatures to improve the efficiency and to enhance power output, but they also have to retain a technically useful strength at these elevated temperatures. In order to meet the requirements for this application, turbine blades are manufactured from monocrystalline alloys, like e.g. the nickel-based CMSX4 superalloy with γ^3-(Ni_3(Al,Ti)) precipitates, showing a strong cubic anisotropy. For the quantitative description of the elastic behavior of this anisotropic material the elastic single crystal constants are needed. The determination of the elastic moduli c_{11}, c_{12} and c_{44} was performed with two independent measuring methods (surface BRINELL scattering and resonant frequency measurement by COMINS ET AL. [21] and HERMANN ET AL. [48], respectively) and show a very good agreement.

	Comins et al. [21]	Hermann et al. [48]
elastic modulus c_{11}	243 ± 2 [GPa]	245 [GPa]
elastic modulus c_{12}	153 ± 2 [GPa]	155 [GPa]
elastic modulus c_{44}	128 ± 1 [GPa]	129 [GPa]

Table 4.2: Elastic moduli for CMSX4 at ambient temperature

The values in row 3 of table 4.2 were calculated from the elastic compliances S, measured in Hermann et al. [48] for CMSX4 superalloy at ambient temperature with the formulae (cf. Dieter [13], Hermann et al. [48])

$$c_{11} = \frac{S_{11} + S_{12}}{(S_{11} - S_{12})(S_{11} + S_{12})} \quad , \tag{4.2}$$

$$c_{12} = \frac{-S_{12}}{(S_{11} - S_{12})(S_{11} + S_{12})} \quad , \tag{4.3}$$

$$c_{44} = \frac{1}{S_{44}} \tag{4.4}$$

for a cubic crystal structure.

$\alpha_1 = 64.0$ [GPa]	$\alpha_2 = 0.0$ [GPa]	$\alpha_3 = 0.0$ [GPa]
$\alpha_4 = 57.5$ [GPa]	$\alpha_5 = -38.0$ [GPa]	$\alpha_6 = -38.0$ [GPa]
$\alpha_7 = 38.0$ [GPa]	$\alpha_8 = 38.0$ [GPa]	$\alpha_9 = -38.0$ [GPa]
$b_1 = 17.5$ [-]	$b_2 = 0.0$ [-]	$b_3 = 0.0$ [-]
$b_4 = 0.0$ [-]	$b_5 = 0.0$ [-]	$b_6 = 0.0$ [-]
$b_7 = 0.0$ [-]	$b_8 = 0.0$ [-]	$b_9 = 0.0$ [-]
$c_1 = 2.0$ [GPa]	$c_2 = 0.0$ [GPa]	$c_3 = 0.0$ [GPa]
$c_4 = 0.0$ [GPa]	$c_5 = 0.0$ [GPa]	$c_6 = 0.0$ [GPa]
$c_7 = 0.0$ [GPa]	$c_8 = 0.0$ [GPa]	$c_9 = 0.0$ [GPa]
$v_1 = 1.0$ [-]	$v_2 = 0.0$ [-]	$v_3 = 0.0$ [-]
$v_4 = 0.0$ [-]	$v_5 = 0.0$ [-]	$v_6 = 0.0$ [-]
$v_7 = 0.0$ [-]	$v_8 = 0.0$ [-]	$v_9 = 0.0$ [-]
$v_{10} = 0.0$ [-]	$v_{11} = 0.0$ [-]	$v_{12} = 0.0$ [-]
$m = 4.0$ [-]	$\eta = 3.0 \times 10^4$ [MPa^m s]	$k_0 = 200.0$ [MPa]
$l_1 = 100.0$ [MPa^{-1}]	$l_2 = 0.0$ [MPa^{-1}]	$l_3 = 0.0$ [MPa^{-1}]

Table 4.3: Material parameters for cubic anisotropy

To determine the material parameters governing the hardening response is a very difficult task and is beyond the scope of this thesis. Devising suitable experimental procedures for

constitutive models and identifying from these experiments material parameters is probably one of the most challenging tasks in today's material research. A good impression of the difficulties encountered is given, among others in HUBER [57], HUBER ET AL. [52]-[56].
However, to go any further we may use the material parameters chosen in HÄUSLER [42], but adjusted for cubic anisotropy, as shown in Table 4.3. It is emphasized that these material parameters are, except for the elastic ones which have been calculated from the measured elasticity moduli (4.2)-(4.4) with (3.214), hypothetical values so that the obtained results can have qualitative meaning only.

4.2 Comparison of numerical with experimental results

The constitutive theory has been implemented in the UMAT subroutine of the finite element code ABAQUS. Details of the numerical time integration as well as the tangent operator are published for example in DIEGELE ET AL. [35], HÄUSLER [42], JANSOHN [62] and are omitted here.
Fig. 4.2 shows the finite element mesh used for spherical indentation, consisting of 3000 solid continuum elements (C3D8) and 3555 nodes. The model has been meshed in a way that accounts for the indentation process, leaving the outer areas relatively coarse and refining the inner, strongly deformed part at the indentation. The initial axis of anisotropy of the cubic anisotropic constitutive model are aligned along the global axis x, y and z of the finite element model, as depicted in 4.2, with the two initial structural tensors being

$$\mathbf{M}_1 := \begin{pmatrix} 1 & 0 & 0 \\ 0 & 0 & 0 \\ 0 & 0 & 0 \end{pmatrix} \quad , \quad \mathbf{M}_2 := \begin{pmatrix} 0 & 0 & 0 \\ 0 & 1 & 0 \\ 0 & 0 & 0 \end{pmatrix} \tag{4.5}$$

in the elasticity law (3.216), the kinematic hardening (3.217), (3.218) and the yield function (3.219), respectively.
Large deformation theory has been used in the analysis, together with the assumption of small elastic strains, which implies $\mathbf{V}_e \approx \mathbf{1}$ (see also HÄUSLER ET AL. [43]). Although the calculation time increases significantly, HUBER [51] has shown that even for small indentations large deformation theory must be applied in order to obtain a consistent result. In Fig. 4.3 the finite element model is shown after the full indentation with a spherical rigid body surface, representing the steel ball indenter. The rigid body surface is not shown here and in any subsequent figures in order to show the deformed underlying finite element mesh. To give a better impression of the bulging of the rim of the indentation, Fig. 4.4 displays the finite element model in the sectional view. Clearly, the bulge shows the relatively coarse structure of the finite element model, but since any further refinement of the solid mesh would result in an intolerable increase of calculation time, the chosen mesh geometry seems to be adequate. The top view of the indented mesh in Fig. 4.5 lets anticipate the anisotropic deformation, especially displayed in the outer rim of the indentation.
The result of a BRINELL hardness indentation experiment, performed by K. Wintrich, is shown in Fig. 4.6. The cubic symmetry of the tested material manifests itself in the square form of the indentation. It also shows, that an anisotropic deformation took place during the process of indenting. Obviously the indenting steel ball was also deformed elastically anisotropic, since the elastic modulus of the ball is significantly lower than c_{11} of the CSMX-4 specimen. But since no experimental data is available this was not further considered in the analysis. The small elastic springback, displayed in the sectional cut in Fig. 4.7 depicts its minor influence on the anisotropic behavior.

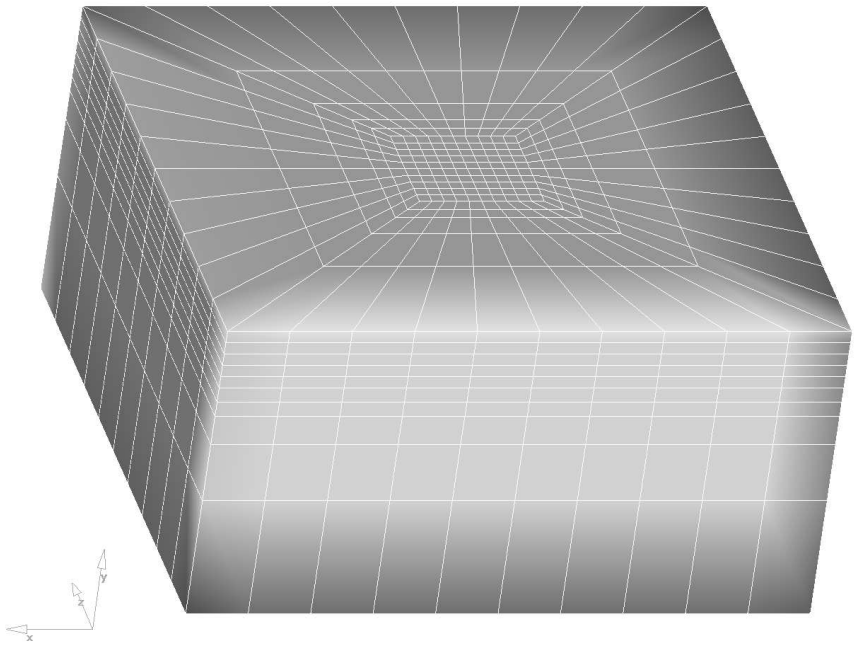

Figure 4.2: Finite element model before indentation

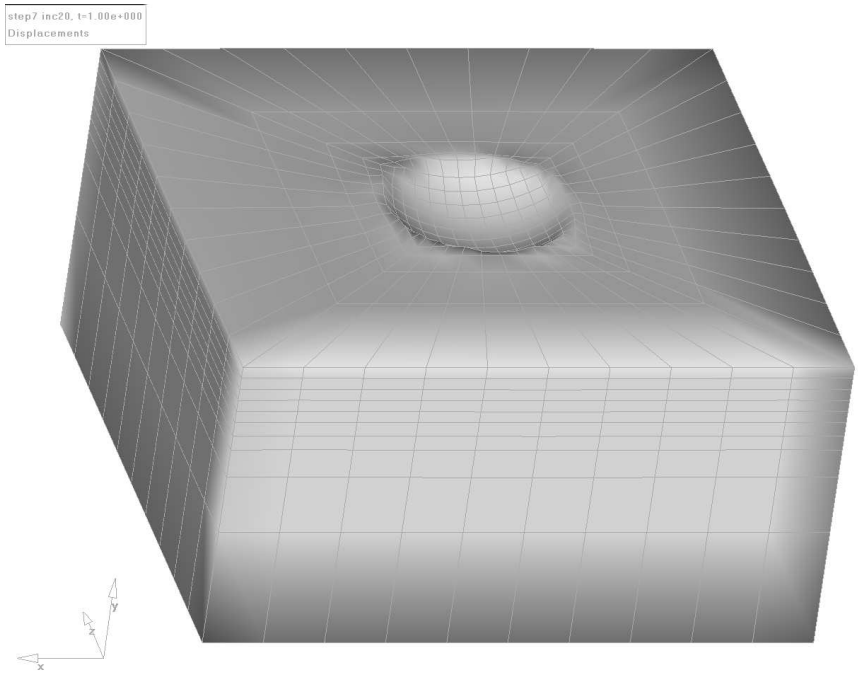

Figure 4.3: Finite element model after full indentation, rigid body indenter not shown

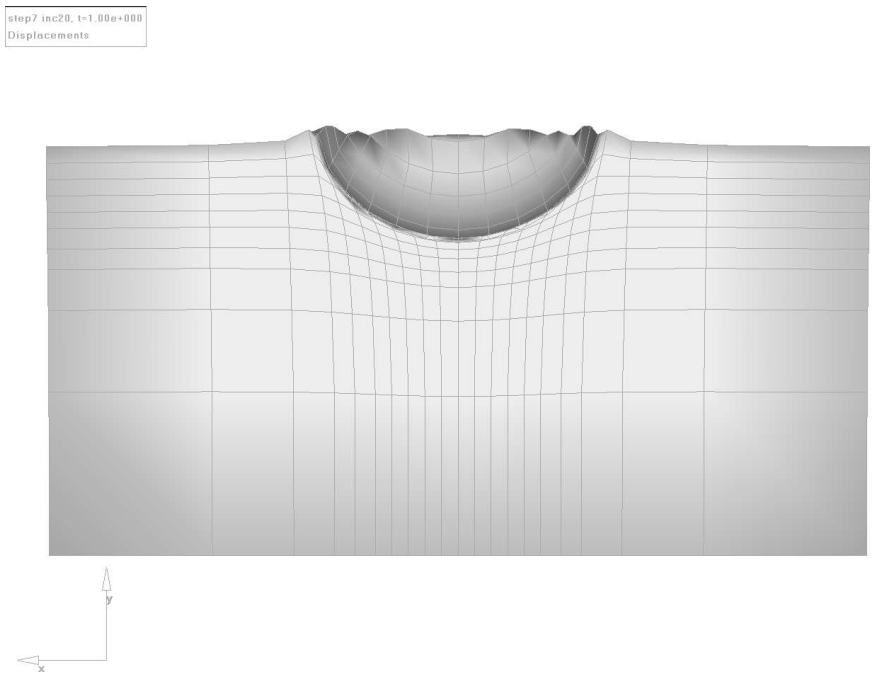

Figure 4.4: Sectional view after full indentation, rigid body indenter not shown

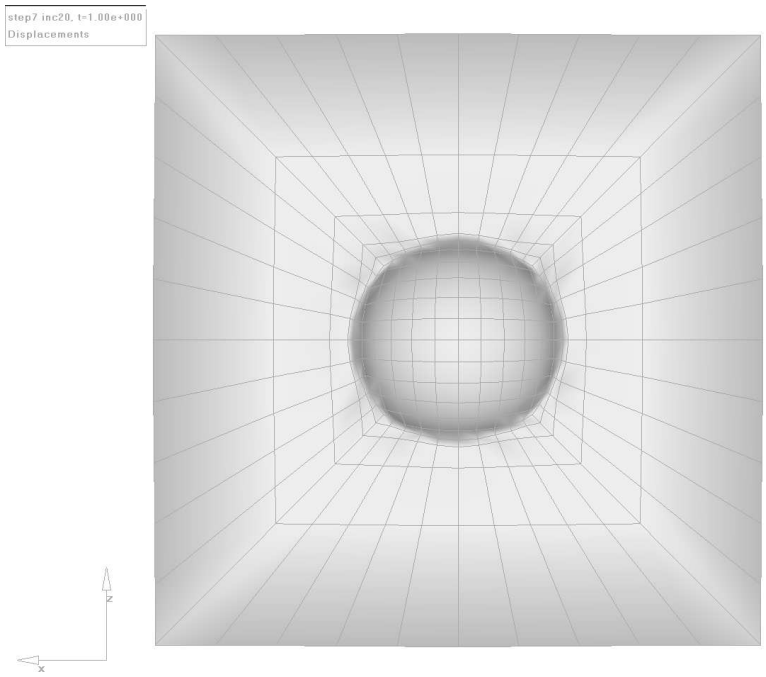

Figure 4.5: Top view after full indentation, rigid body indenter not shown

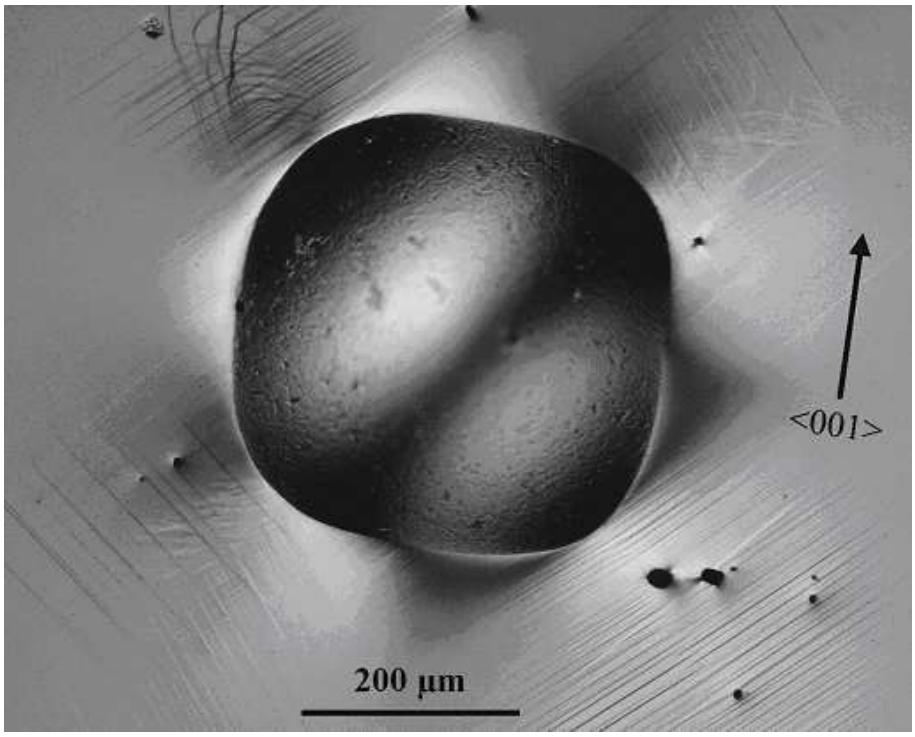

Figure 4.6: Photograph of the indentation experiment, after the indenter has been removed (courtesy of K. Wintrich, TU-Darmstadt)

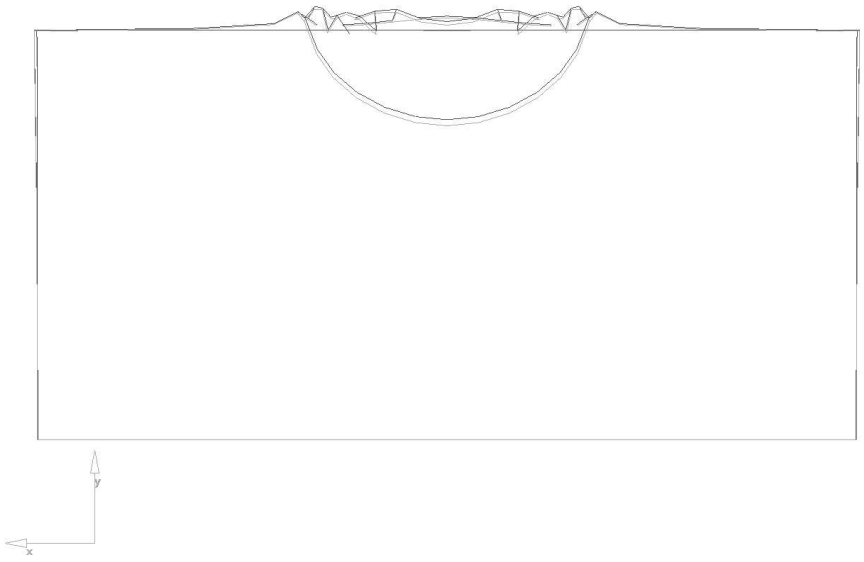

Figure 4.7: Sectional cut at maximum indentation (grey) and after springback

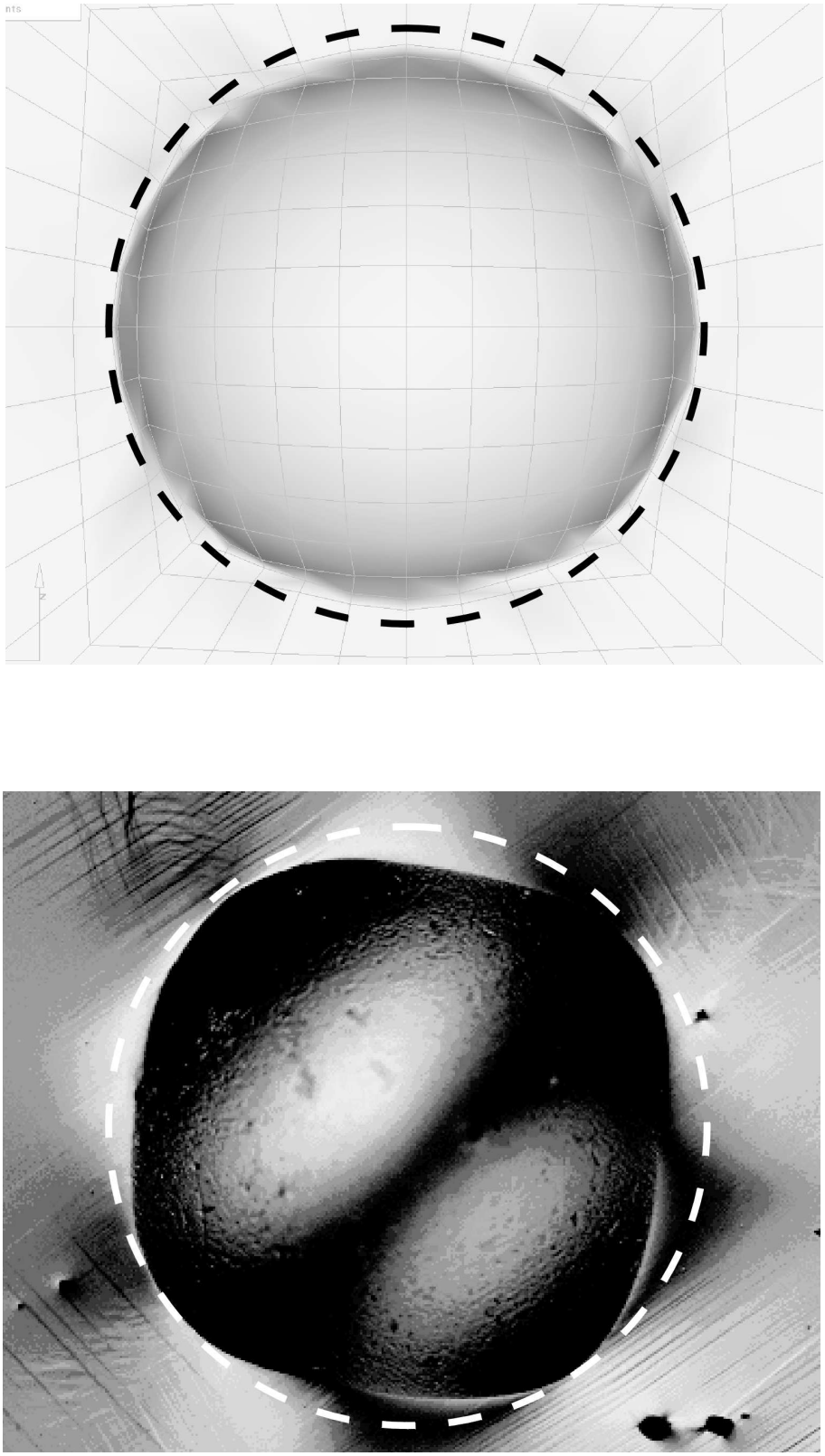

Figure 4.8: Enhancements of Figs. 4.5 and 4.6, circles added for clarification purpose

Generally, the constitutive model shows the expected distinct difference of the indentation from a circular form due to anisotropy. This can be seen in Fig. 4.8, which compares the numerical result (enhancement of Fig. 4.5) with the experiment (enhancement of Fig. 4.6). For clarification, circles have been drawn around the indentations. The Brinell experiment shows an indentation that resembles a square with four round edges, whereas the finite element calculation produced an elliptical indentation. Currently it is still an open question, whether just different material parameters would be capable to produce more satisfying results or if other material functions, as for example a different yield function, should be chosen to obtain a better outcome.

Chapter 5

Phenomenological model to describe yield surface evolution during plastic flow for small deformations

The analysis in this chapter corresponds essentially to that one given in DAFALIAS ET AL. [34] and addresses some features of the description of subsequent yield surfaces after various preloadings. The aim of this work is to show how deformation induced anisotropy of the yield surface may be formulated in a thermodynamically consistent manner. This is achieved by establishing sufficient conditions for the satisfaction of the so-called dissipation inequality. For reasons of simplicity, the proposed model is outlined for yield surfaces which initially are isotropic and the initial yield surface may be approximated with sufficient accuracy by a VON MISES yield function. This refers to e.g. the experiments by ISHIKAWA [59], which will be used in order to discuss the capabilities of the model. A brief summary of the experimental results by ISHIKAWA [59], will be given in the following.

5.1 Subsequent Yield Surfaces of Stainless Steel

The specimens used in ISHIKAWA's [59] investigations are drawing tubes of type AISI SUS304 stainless steel, subjected to solution heat treatment. Stress controlled deformation processes, with a constant stress rate of 4.3 MPa/s have been imposed, consisting of axial-torsional loadings. Yielding was defined by a VON MISES effective strain of 50 μm/m, which is small enough to detect yield surfaces in stress space by using a single specimen. The yield surfaces are determined by partially unloading the specimen from the actual stress state to the center of the yield surface, the location of which has been approximated during the preloading part of the stress path. More precisely, the center of the subsequent yield surface in the experiment is simulated by using the constitutive model given in ISHIKAWA AND SASAKI [60]. Figs. 5.1-5.7 illustrate the imposed stress paths, and the resulting yield surfaces, with respect to the σ-$\sqrt{3}\tau$-coordinate system (used stress space), where σ, τ are the axial and shear stress components, respectively. For all specimens, the initial yield locus may be approximated well by a VON MISES yield circle. These approximated initial yield circles are denoted by broken lines, the corresponding radii being taken from Table 1 in ISHIKAWA [59]. All detected subsequent yield loci may be approximated well by ellipses, as shown in the figures by solid lines. During proportional loading the ellipses are translated and compressed in the direction of the prestress. During non-proportional loading the subsequent yield ellipses translate, rotate and change their shape. The approximations of the subsequent yield loci indicated in Figs. 5.1-5.7 are constructed from

the experimental data by using a fitting procedure. Note that, because of time effects (rate-dependence) in the material behavior, the subsequent yield loci do generally not contain the prestress points. The experimental results e.g. in Figs. 5.1, 5.2 indicate that isotropic hardening is not present. In fact, existence of isotropic hardening (softening) would imply subsequent yield loci, after radial loading, which are broader (smaller) in the direction perpendicular to the preloading path. But such behavior is not observed (see Figs. 5.1c, 5.2c). Therefore, the experimental results in Figs. 5.1-5.7 are interpreted as to that isotropic hardening is generally absent, the mean value of the constant yield stress being $k_0 = 194$ MPa.

5.2 Proposed Constitutive Model

5.2.1 Basic Relations

Attention is confined to small elastic-viscoplastic (rate-dependent) deformations and by $\mathbf{E}$ and $\mathbf{T}$ the linearized strain tensor and the CAUCHY stress tensor are denoted, respectively. Since the formulation is not affected by a space dependence, an explicit reference to space will be dropped. Only isothermal deformations with homogeneous temperature distribution will be considered, so that a temperature dependence will be dropped as well. As usually, the strain tensor is assumed to satisfy the decomposition

$$\mathbf{E} = \mathbf{E}_e + \mathbf{E}_p \quad , \tag{5.1}$$

where $\mathbf{E}_e$ and $\mathbf{E}_p$ are the elastic and the plastic strain parts, respectively. Furthermore, the existence of a specific free energy ψ is assumed, with a corresponding elastic and plastic decomposition as (cf. (3.18))

$$\psi = \psi_e + \psi_p \quad . \tag{5.2}$$

For simplicity, ψ_e is supposed to be an isotropic function of $\mathbf{E}_e$, of the form

$$\psi_e = \hat{\psi}_e(\mathbf{E}_e) = \frac{1}{2\varrho}\mathbf{E}_e \cdot \boldsymbol{\mathcal{C}}[\mathbf{E}_e] \quad , \tag{5.3}$$

$$\boldsymbol{\mathcal{C}} = 2\mu\, \boldsymbol{\mathcal{E}} + \lambda\, \mathbf{1} \otimes \mathbf{1} \quad . \tag{5.4}$$

Here, ϱ is the mass density and μ, λ are the elasticity parameters. Let $\mathcal{C}_{ijkl}$ be the components of the fourth-order tensor $\boldsymbol{\mathcal{C}}$ with respect to the orthonormal basis, $\mathbf{e}_i$. Then $\boldsymbol{\mathcal{C}}$ has the properties

$$\mathcal{C}_{ijkl} = \mathcal{C}_{klij} = \mathcal{C}_{jikl} \quad . \tag{5.5}$$

Eq. $(5.5)_1$ states that the tensor $\boldsymbol{\mathcal{C}}$ is symmetric, i.e. $\boldsymbol{\mathcal{C}} = \boldsymbol{\mathcal{C}}^T$.
According to the assumptions made, the second law of thermodynamics, in the form of the CLAUSIUS-DUHEM-inequality, reads

$$\mathcal{D}_{C-D} = \mathbf{T} \cdot \dot{\mathbf{E}} - \varrho\, \dot{\psi} = \left(\mathbf{T} - \varrho \frac{\partial \hat{\psi}_e}{\partial \mathbf{E}_e} \right) \cdot \dot{\mathbf{E}} - \varrho\, \dot{\psi}_p \geq 0 \quad . \tag{5.6}$$

Using standard arguments, it can be shown that the relations

$$\mathbf{T} = \varrho\, \frac{\partial \hat{\psi}_e}{\partial \mathbf{E}_e} = \boldsymbol{\mathcal{C}}[\mathbf{E}_e] \quad , \tag{5.7}$$

$$\mathcal{D}_d := \mathbf{T} \cdot \dot{\mathbf{E}}_p - \varrho\, \dot{\psi}_p \geq 0 \tag{5.8}$$

are necessary and sufficient conditions for inequality (5.6) to be satisfied in the case of rate-dependent (visco-)plasticity, considered in the present work. Relation (5.8) is known as the dissipation inequality.

5.2.2 Yield Function - Flow Rule

ISHIKAWA's experimental results are interpreted as follows. Kinematic hardening effects are present, whereas isotropic hardening is absent. All subsequent yield loci may be approximated well by ellipses. This means, after prestressing, the subsequent yield loci translate and distort. For simplicity, rotation of the subsequent yield loci is not assumed explicitly. To model these phenomena, the existence of a yield function $\hat{F}(\mathbf{T}, \boldsymbol{\xi}, \boldsymbol{\mathcal{H}})$ is assumed in terms of a fourth-order tensor $\boldsymbol{\mathcal{H}}$ of the form

$$F = \hat{F}(\mathbf{T}, \boldsymbol{\xi}, \boldsymbol{\mathcal{H}}) = \hat{f}(\mathbf{T}, \boldsymbol{\xi}, \boldsymbol{\mathcal{H}}) - k_0 \quad , \tag{5.9}$$

$$f = \hat{f}(\mathbf{T}, \boldsymbol{\xi}, \boldsymbol{\mathcal{H}}) := \sqrt{(\mathbf{T} - \boldsymbol{\xi})^D \cdot \boldsymbol{\mathcal{H}}[(\mathbf{T} - \boldsymbol{\xi})^D]} \quad , \tag{5.10}$$

with

$$\boldsymbol{\mathcal{H}} = \boldsymbol{\mathcal{H}}_0 + \varphi \boldsymbol{\mathcal{A}} \tag{5.11}$$

and where yield occurs when $F = 0$.
In these equations, $\boldsymbol{\xi}$ is the so-called back stress tensor and k_0 is a material parameter representing constant yield stress. $\boldsymbol{\mathcal{H}}_0$ and $\boldsymbol{\mathcal{A}}$ are fourth-order tensors modelling distortion, but not explicitly rotation of the subsequent yield surfaces. In particular, $\boldsymbol{\mathcal{H}}_0$ is assumed to be constant, representing the initial value of $\boldsymbol{\mathcal{H}}$, while $\boldsymbol{\mathcal{A}}$ evolves with plastic flow from its initial zero value, representing the anisotropic development, and satisfies homogeneous initial conditions. The scalar φ will be discussed subsequently. The experiments by ISHIKAWA suggest modelling of the initial yield surface by using the VON MISES yield function. Therefore,

$$\boldsymbol{\mathcal{H}}_0 = \tfrac{3}{2} \left(\boldsymbol{\mathcal{E}} - \tfrac{1}{3} \, \mathbf{1} \otimes \mathbf{1} \right) \quad , \tag{5.12}$$

is set to be deviatoric. With respect to the orthonormal basis $\mathbf{e}_i$, $\boldsymbol{\mathcal{H}}_0$ exhibits the properties (5.5) as well as the property

$$(\mathcal{H}_0)_{iikl} = 0 \quad . \tag{5.13}$$

Accordingly, from $\mathcal{A}_{ijkl}$ the properties (5.5), (5.13) are required as well, where $\mathcal{A}_{ijkl}$ are the components of $\boldsymbol{\mathcal{A}}$ with respect to the orthonormal basis $\mathbf{e}_i$. Notice that (5.10) together with normality $\dot{\mathbf{E}}_p \sim \partial f / \partial \mathbf{T}$, satisfies the incompressibility condition $\operatorname{tr} \dot{\mathbf{E}}_p = 0$ without any restriction on $\boldsymbol{\mathcal{H}}$. But since there are only five independent components of $(\mathbf{T} - \boldsymbol{\xi})^D$, the 21 components of $\boldsymbol{\mathcal{H}}$ must reduce to 15 independent ones. This is in fact achieved by the six equations (5.13) for both $\boldsymbol{\mathcal{H}}_0$ and $\boldsymbol{\mathcal{A}}$, hence, for $\boldsymbol{\mathcal{H}}$ (cf. DAFALIAS [25]).
The experiments illustrated in Figs. 5.5, 5.6 show that the yield loci shrink after prestressing and expand after unloading to the state where the back stress tensor is nearly vanishing. To incorporate such phenomena into the constitutive model, φ is assumed to be a constitutive function of $\boldsymbol{\xi}$. For the range of experimental results by ISHIKAWA, the assumption

$$\varphi = 1 + \varphi_0 \left(1 - e^{\, \varphi_1 \|\boldsymbol{\xi}\|} \right) \tag{5.14}$$

seems to be appropriate for the purposes of the present work, with φ_0 and φ_1 being material constants.
Now, inelastic flow is postulated to occur, if a positive overstress applies. Consequently, on defining overstress to be given by F, inelastic flow occurs only if $F > 0$. Moreover, for an associated flow rule the yield function serves also as a plastic potential, thus

$$\dot{\mathbf{E}}_p = \dot{s} \sqrt{\frac{3}{2}} \frac{\frac{\partial \hat{f}}{\partial \mathbf{T}}}{\| \frac{\partial \hat{f}}{\partial \mathbf{T}} \|} = \frac{\dot{s}}{\zeta} \frac{\partial \hat{f}}{\partial \mathbf{T}} \quad , \tag{5.15}$$

$$\frac{\partial \hat{f}}{\partial \mathbf{T}} = \frac{1}{f}(\boldsymbol{\mathcal{H}}_0 + \varphi\, \boldsymbol{\mathcal{A}})[(\mathbf{T} - \boldsymbol{\xi})^D] \quad , \tag{5.16}$$

$$\zeta := \sqrt{\frac{2}{3}} \left\| \frac{\partial \hat{f}}{\partial \mathbf{T}} \right\| \quad , \tag{5.17}$$

$$\dot{s} := \sqrt{\frac{2}{3} \dot{\mathbf{E}}_p \cdot \dot{\mathbf{E}}_p} \quad . \tag{5.18}$$

It is common use in the framework of unified viscoplasticity to assume $\dot{s}$ as a function of the overstress F. In particular,

$$\dot{s} = \frac{\langle F \rangle^m}{\eta} \tag{5.19}$$

is set, where m, η are positive material parameters, and the function $\langle x \rangle$ is defined by

$$\langle x \rangle := \begin{cases} x & \text{if} \quad x \geq 0 \\ 0 & \text{if} \quad x < 0 \end{cases} \quad , \tag{5.20}$$

for all real x.

5.2.3 Hardening Rules

Consider the case that kinematic hardening and distortional hardening are not coupled. This may be taken into account by an additive decomposition of ψ_p into two parts, ψ_p^{kin} and ψ_p^{dist}, which are related to the kinematic hardening and the distortional hardening effects, respectively,

$$\psi_p = \psi_p^{kin} + \psi_p^{dist} \quad . \tag{5.21}$$

During inelastic flow, a part of the plastic power $\mathbf{T} \cdot \dot{\mathbf{E}}_p$ will be dissipated into heat, while the remainder will be stored in the material in form of internal structure rearrangements. The parts $\varrho\, \psi_p^{kin}$ and $\varrho\, \psi_p^{dist}$ represent just the energy stored in the material due to kinematic hardening and distortional hardening, respectively. Following Chaboche et al. [19], the existence of internal, second-order strain tensors $\mathbf{Y}_i,\ i = 1, .., k$ is assumed, so that ψ_p^{kin} is a function of the strains $\mathbf{Y}_i$. For simplicity, ψ_p^{kin} is assumed to be an isotropic function of the form

$$\psi_p^{kin} = \hat{\psi}_p^{kin}(\mathbf{Y}_i) = \sum_{i=1}^{k} \frac{c_i}{2\varrho} \mathbf{Y}_i \cdot \mathbf{Y}_i \quad . \tag{5.22}$$

The internal stress tensors, thermodynamically conjugate to the strains $\mathbf{Y}_i$ are

$$\boldsymbol{\xi}_i := \varrho \frac{\partial \hat{\psi}_p^{kin}}{\partial \mathbf{Y}_i} = c_i \mathbf{Y}_i \quad \text{(no sum on i)} \quad . \tag{5.23}$$

According to this approach, the back stress tensor $\boldsymbol{\xi}$ is given by the formula

$$\boldsymbol{\xi} = \sum_{i=1}^{k} \boldsymbol{\xi}_i \quad . \tag{5.24}$$

In a similar fashion, the existence of internal, symmetric fourth-order tensors $\boldsymbol{\mathcal{D}}_j$, $j = 1, .., d$ is assumed, and

$$\psi_p^{dist} = \hat{\psi}_p^{dist}(\boldsymbol{\mathcal{D}}_j) = \sum_{j=1}^{d} \frac{\alpha_j}{2\varrho}\, \boldsymbol{\mathcal{D}}_j \cdot \boldsymbol{\mathcal{D}}_j \quad . \tag{5.25}$$

By $\boldsymbol{\mathcal{A}}_j$ the fourth-order tensors, which are thermodynamically conjugate to $\boldsymbol{\mathcal{D}}_j$, are denoted

$$\boldsymbol{\mathcal{A}}_j := \varrho \frac{\partial \hat{\psi}_p^{dist}}{\partial \boldsymbol{\mathcal{D}}_j} = \alpha_j \boldsymbol{\mathcal{D}}_j \quad \text{(no sum on j)} \quad , \tag{5.26}$$

and $\boldsymbol{\mathcal{A}}$ is defined by

$$\boldsymbol{\mathcal{A}} = \sum_{j=1}^{d} \boldsymbol{\mathcal{A}}_j \quad . \tag{5.27}$$

In relations (5.22), (5.25), c_i, α_j are non-negative material parameters. To accomplish the hardening laws, evolution equations for the internal variables $\mathbf{Y}_i$ and $\boldsymbol{\mathcal{D}}_j$ must be formulated, which must be compatible with the dissipation inequality.
After using (5.21)-(5.27) in (5.8),

$$\begin{aligned} \mathcal{D}_d &= \mathbf{T} \cdot \dot{\mathbf{E}}_p - \sum_{i=1}^{k} \boldsymbol{\xi}_i \cdot \dot{\mathbf{Y}}_i - \sum_{j=1}^{d} \boldsymbol{\mathcal{A}}_j \cdot \dot{\boldsymbol{\mathcal{D}}}_j \\ &= (\mathbf{T} - \boldsymbol{\xi}) \cdot \dot{\mathbf{E}}_p + \sum_{i=1}^{k} \boldsymbol{\xi}_i \cdot (\dot{\mathbf{E}}_p - \dot{\mathbf{Y}}_i) - \sum_{j=1}^{d} \boldsymbol{\mathcal{A}}_j \cdot \dot{\boldsymbol{\mathcal{D}}}_j \geq 0 \quad , \end{aligned} \tag{5.28}$$

or, by virtue of (5.15)-(5.18),

$$\begin{aligned} \mathcal{D}_d &= \frac{\dot{s}}{f\,\zeta} (\mathbf{T} - \boldsymbol{\xi})^D \cdot \boldsymbol{\mathcal{H}}_0[(\mathbf{T} - \boldsymbol{\xi})^D] \\ &\quad + \sum_{j=1}^{d} \boldsymbol{\mathcal{A}}_j \cdot \left\{ \frac{\dot{s}\,\varphi}{f\,\zeta} (\mathbf{T} - \boldsymbol{\xi})^D \otimes (\mathbf{T} - \boldsymbol{\xi})^D \right\} \\ &\quad + \sum_{i=1}^{k} \boldsymbol{\xi}_i \cdot (\dot{\mathbf{E}}_p - \dot{\mathbf{Y}}_i) - \sum_{j=1}^{d} \boldsymbol{\mathcal{A}}_j \cdot \dot{\boldsymbol{\mathcal{D}}}_j \\ &= \mathcal{D}_d^{(0)} + \mathcal{D}_d^{(kin)} + \mathcal{D}_d^{(dist)} \geq 0 \quad , \end{aligned} \tag{5.29}$$

where

$$\mathcal{D}_d^{(0)} = \frac{\dot{s}}{f\,\zeta} (\mathbf{T} - \boldsymbol{\xi})^D \cdot \boldsymbol{\mathcal{H}}_0[(\mathbf{T} - \boldsymbol{\xi})^D] \quad , \tag{5.30}$$

$$\mathcal{D}_d^{(kin)} = \sum_{i=1}^{k} \boldsymbol{\xi}_i \cdot (\dot{\mathbf{E}}_p - \dot{\mathbf{Y}}_i) \quad , \tag{5.31}$$

$$\mathcal{D}_d^{(dist)} = \sum_{j=1}^{d} \boldsymbol{\mathcal{A}}_j \cdot \left\{ \frac{\dot{s}\,\varphi}{f\,\zeta} (\mathbf{T} - \boldsymbol{\xi})^D \otimes (\mathbf{T} - \boldsymbol{\xi})^D - \dot{\boldsymbol{\mathcal{D}}}_j \right\} \quad . \tag{5.32}$$

Since $\boldsymbol{\mathcal{H}}_0$ is positive definite for all deviatoric second-order tensors, $\mathcal{D}_d^{(0)} \geq 0$ will be set. Therefore, (5.29) will always be satisfied if

$$\mathcal{D}_d^{(kin)} \geq 0 \quad , \quad \mathcal{D}_d^{(dist)} \geq 0 \quad . \tag{5.33}$$

Clearly the relations (no sum on i, j)

$$\dot{\mathbf{E}}_p - \dot{\mathbf{Y}}_i = \dot{s}\, b_i\, \boldsymbol{\xi}_i \quad ,$$

$$\frac{\dot{s}\,\varphi}{f\,\zeta}(\mathbf{T}-\boldsymbol{\xi})^D \otimes (\mathbf{T}-\boldsymbol{\xi})^D - \dot{\boldsymbol{\mathcal{D}}}_j = \dot{s} f\; B_j \boldsymbol{\mathcal{A}}_j \quad ,$$

or

$$\dot{\mathbf{Y}}_i \;=\; \dot{\mathbf{E}}_p - \dot{s}\, b_i\, \boldsymbol{\xi}_i \quad , \tag{5.34}$$

$$\dot{\boldsymbol{\mathcal{D}}}_j \;=\; \dot{s}\left\{\frac{\varphi}{f\,\zeta}(\mathbf{T}-\boldsymbol{\xi})^D \otimes (\mathbf{T}-\boldsymbol{\xi})^D - f\; B_j \boldsymbol{\mathcal{A}}_j\right\} \tag{5.35}$$

are sufficient conditions for (5.33) to hold, with b_i, B_j being non-negative material parameters. Eqs. (5.34), together with (5.23), (5.24), represent the kinematic hardening law introduced by Chaboche et al. [19]. For $k = 1$, one obtains the so-called Armstrong-Frederick kinematic hardening model (see Armstrong and Frederick [6]). Marquis [77] showed that the Armstrong-Frederick rule may be derived in a purely mechanical context by using a two-surface model (see also Dafalias and Popov [22]). Later, Tsakmakis [100] derived the model of Chaboche et al. [19] from a so-called multisurface model. Generally, the concept of multisurface plasticity has been introduced by Mroz [81]. Dafalias and Popov [22], [23] were the first to introduce the two-surface (yield and bounding) model in order to describe cyclic loading processes. Today, a large number of similar approaches can be found in the literature.

The equations governing the response of distortional hardening are given by (5.26), (5.27) and (5.35). Alternatively, (5.35) may be rewritten as (no sum on j)

$$\dot{\boldsymbol{\mathcal{A}}}_j = \dot{z}\left\{\Theta_j\,(\mathbf{T}-\boldsymbol{\xi})^D \otimes (\mathbf{T}-\boldsymbol{\xi})^D - \alpha_j\, B_j\, \boldsymbol{\mathcal{A}}_j\right\} \quad , \tag{5.36}$$

$$\Theta_j := \frac{\varphi\,\alpha_j}{f^2\,\zeta} \quad , \quad \dot{z} := \dot{s} f \quad , \tag{5.37}$$

in view of (5.26). On assuming homogeneous initial conditions, $\boldsymbol{\mathcal{A}}_j$ may be integrated to get (no sum on j)

$$\boldsymbol{\mathcal{A}}_j(z) = \int_0^z e^{-\alpha_j B_j\,(z-\overline{z})}\; \Theta_j(\overline{z})\; (\mathbf{T}(\overline{z}) - \boldsymbol{\xi}(\overline{z}))^D \otimes (\mathbf{T}(\overline{z}) - \boldsymbol{\xi}(\overline{z}))^D d\overline{z} \quad . \tag{5.38}$$

From this, it is not difficult to see that every $\boldsymbol{\mathcal{A}}_j$ satisfies the required properties (5.5), (5.13), and therefore $\boldsymbol{\mathcal{A}}$ too.

5.3 Comparison with Experiments - Concluding Remarks

Figs. 5.8-5.14 illustrate yield loci predicted by the proposed model for the loading paths given in Figs. 5.1-5.7, respectively. ISHIKAWA's experimental data are also displayed in Figs. 5.8-5.14. The predicted responses are calculated by assuming $\boldsymbol{\xi}$ and $\boldsymbol{\mathcal{A}}$ to consist of two parts, respectively, i.e. $\boldsymbol{\xi} = \boldsymbol{\xi}_1 + \boldsymbol{\xi}_2$, $\boldsymbol{\mathcal{A}} = \boldsymbol{\mathcal{A}}_1 + \boldsymbol{\mathcal{A}}_2$. The material parameters are chosen as shown in Table 5.1.

$\mu = 7.88 \times 10^4$ [MPa]	$\lambda = 1.18 \times 10^5$ [MPa]
$m = 2.25$ [-]	$\eta = 1.50 \times 10^7$ [MPa^{m}s]
$k_0 = 1.94 \times 10^2$ [MPa]	
$\varphi_0 = 1.00$ [-]	$\varphi_1 = 1.80 \times 10^{-2}$ [MPa^{-1}]
$\alpha_1 = 4.50$ [MPa^{-1}]	B_1=1.60 [MPa s^{-1}]
$\alpha_2 = 0.80$ [MPa^{-1}]	B_2=0.50 [MPa s^{-1}]
$c_1 = 4.50 \times 10^4$ [MPa^{-1}]	$b_1 = 3.30 \times 10^{-2}$ [-]
$c_2 = 9.00 \times 10^3$ [MPa^{-1}]	$b_2 = 0$ [-]

Table 5.1: Material parameters

It is emphasized that these values are chosen based on trial and error. A systematic identification of material parameters by using established optimization algorithms is beyond the scope of the work. Therefore, comparison of the predicted responses with the experimental data has qualitative meaning only.
For monotonous tension, Fig. 5.8b indicates that the translation of the yield locus, controlled by the back stress $\boldsymbol{\xi}$, is well predicted. The subsequent yield locus, placed in the origin of stress space in Fig. 5.8c shows a good agreement between experimental and predicted results for the distortion of the yield surface. The same is also true for monotonous torsional loading (see Figs. 5.9b, 5.9c). Figs. 5.10b, 5.10c reveal that translation and distortion of the yield locus are in essence well predicted for the case of monotonous radial loading conditions. However, from Figs. 5.10b and 5.10c, some differences between the predicted and experimental results can be recognized, which arise from a missing explicit rotation in the theoretical model. In the case of a combined tension-torsion loading history, the numerical results in Figs. 5.11b and 5.11c show a very good agreement with the experiment for the tensile part A, but less good for the following torsional part C due to the aforementioned missing explicit rotation in the model. During uniaxial cyclic loading, the model predicts the behavior of the yield surface very well for the tension and compression phase (see Figs. 5.12b, 5.12c, 5.12d), but less good for the reloading tensile part (see Fig. 5.12e). This may be due to the chosen values of the material parameters φ_0 and φ_1, or due to the chosen constitutive function φ itself or due to the fact that the present model is not amplified by further internal variables describing cyclic loading effects. More complex loading histories, including tensile loading followed by torsional loading, are displayed in Figs. 5.13 and 5.14. It can be seen that the initial tensile loading behavior is described well, whereas the subsequent yield surfaces after the torsional loading part are not very well predicted, which may be interpreted to be caused by the missing explicit rotation in the constitutive model.
From this discussion, it can be concluded that the model is generally able to predict the experimentally measured yield loci. For the observed deviations from the experimental results

in essence two reasons are likely to account for. On the one hand, since the model is highly nonlinear, it is very difficult to choose the material parameters appropriately. This means, one may assume that other values for the material parameters, which will be identified by using established optimization procedures, may furnish better agreement with the experimental data. On the other hand, only translation and distortion of the yield surface can be described by the proposed constitutive theory. The measured yield loci, however, translate, distort and rotate, depending on the imposed loading history. Therefore, one may expect improved predicted results, if the constitutive theory will be amplified to model rotations of the yield surface explicitly. To clarify this point will be the subject of future work.

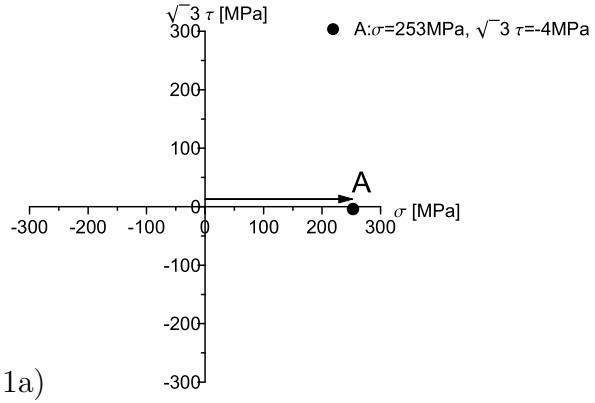

1a)

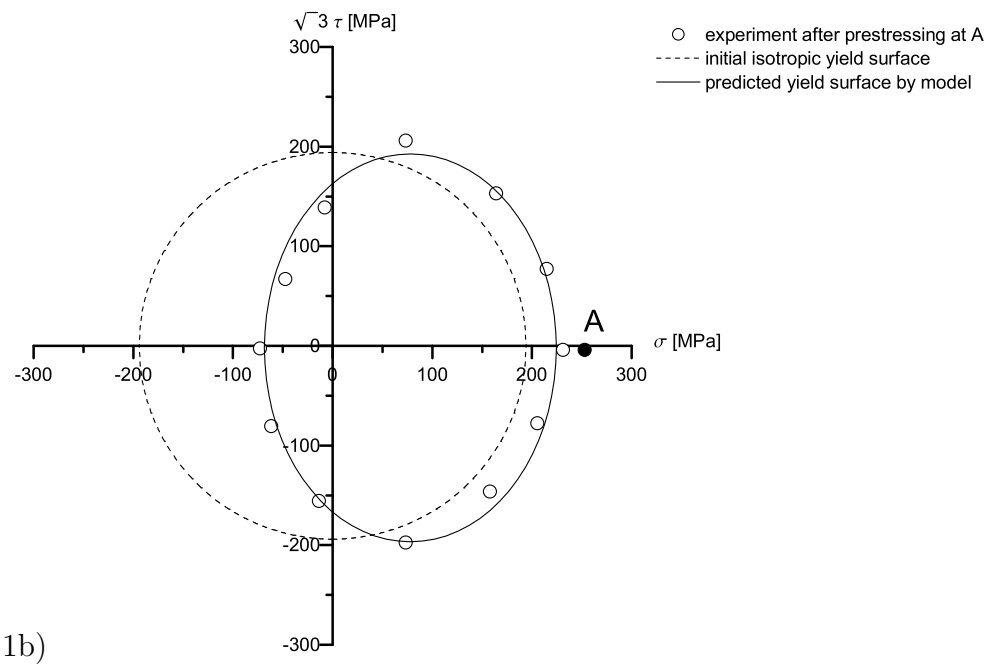

1b)

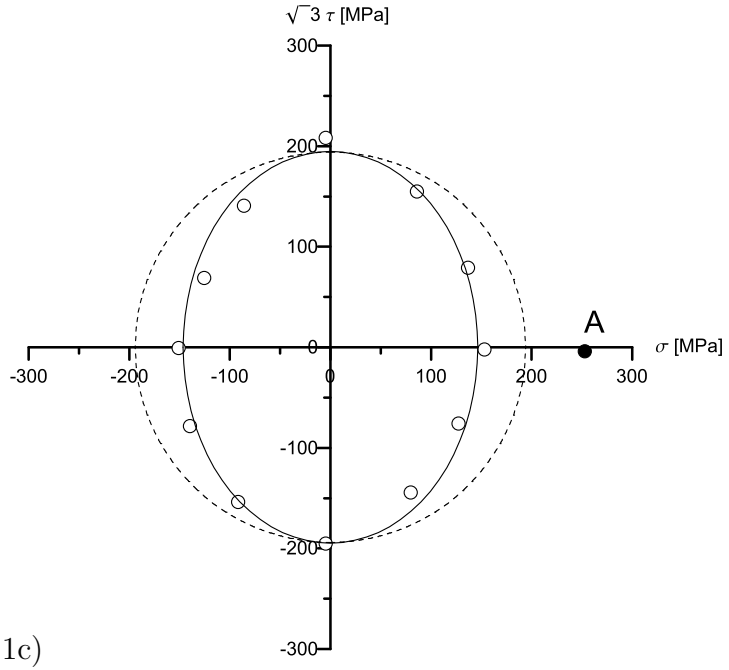

1c)

Figure 5.1: Monotonous tensile loading. 5.1a) Loading path imposed. 5.1b) Yield locus after prestressing at A. 5.1c) Subsequent yield locus from 5.1b) placed in the origin of the stress space

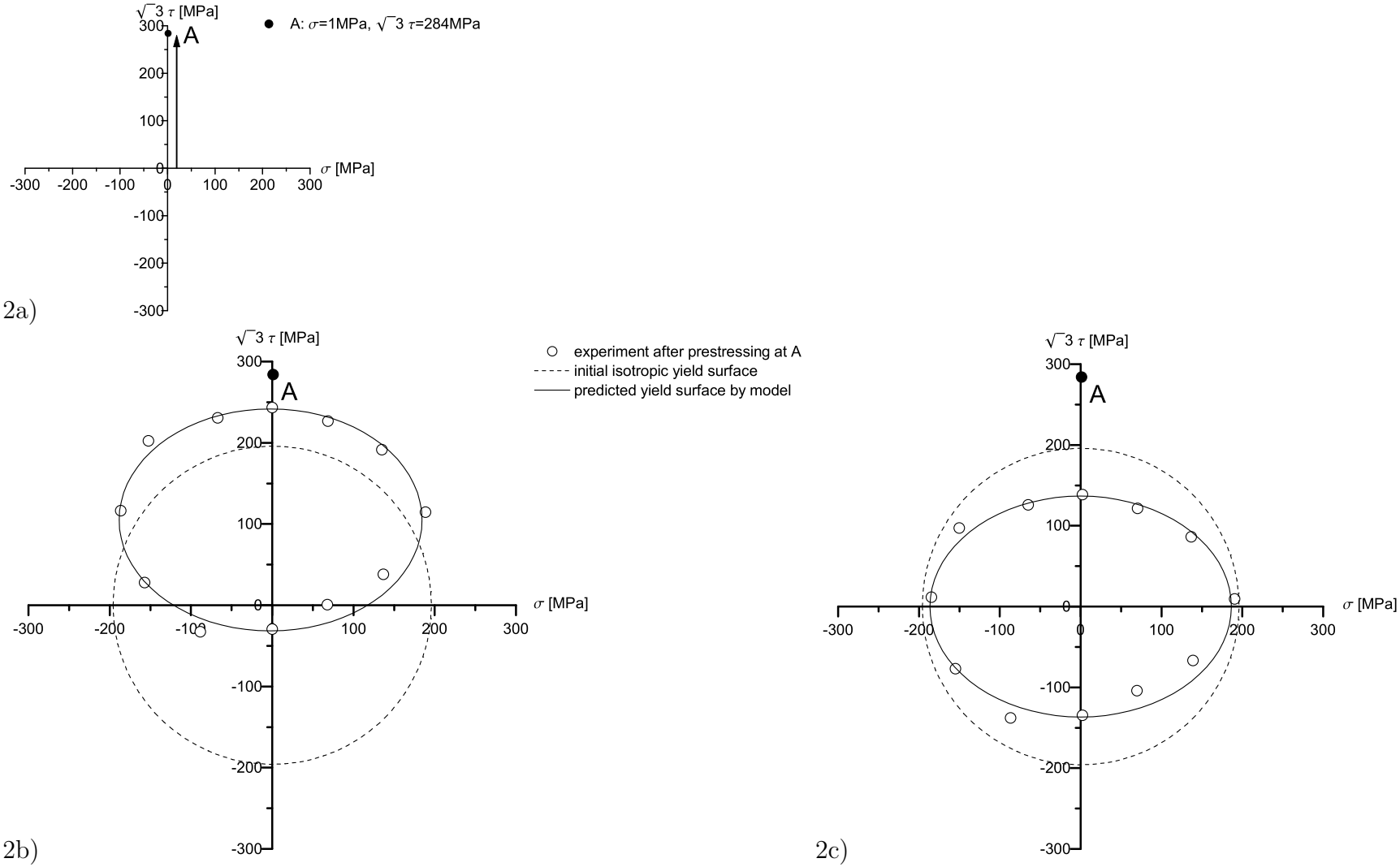

Figure 5.2: Monotonous torsional loading. 5.2a) Loading path imposed. 5.2b) Yield locus after prestressing at A. 5.2c) Subsequent yield locus from 5.2b) placed in the origin of the stress space

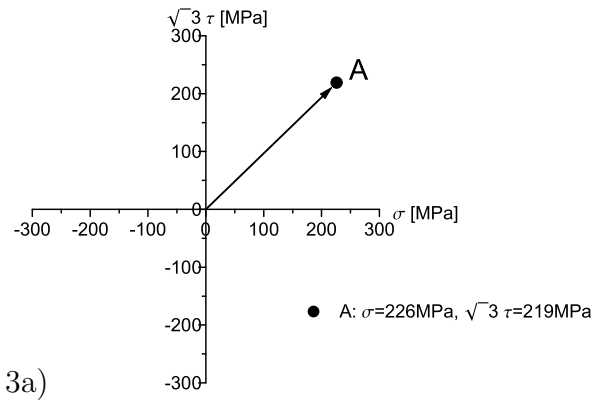

3a)

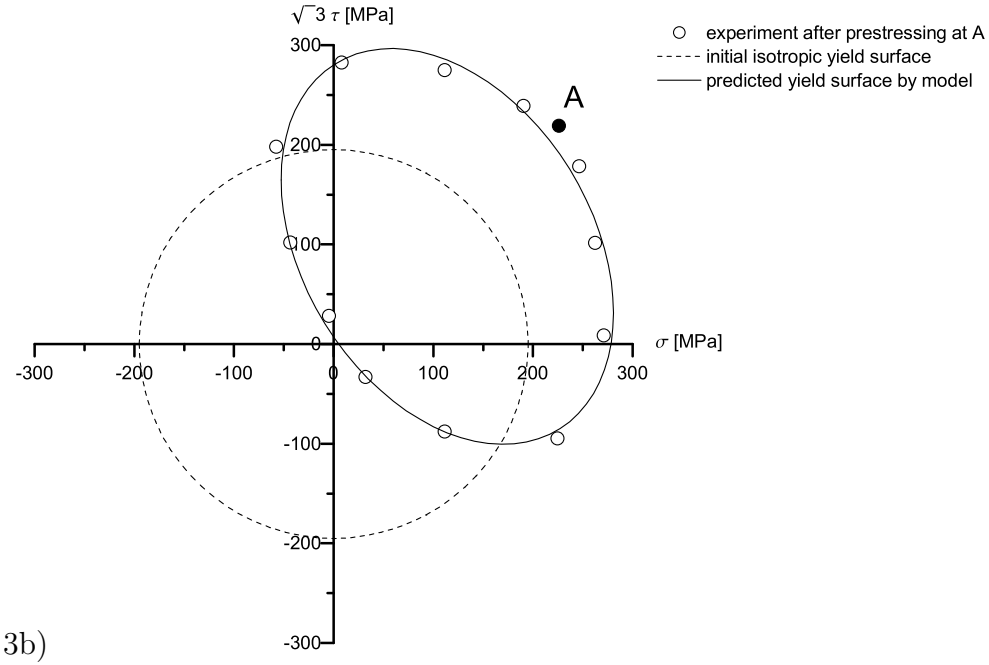

3b)

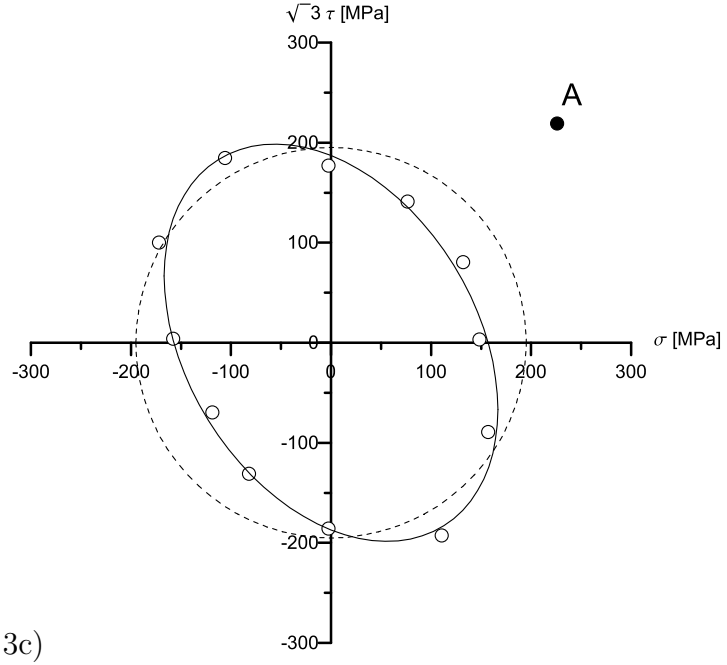

3c)

Figure 5.3: Monotonous radial loading. 5.3a) Loading path imposed. 5.3b) Yield locus after prestressing at A. 5.3c) Subsequent yield locus from 5.3b) placed in the origin of the stress space

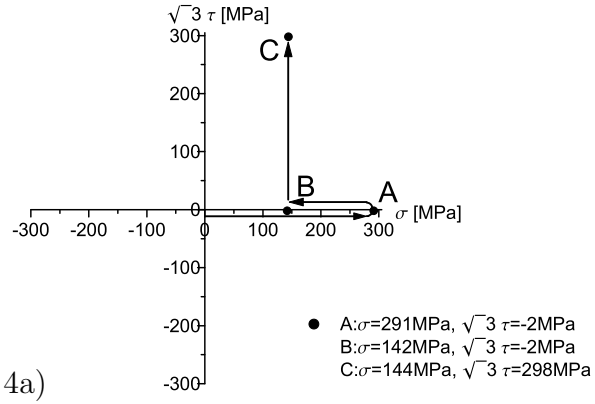

4a)

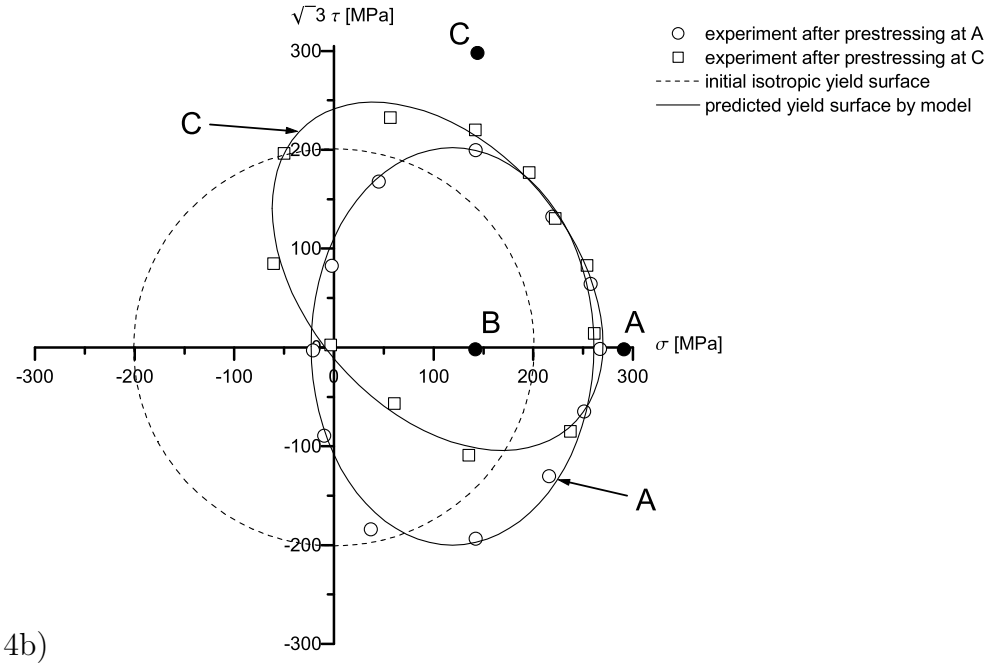

4b)

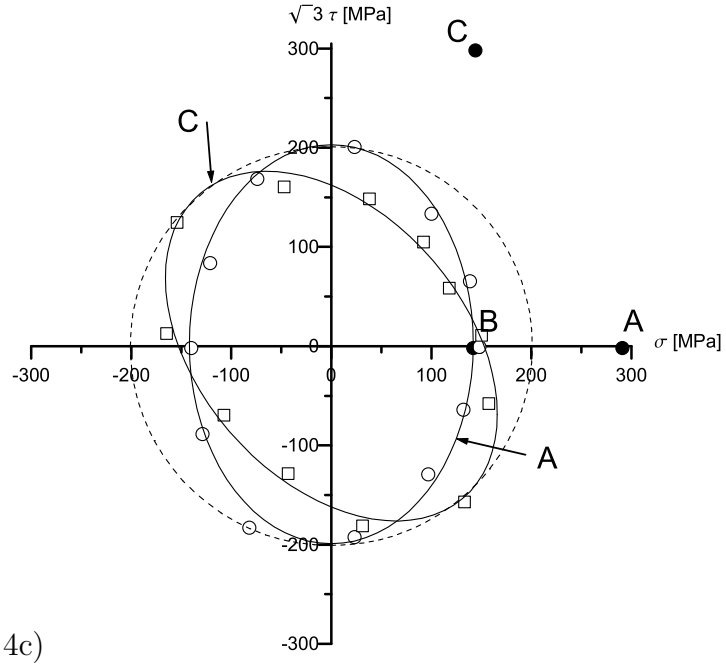

4c)

Figure 5.4: Combined tension-torsion loading history. 5.4a) Loading path imposed. 5.4b) Yield loci after prestressing at A and C. 5.4c) Subsequent yield loci from 5.4b) placed in the origin of the stress space

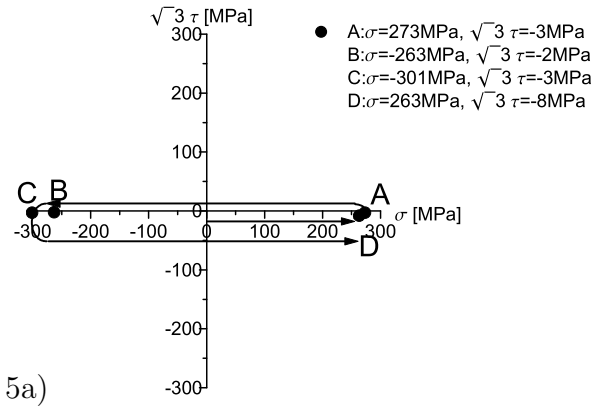

5a)

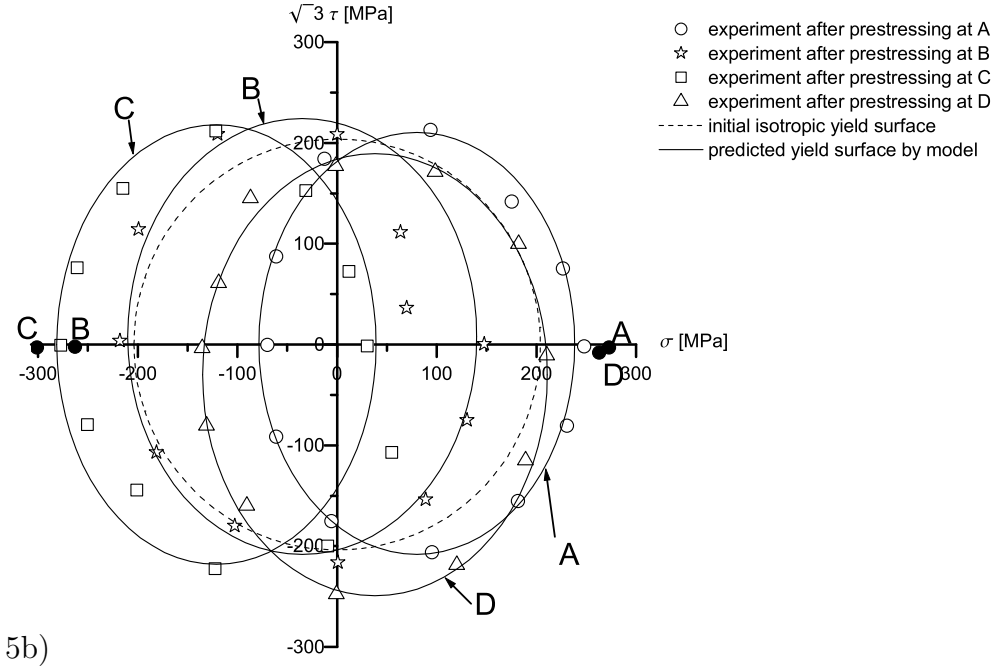

5b)

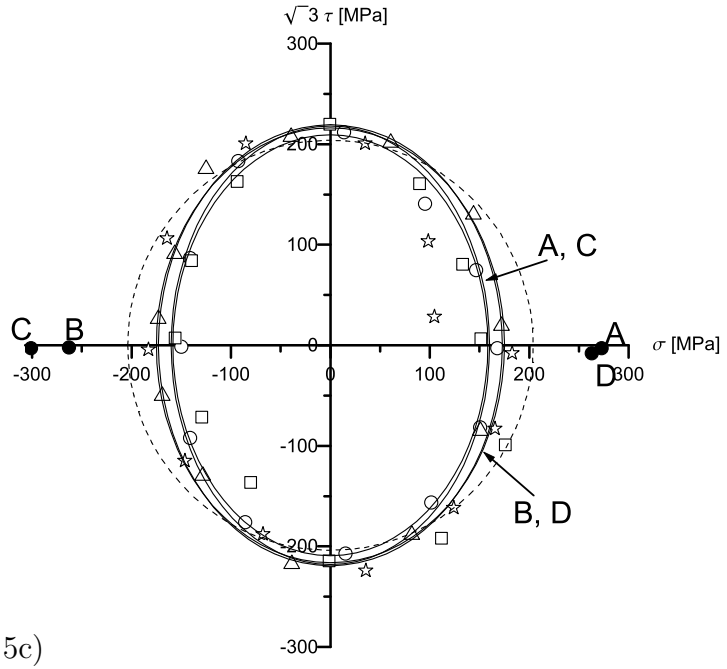

5c)

Figure 5.5: Uniaxial, cyclic loading. 5.5a) Loading path imposed. 5.5b) Yield loci after prestressing at A, B, C and D. 5.5c) Subsequent yield loci from 5.5b) placed in the origin of the stress space

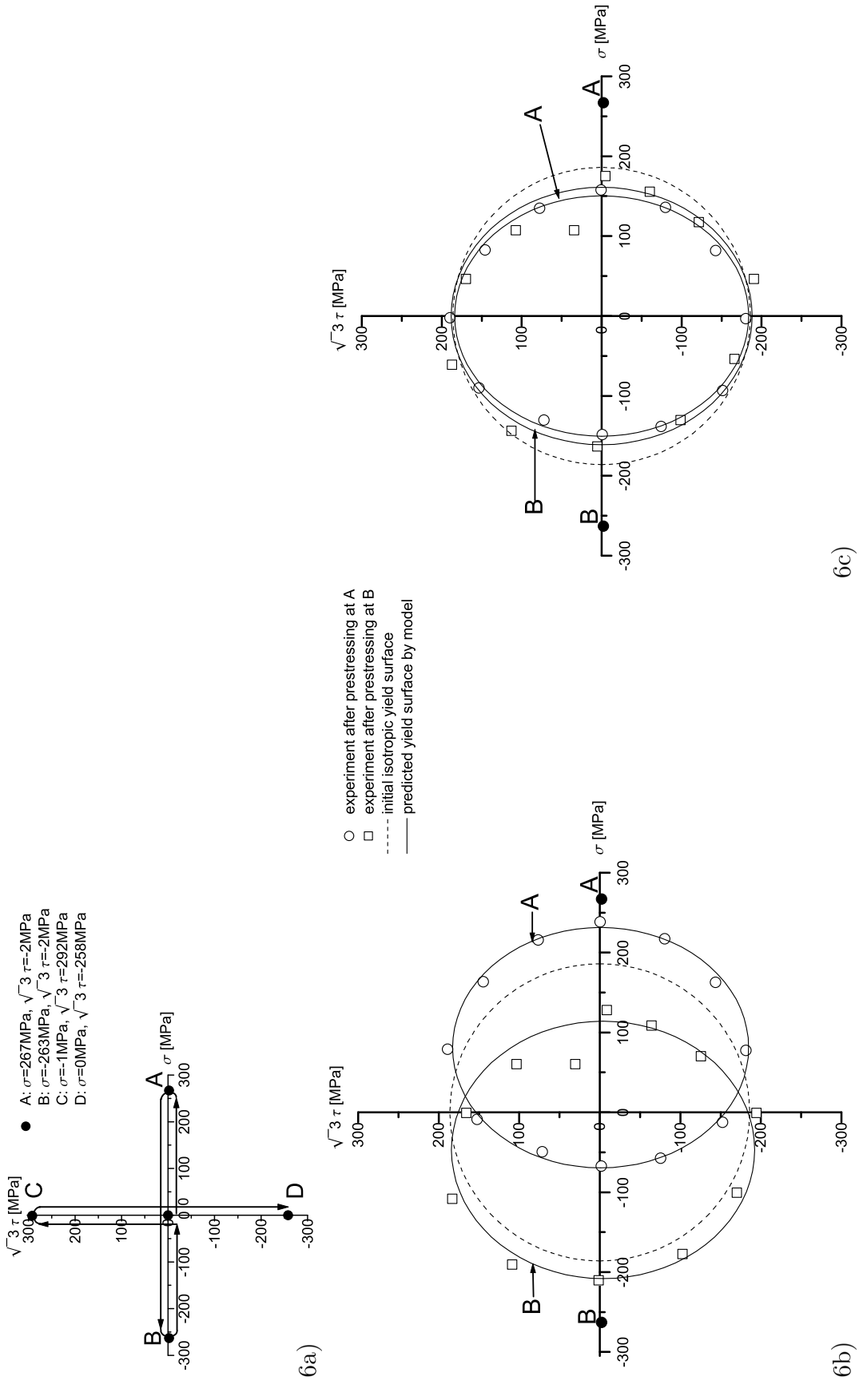
A: σ=267MPa, √3 τ=-2MPa
B: σ=-263MPa, √3 τ=-2MPa
C: σ=-1MPa, √3 τ=292MPa
D: σ=0MPa, √3 τ=-258MPa
√3 τ [MPa]
σ [MPa]
A
B
C
D
experiment after prestressing at A
experiment after prestressing at B
initial isotropic yield surface
predicted yield surface by model
6a)
6b)
6c)

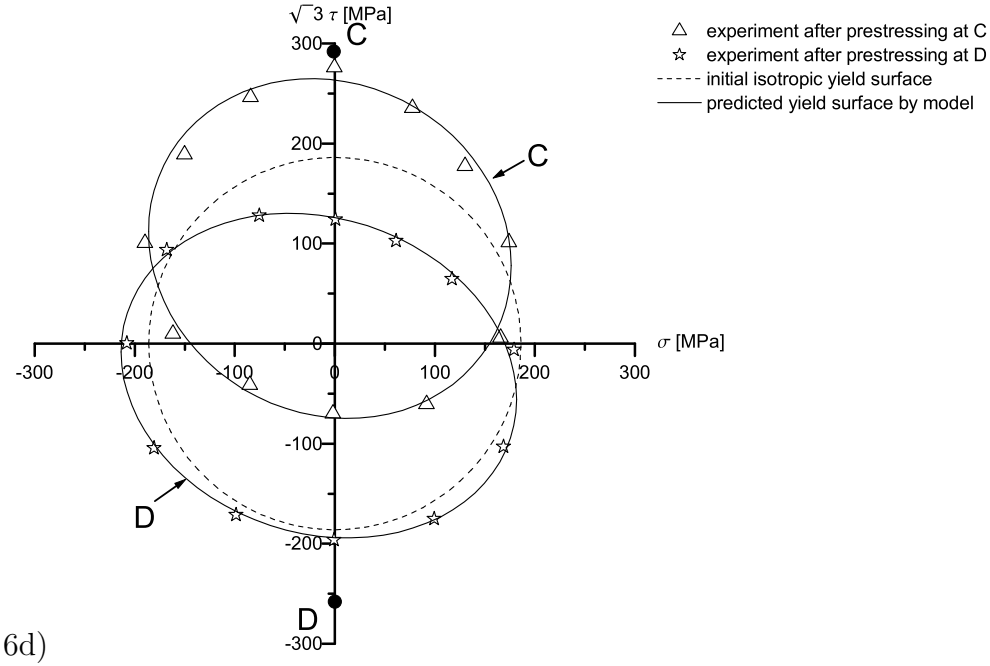

6d)

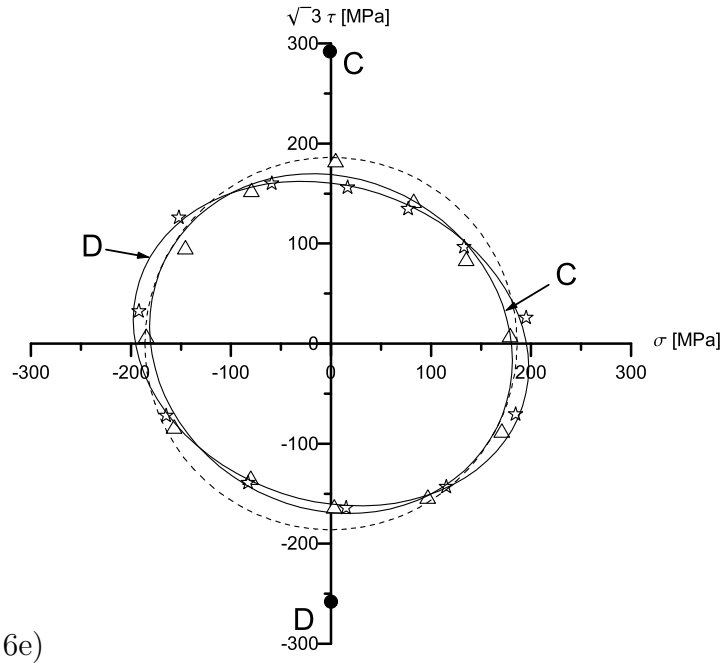

6e)

Figure 5.6: Combined tension-torsion loading history. 5.6a) Loading path imposed. 5.6b) Yield loci after prestressing at A and B. 5.6c) Subsequent yield loci from 5.6b) placed in the origin of the stress space. 5.6d) Yield loci after prestressing at C and D. 5.6e) Subsequent yield loci from 5.6d) placed in the origin of the stress space

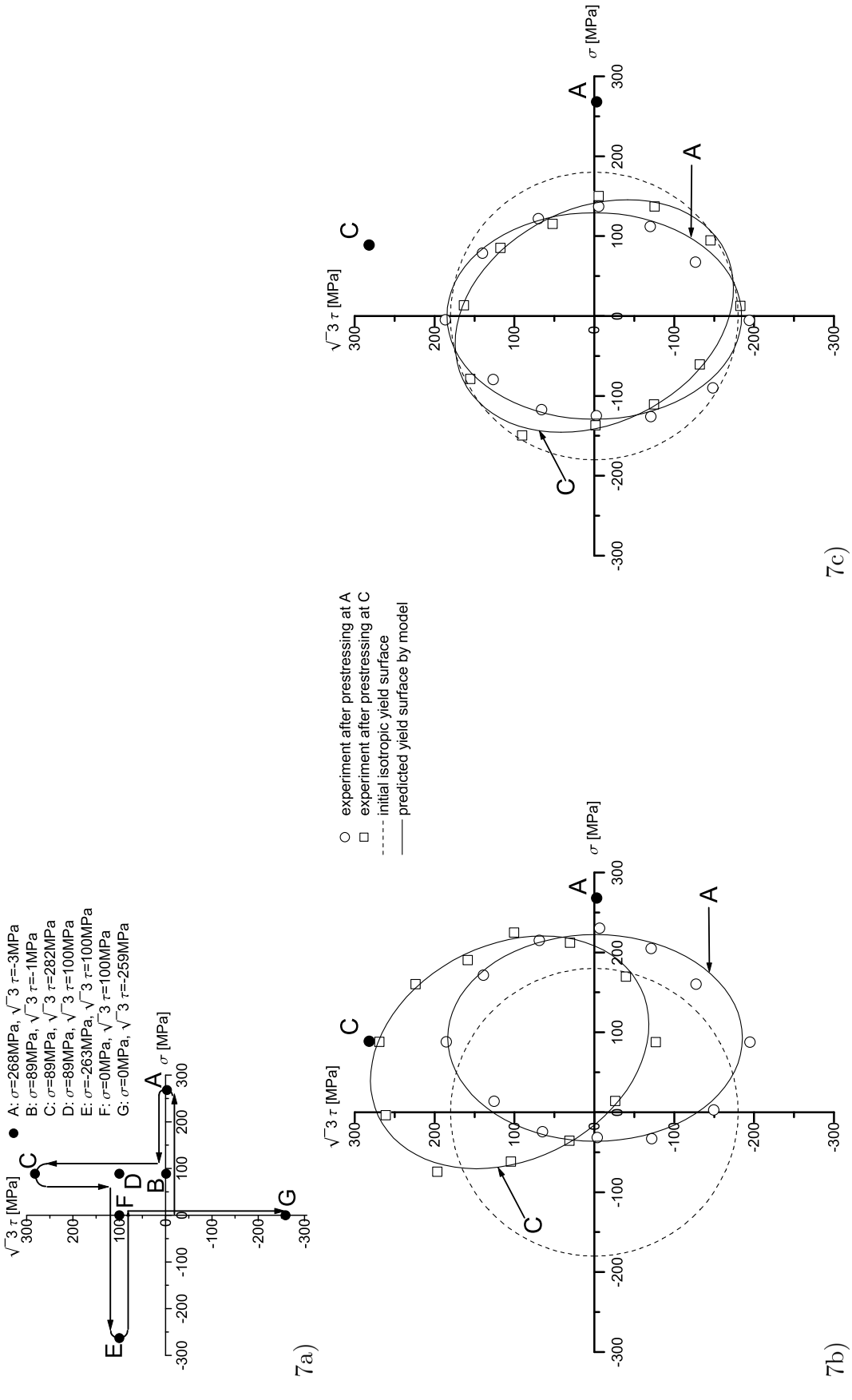
A: σ=268MPa, √3 τ=-3MPa
B: σ=89MPa, √3 τ=-1MPa
C: σ=89MPa, √3 τ=282MPa
D: σ=89MPa, √3 τ=100MPa
E: σ=-263MPa, √3 τ=100MPa
F: σ=0MPa, √3 τ=100MPa
G: σ=0MPa, √3 τ=-259MPa
√3 τ [MPa]
σ [MPa]
experiment after prestressing at A
experiment after prestressing at C
initial isotropic yield surface
predicted yield surface by model
7a)
7b)
7c)

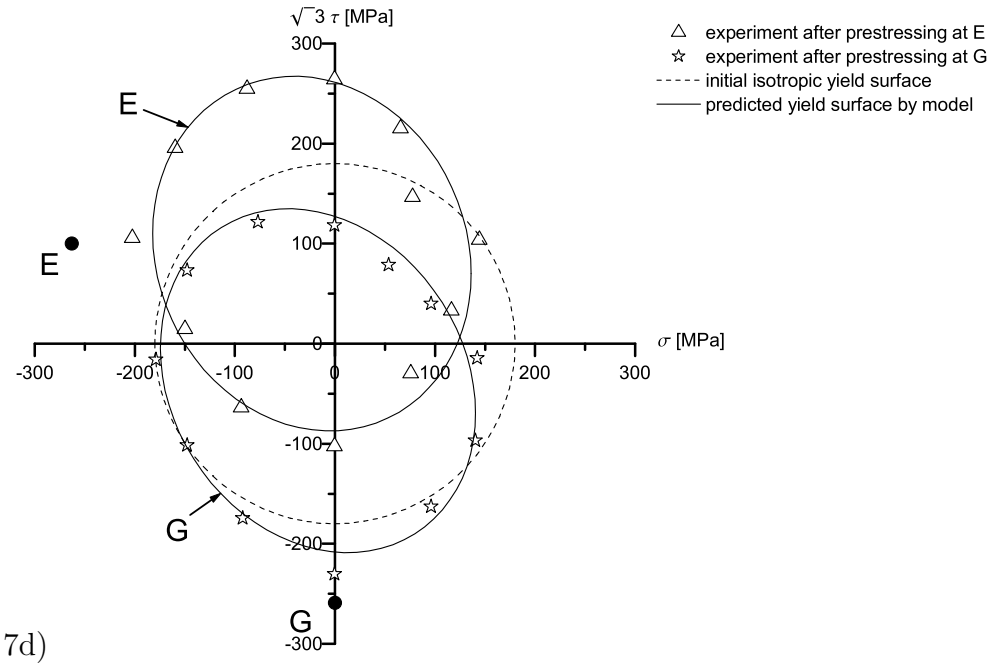

7d)

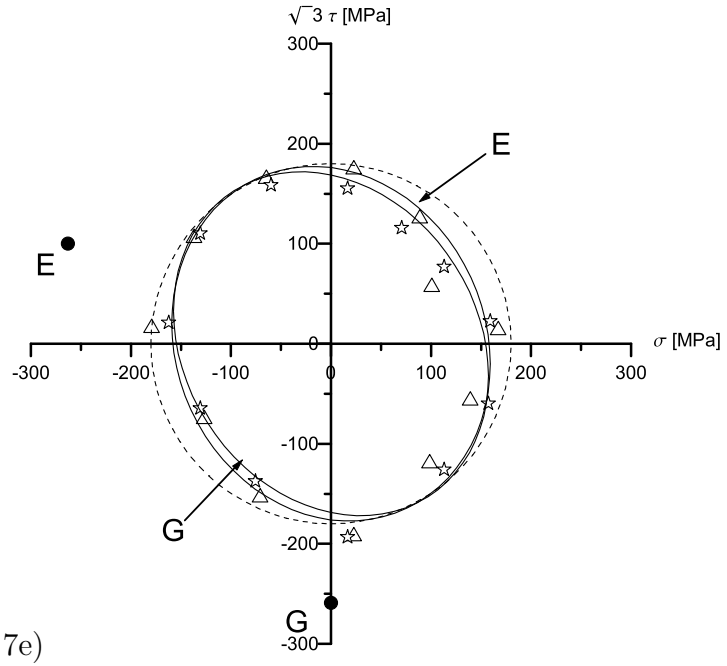

7e)

Figure 5.7: Combined tension-torsion loading history. 5.7a) Loading path imposed. 5.7b) Yield loci after prestressing at A and C. 5.7c) Subsequent yield loci from 5.7b) placed in the origin of the stress space. 5.7d) Yield loci after prestressing at E and G. 5.7e) Subsequent yield loci from 5.7d) placed in the origin of the stress space

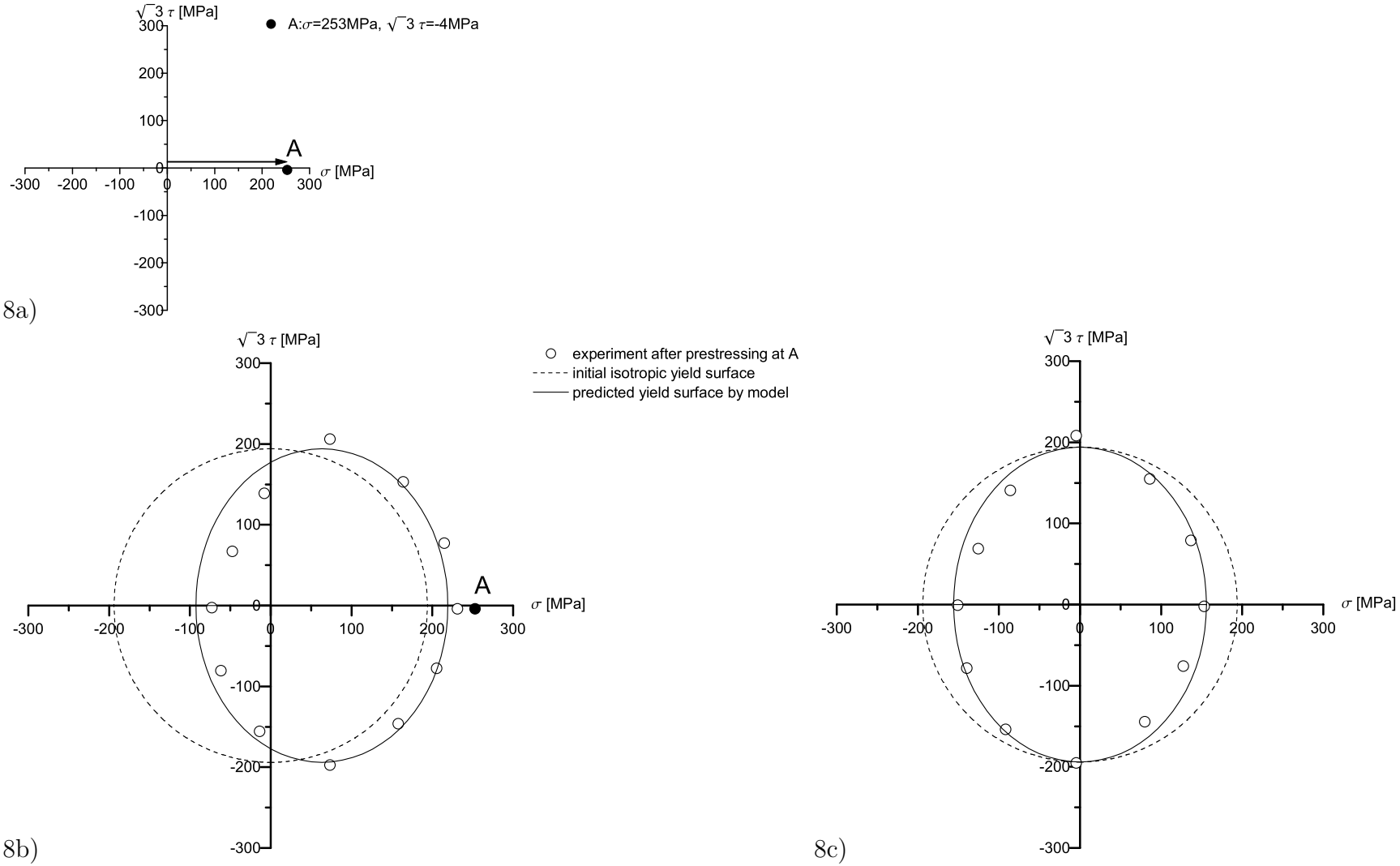

Figure 5.8: Comparison of predicted responses with experimental data, displayed in Fig. 5.8a) Loading path imposed. 5.8b) Yield locus after prestressing at A. 5.8c) Subsequent yield locus from b) placed in the origin of the stress space

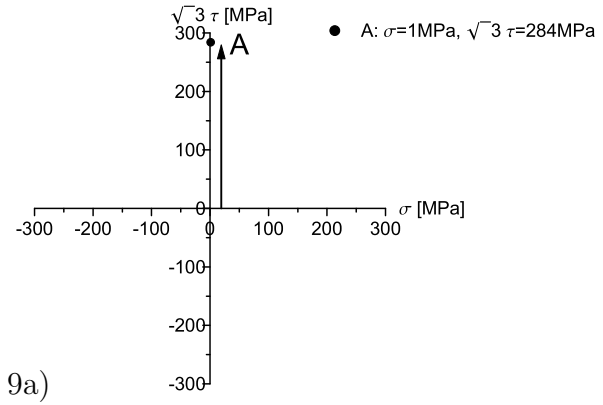

9a)

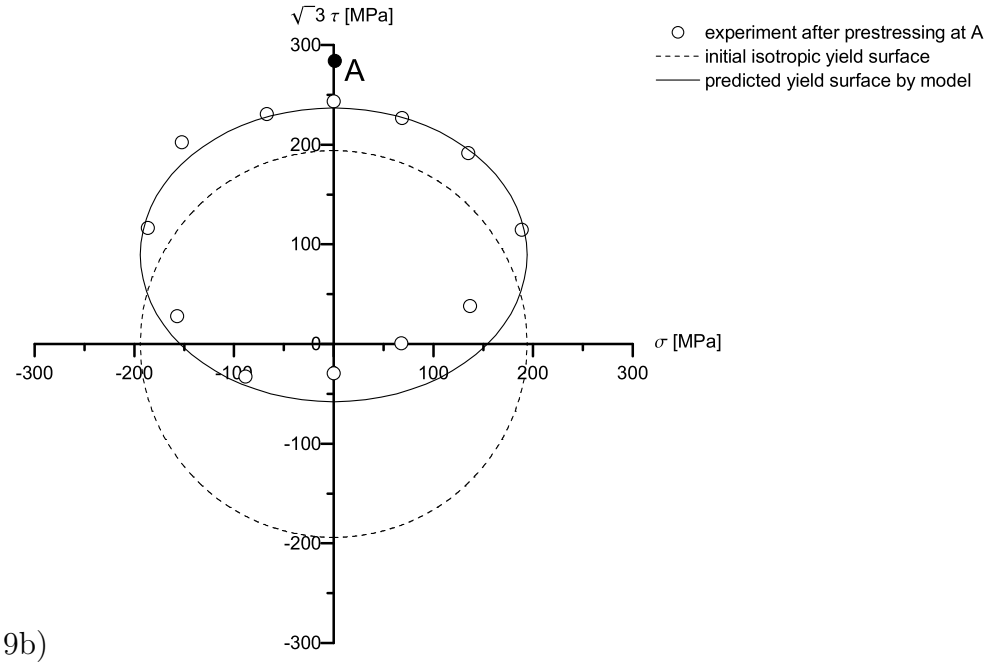

9b)

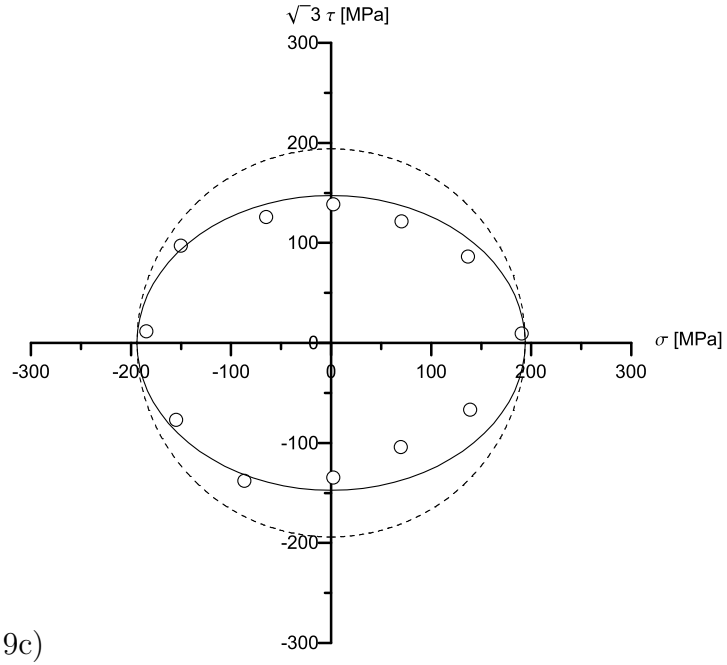

9c)

Figure 5.9: Comparison of predicted responses with experimental data, displayed in Fig. 5.9a) Loading path imposed. 5.9b) Yield locus after prestressing at A. 5.9c) Subsequent yield locus from 5.9b) placed in the origin of the stress space

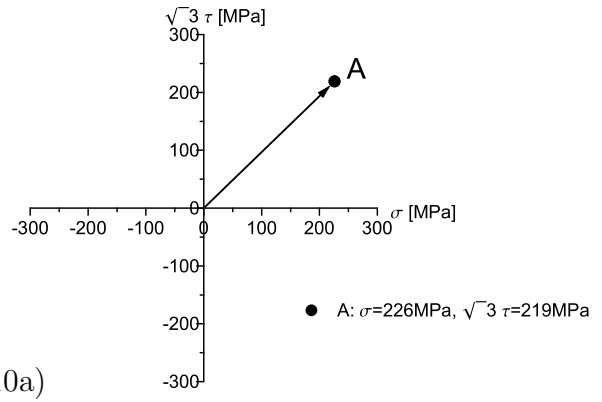

10a)

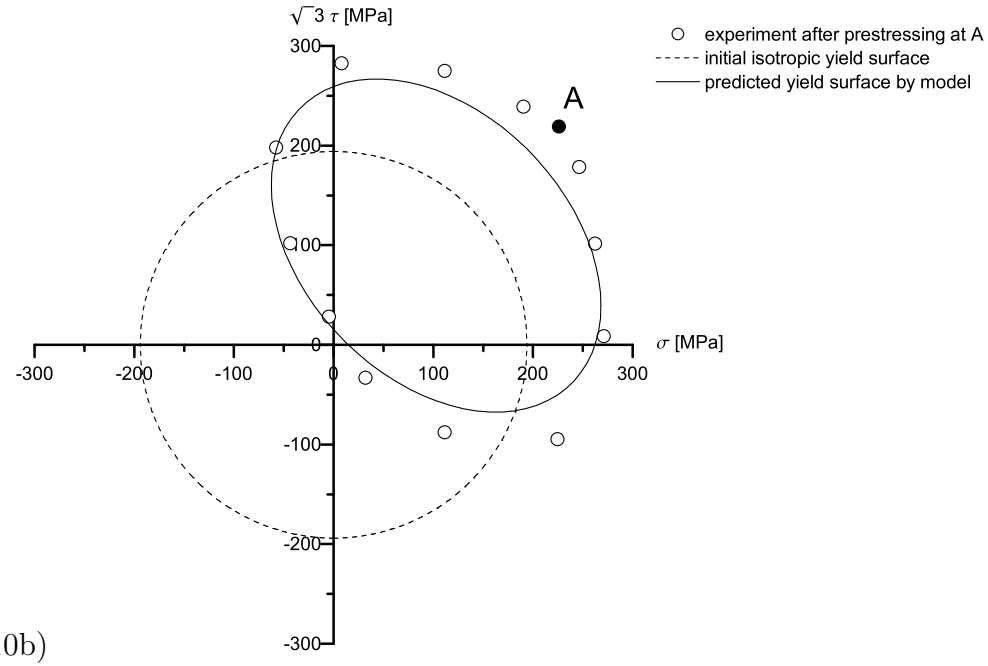

10b)

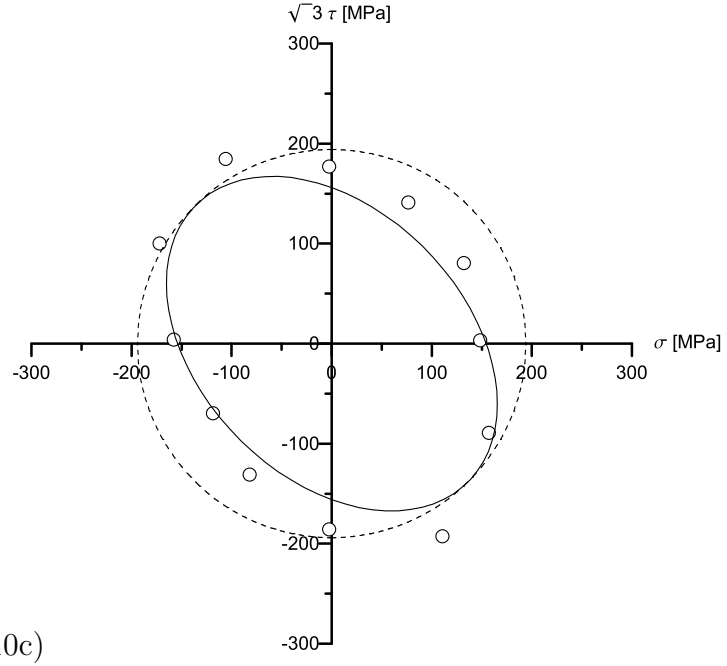

10c)

Figure 5.10: Comparison of predicted responses with experimental data, displayed in Fig. 5.10a) Loading path imposed. 5.10b) Yield locus after prestressing at A. 5.10c) Subsequent yield locus from 5.10b) placed in the origin of the stress space

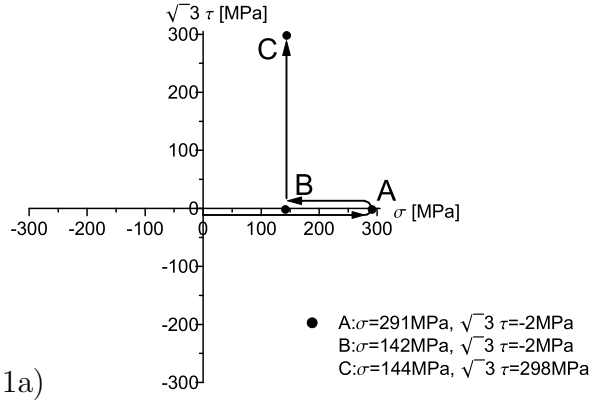

11a)

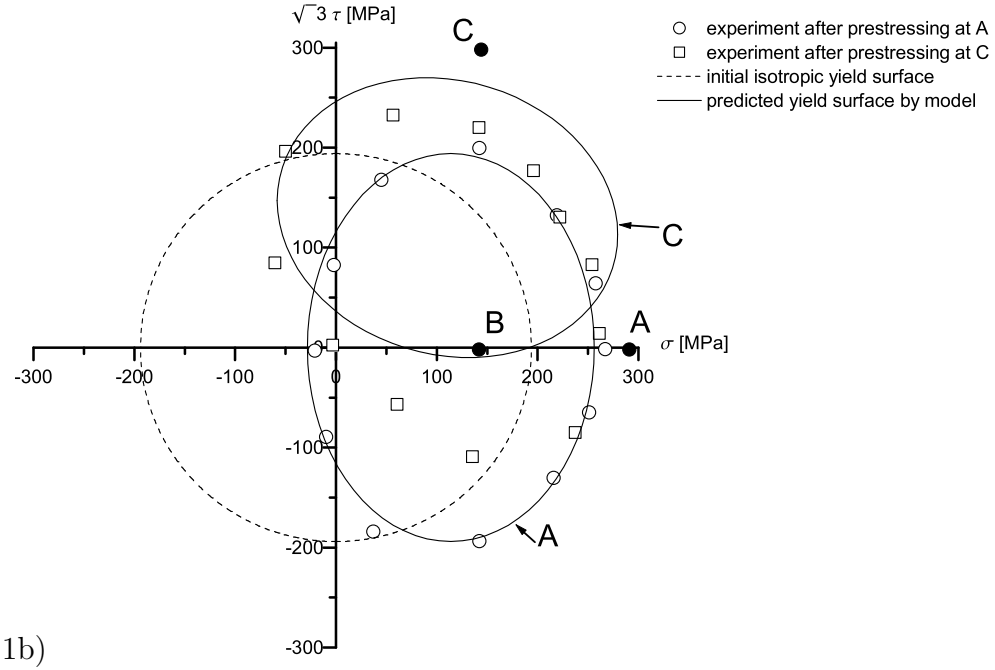

11b)

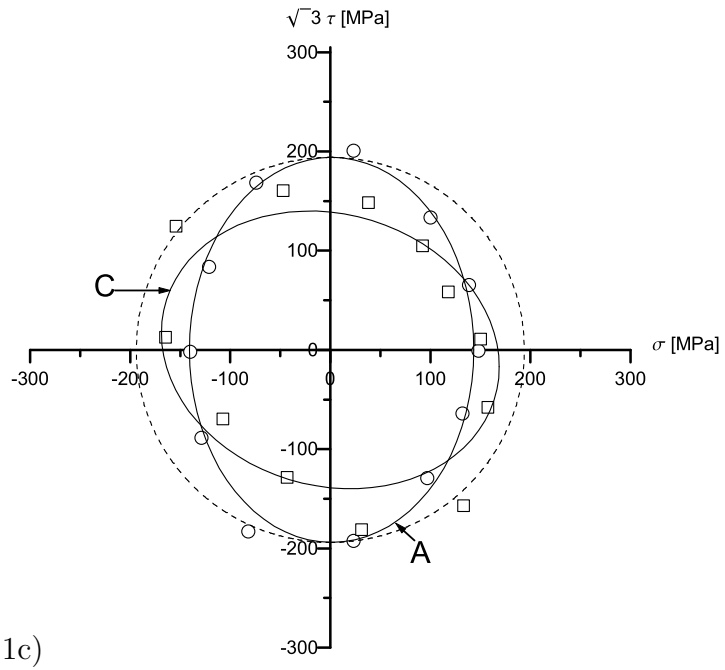

11c)

Figure 5.11: Comparison of predicted responses with experimental data, displayed in Fig. 5.11a) Loading path imposed. 5.11b) Yield loci after prestressing at A and C. 5.11c) Subsequent yield loci from 5.11b) placed in the origin of the stress space

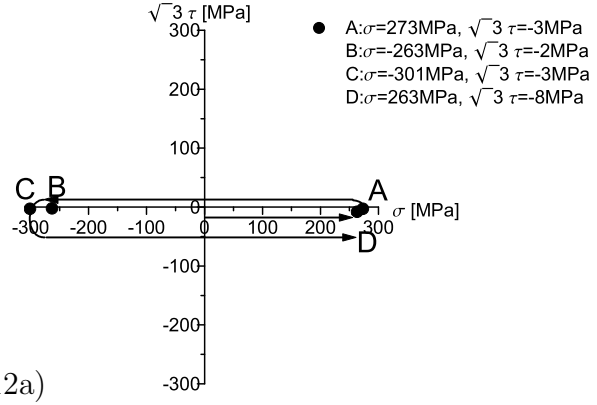
√3 τ [MPa]
A:σ=273MPa, √3 τ=-3MPa
B:σ=-263MPa, √3 τ=-2MPa
C:σ=-301MPa, √3 τ=-3MPa
D:σ=263MPa, √3 τ=-8MPa
C
B
A
D
σ [MPa]

12a)

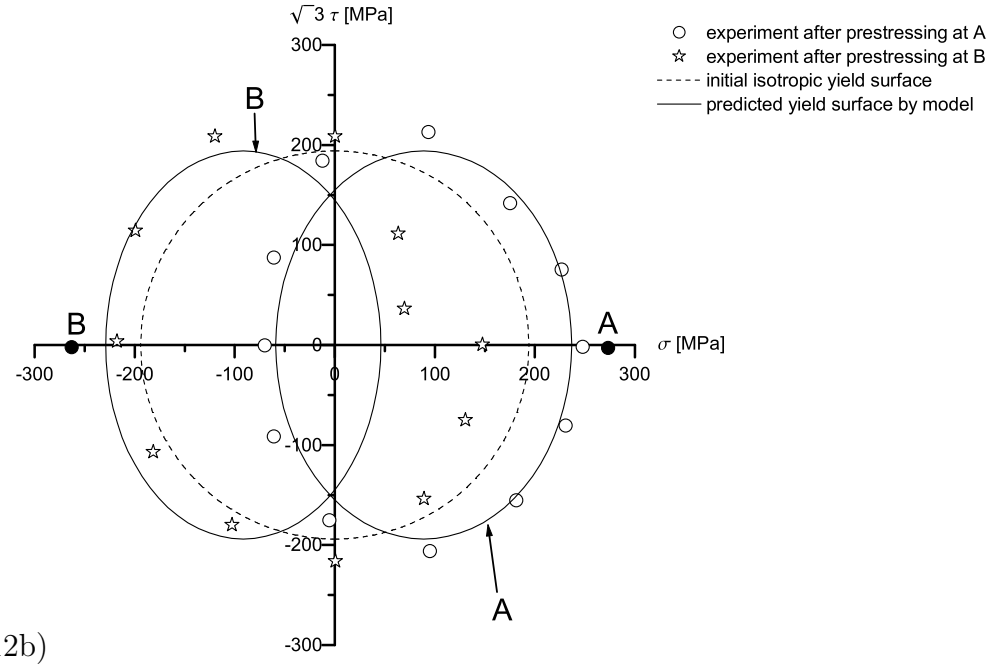
√3 τ [MPa]
experiment after prestressing at A
experiment after prestressing at B
initial isotropic yield surface
predicted yield surface by model
B
B
A
A
σ [MPa]

12b)

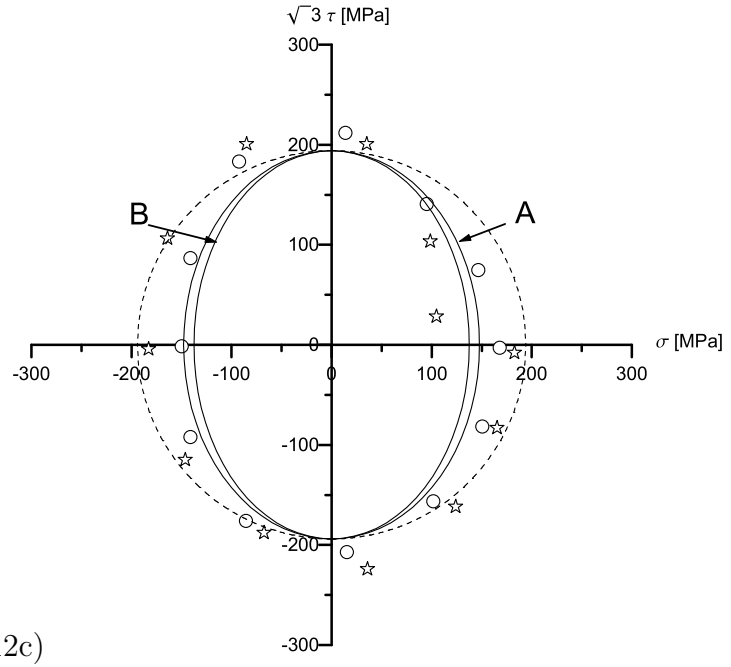
√3 τ [MPa]
B
A
σ [MPa]

12c)

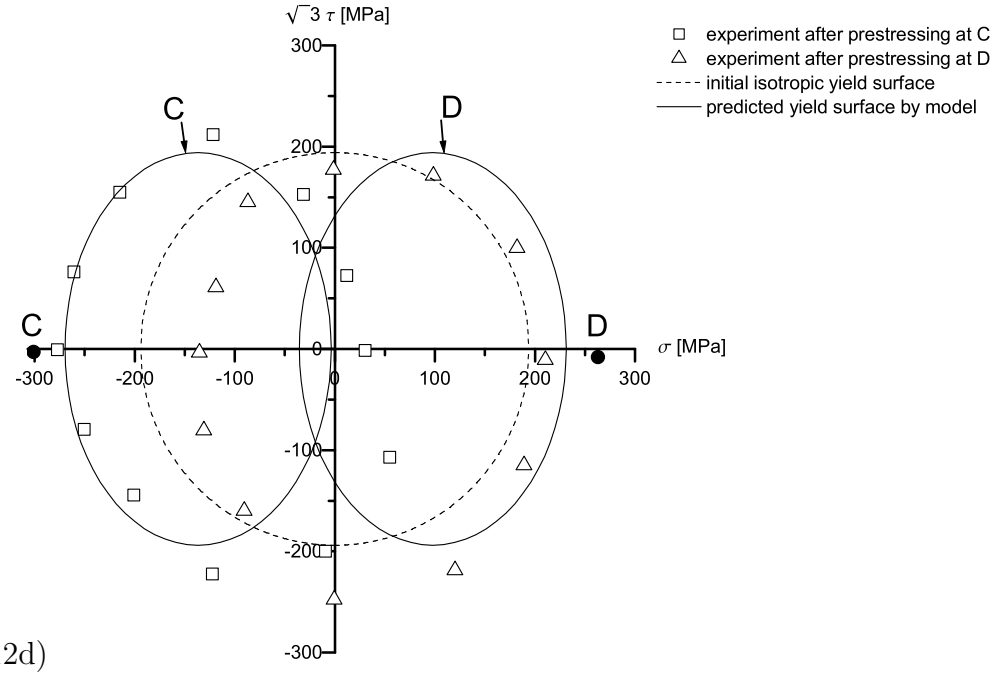

12d)

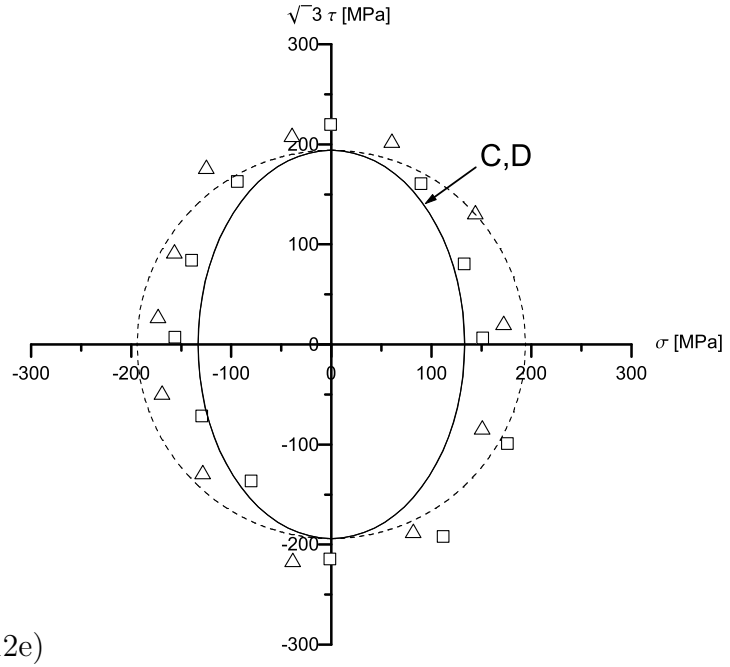

12e)

Figure 5.12: Comparison of predicted responses with experimental data, displayed in Fig. 5.12a) Loading path imposed. 5.12b) Yield loci after prestressing at A and B. 5.12c) Subsequent yield loci from 5.12b) placed in the origin of the stress space. 5.12d) Yield loci after prestressing at C and D. 5.12e) Subsequent yield loci from 5.12d) placed in the origin of the stress space

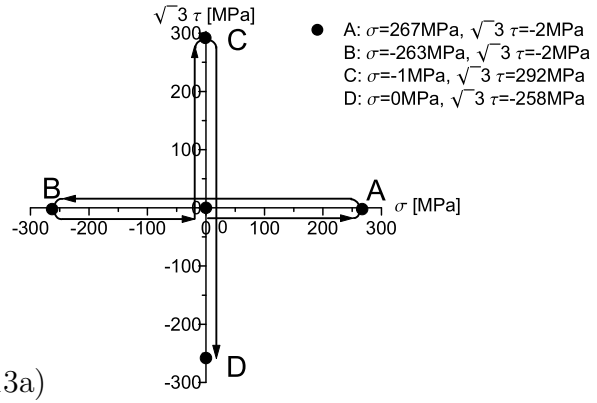
√3 τ [MPa]
A: σ=267MPa, √3 τ=-2MPa
B: σ=-263MPa, √3 τ=-2MPa
C: σ=-1MPa, √3 τ=292MPa
D: σ=0MPa, √3 τ=-258MPa
A
B
C
D
σ [MPa]

13a)

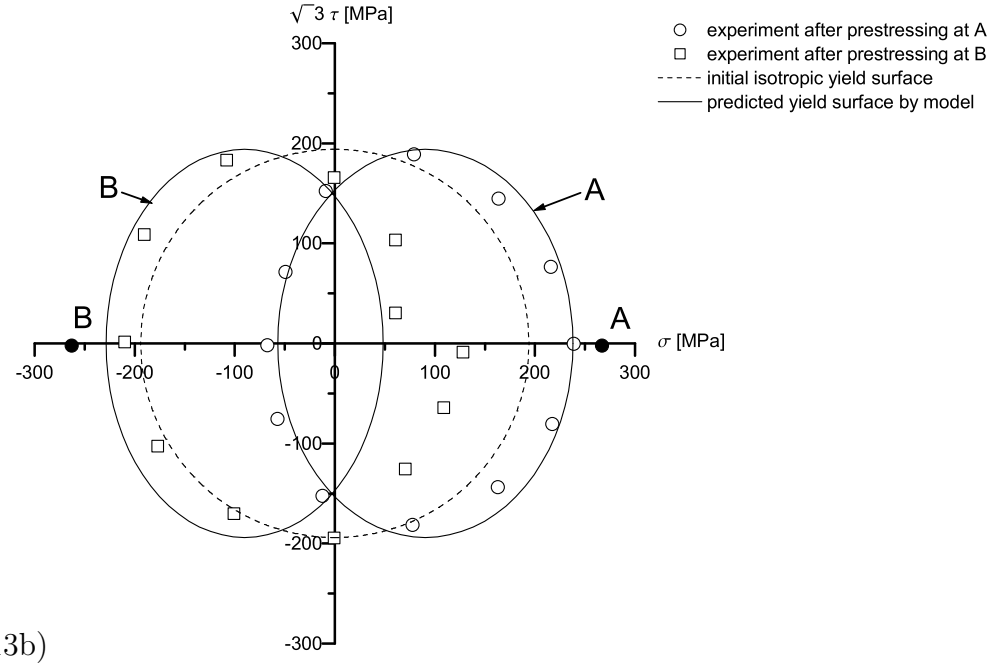
√3 τ [MPa]
experiment after prestressing at A
experiment after prestressing at B
initial isotropic yield surface
predicted yield surface by model
A
B
σ [MPa]

13b)

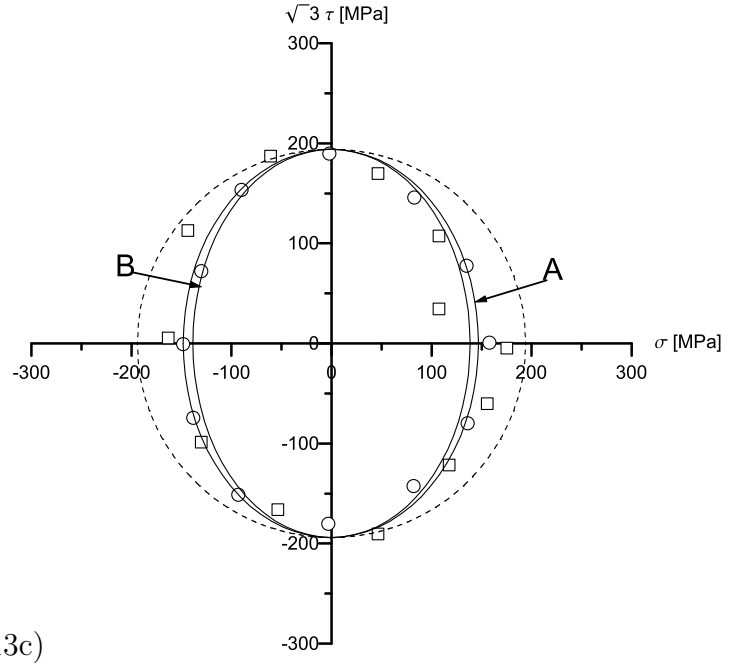
√3 τ [MPa]
A
B
σ [MPa]

13c)

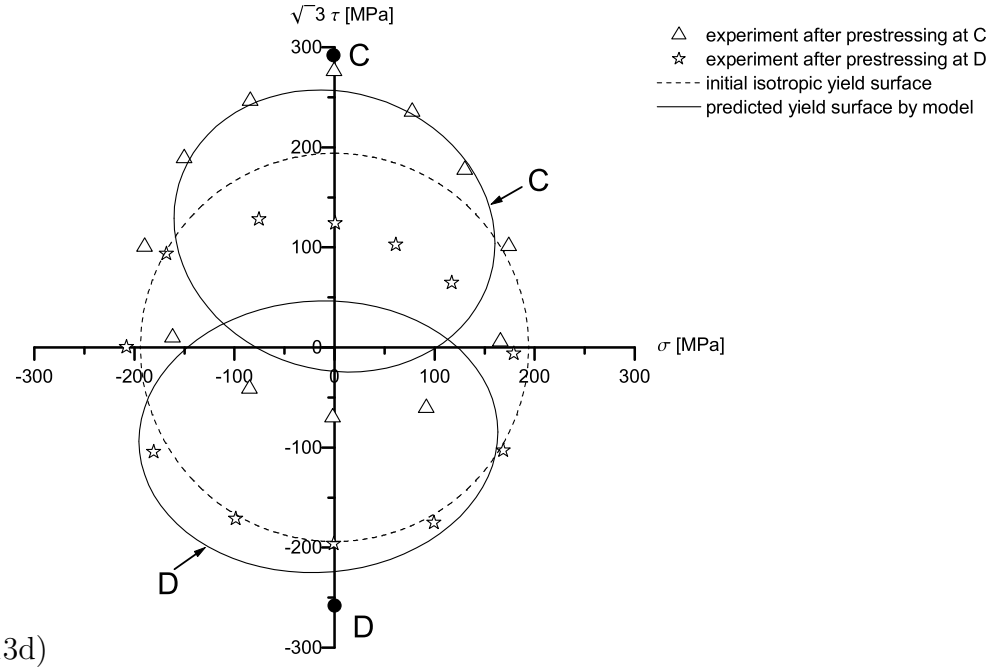

13d)

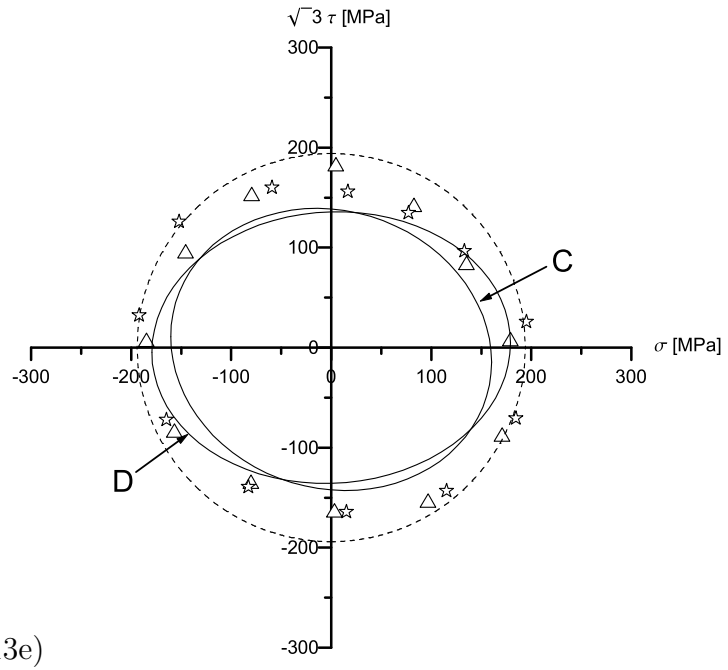

13e)

Figure 5.13: Comparison of predicted responses with experimental data, displayed in Fig. 5.13a) Loading path imposed. 5.13b) Yield loci after prestressing at A and B. 5.13c) Subsequent yield loci from 5.13b) placed in the origin of the stress space. 5.13d) Yield loci after prestressing at C and D. 5.13e) Subsequent yield loci from 5.13d) placed in the origin of the stress space

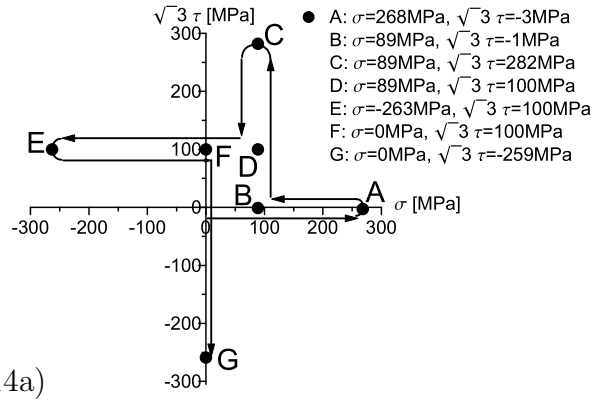
√3 τ [MPa]
σ [MPa]
A: σ=268MPa, √3 τ=-3MPa
B: σ=89MPa, √3 τ=-1MPa
C: σ=89MPa, √3 τ=282MPa
D: σ=89MPa, √3 τ=100MPa
E: σ=-263MPa, √3 τ=100MPa
F: σ=0MPa, √3 τ=100MPa
G: σ=0MPa, √3 τ=-259MPa

14a)

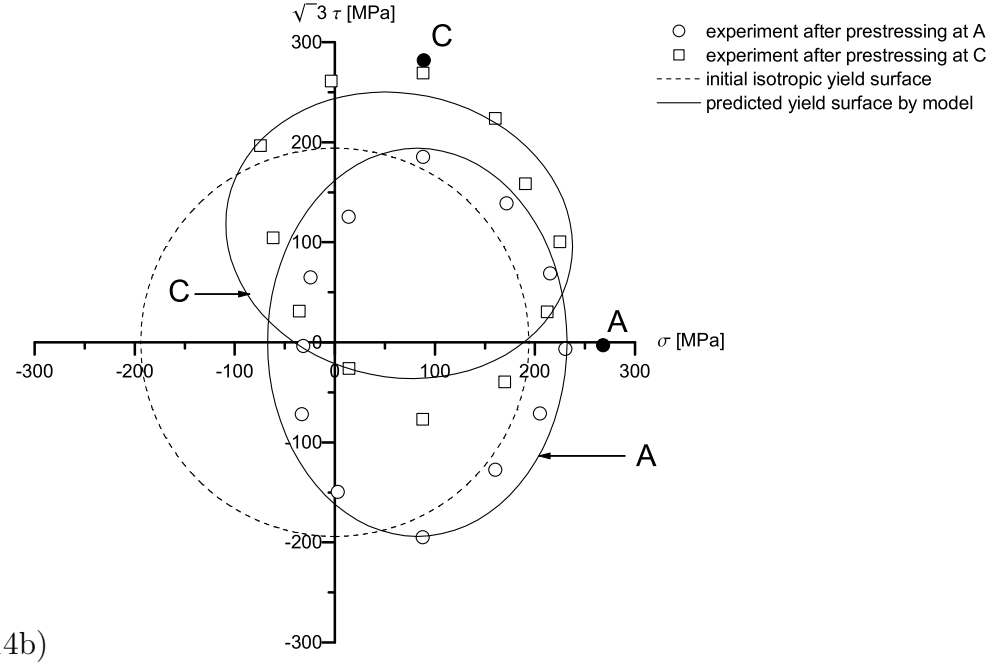
√3 τ [MPa]
σ [MPa]
experiment after prestressing at A
experiment after prestressing at C
initial isotropic yield surface
predicted yield surface by model

14b)

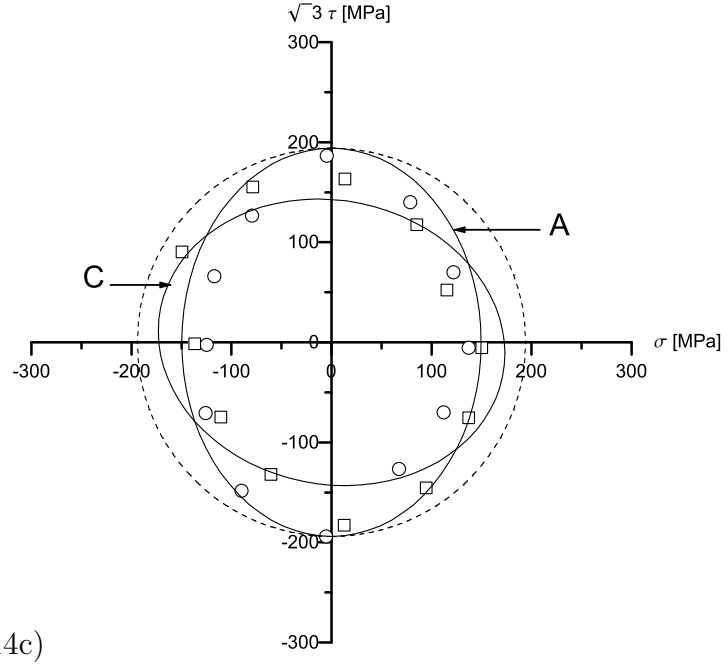
√3 τ [MPa]
σ [MPa]

14c)

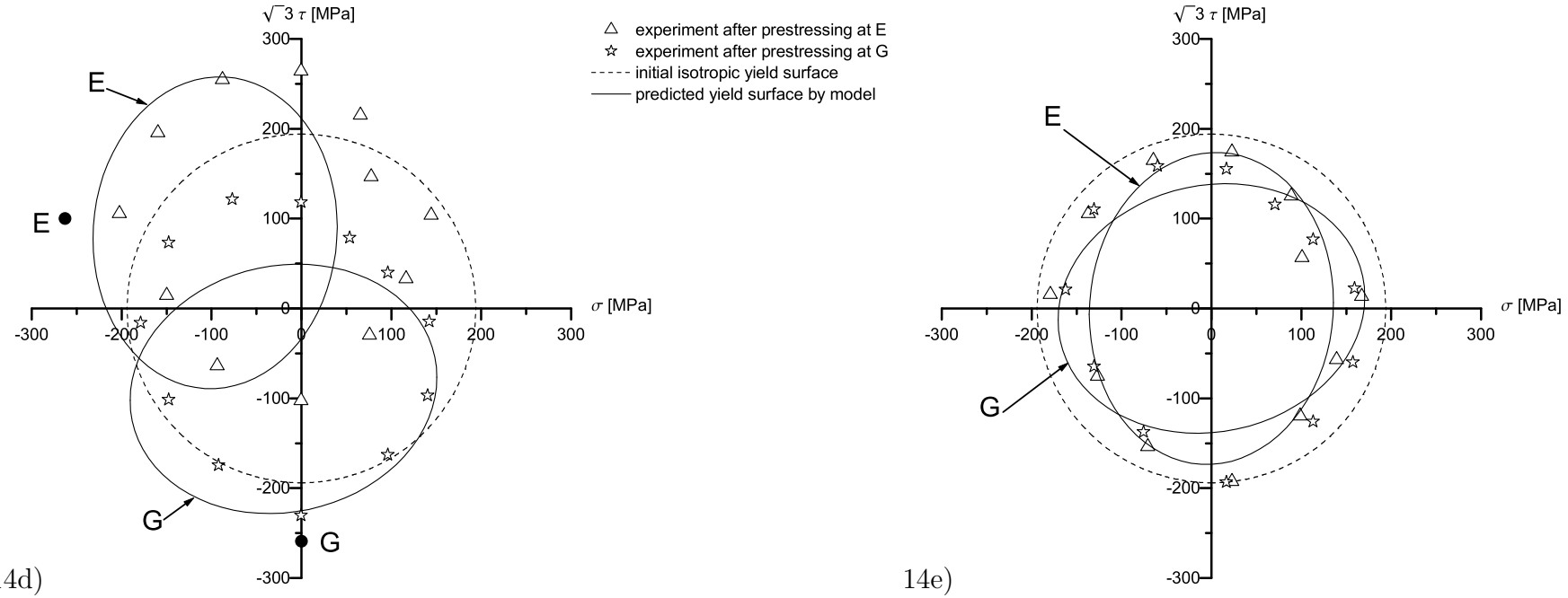

14d) 14e)

Figure 5.14: Comparison of predicted responses with experimental data, displayed in Fig. 5.14a) Loading path imposed. 5.14b) Yield loci after prestressing at A and C. 5.14c) Subsequent yield loci from 5.14b) placed in the origin of the stress space. 5.14d) Yield loci after prestressing at E and G. 5.14e) space

Chapter 6

Summary

This work is basically divided in two parts. In the first one, a thermodynamically consistent constitutive model describing plastic anisotropy at large deformations has been adjusted to predict the mechanical response of single crystal alloys showing cubic symmetry. The model is based on the multiplicative decomposition of the deformation gradient tensor into an elastic and an inelastic part and is invariant under arbitrary rigid body rotations superposed on both the actual and the plastic intermediate configuration. In order to describe the hardening response, an internal back stress tensor of MANDEL type is introduced and evolution equations are derived as sufficient conditions for the validity of the dissipation inequality in every admissible process. Structural tensors, representing local axes of symmetry are used to describe anisotropic constitutive properties. The constitutive theory allows to predict a deformation induced rotation of the symmetry axes. This is possible by incorporating rotation tensors, following DAFALIAS [26] [31] and DAFALIAS AND RASHID [28], which correspond to the independent evolution of anisotropy in the elasticity law, the kinematic hardening and the flow rule. For the rotation tensors in the elasticity law and the kinematic hardening, evolution equations are derived as sufficient conditions for the second law of thermodynamics in form of the CLAUSIUS-DUHEM inequality. The constitutive model was developed for large deformations using the concept of dual variables (see HAUPT AND TSAKMAKIS [40]) and was formulated in the stress-free plastic intermediate configuration.
For small elastic strains, the anisotropic plasticity model was implemented in the finite element code ABAQUS through the user subroutine UMAT (see ABAQUS STANDARD USER'S MANUAL [2], 24.2.30). No further simplification has been made, but the complete expression for kinematic hardening and a hyperelasticity law were used. The system of differential equations has been resolved through an operator-split procedure. In the first operator the elastic part is solved, using a midpoint rule and in the second operator the inelastic part is solved via an implicit-EULER-procedure. ABAQUS requires the so-called material JACOBIAN matrix, which has been computed numerically, since an analytical solution of this would be very fault sensitive and inflexible to any change in the constitutive equations. Here the dearest part of the computation is the solution of the system of nonlinear equations in the second operator (50 for orthotropy), for which no really efficient algorithm exists. The following quotation expresses this quite well:

"We make an extreme, but wholly defensible, statement: There are *no* good, general methods for solving systems of more than one nonlinear equation"(PRESS ET AL. [92], chapter 9.6).

To demonstrate the capabilities of the proposed constitutive model, a BRINELL hardness indentation test was simulated and compared with experimental results. It could be shown, that the

constitutive model is able to predict the physical behavior of the material correctly, although an explicit determination of material parameters, describing the experiment, was not done. The question still remains, whether it is possible to obtain better results through a simple change of material parameters, or if other material functions, namely a different yield function, would lead to more realistic findings.

In the second part of this work a thermodynamically consistent model was proposed, describing the evolution of anisotropy in the yield surface for polycrystalline materials. The model is based on the derivation of sufficient conditions for the so-called dissipation inequality. Attention was confined to small elastic-viscoplastic deformations, for which the equations, constituting the material model, were derived. As the experimental results by ISHIKAWA [59] suggested, an initial isotropic yield surface using the VON MISES yield function was supposed and isotropic hardening could be neglected. Inelastic flow was postulated to occur, whenever a positive overstress applies. The hardening rules were formulated in a way that kinematic hardening and distortional hardening were considered separately, whereas rotational hardening was not involved. Comparison between the experimental results of ISHIKAWA [59] and the proposed constitutive model showed its capabilities to predict material response well for the case of tensile and torsional loading alone, but also revealed its shortcomings in the case of combined tensile and torsional loading due to the lack of both, a suitable description of the rotation of the yield surface and an appropriate set of material parameters.

Appendix A

Transformations under rigid body rotations superposed on both, the actual and the plastic intermediate configuration

It can be seen (cf. Casey and Naghdi [14], [16], Green and Naghdi [39]) that under rigid body rotations $\mathbf{Q} = \mathbf{Q}(t)$ superposed on the actual configuration, and rigid body rotations $\overline{\mathbf{Q}} = \overline{\mathbf{Q}}(t)$ superposed on the plastic intermediate configuration simultaneously, the following transformations for the deformation and stress tensors apply.

Deformation gradient tensor:

$$\mathbf{F} \to \mathbf{F}^{\star} = \mathbf{Q}\mathbf{F} = \mathbf{Q}\mathbf{F}_e\overline{\mathbf{Q}}^T\overline{\mathbf{Q}}\mathbf{F}_p \quad . \tag{A.1}$$

Elastic deformation tensors:

$$\mathbf{F}_e \to \mathbf{F}_e^{\star} = \mathbf{Q}\mathbf{F}_e\overline{\mathbf{Q}}^T \quad , \tag{A.2}$$
$$\mathbf{Q}_e \to \mathbf{Q}_e^{\star} = \mathbf{Q}\mathbf{Q}_e\overline{\mathbf{Q}}^T \quad , \tag{A.3}$$
$$\hat{\mathbf{U}}_e \to \hat{\mathbf{U}}_e^{\star} = \overline{\mathbf{Q}}\hat{\mathbf{U}}_e\overline{\mathbf{Q}}^T \quad , \tag{A.4}$$
$$\mathbf{V}_e \to \mathbf{V}_e^{\star} = \mathbf{Q}\mathbf{V}_e\mathbf{Q}^T \quad , \tag{A.5}$$
$$\hat{\mathbf{C}}_e \to \hat{\mathbf{C}}_e^{\star} = \overline{\mathbf{Q}}\hat{\mathbf{C}}_e\overline{\mathbf{Q}}^T \quad , \tag{A.6}$$
$$\hat{\mathbf{\Gamma}}_e \to \hat{\mathbf{\Gamma}}_e^{\star} = \overline{\mathbf{Q}}\hat{\mathbf{\Gamma}}_e\overline{\mathbf{Q}}^T \quad . \tag{A.7}$$

Plastic deformation tensors:

$$\mathbf{F}_p \to \mathbf{F}_p^{\star} = \overline{\mathbf{Q}}\mathbf{F}_p \quad , \tag{A.8}$$
$$\mathbf{Q}_p \to \mathbf{Q}_p^{\star} = \overline{\mathbf{Q}}\mathbf{Q}_p \quad , \tag{A.9}$$
$$\mathbf{U}_p \to \mathbf{U}_p^{\star} = \mathbf{U}_p \quad , \tag{A.10}$$
$$\hat{\mathbf{V}}_p \to \hat{\mathbf{V}}_p^{\star} = \overline{\mathbf{Q}}\hat{\mathbf{V}}_p\overline{\mathbf{Q}}^T \quad , \tag{A.11}$$
$$\hat{\mathbf{B}}_p \to \hat{\mathbf{B}}_p^{*} = \overline{\mathbf{Q}}\hat{\mathbf{B}}_p\overline{\mathbf{Q}}^T \quad , \tag{A.12}$$
$$\hat{\mathbf{\Gamma}}_p \to \hat{\mathbf{\Gamma}}_p^{\star} = \overline{\mathbf{Q}}\hat{\mathbf{\Gamma}}_p\overline{\mathbf{Q}}^T \quad . \tag{A.13}$$

Plastic velocity gradients:

$$\hat{\mathbf{L}}_p \to \hat{\mathbf{L}}_p^\star = \overline{\mathbf{Q}}\hat{\mathbf{L}}_p\overline{\mathbf{Q}}^T + \dot{\overline{\mathbf{Q}}}\,\overline{\mathbf{Q}}^T \quad , \tag{A.14}$$

$$\hat{\mathbf{W}}_p \to \hat{\mathbf{W}}_p^\star = \overline{\mathbf{Q}}\hat{\mathbf{W}}_p\overline{\mathbf{Q}}^T + \dot{\overline{\mathbf{Q}}}\,\overline{\mathbf{Q}}^T \quad , \tag{A.15}$$

$$\hat{\mathbf{D}}_p \to \hat{\mathbf{D}}_p^\star = \overline{\mathbf{Q}}\hat{\mathbf{D}}_p\overline{\mathbf{Q}}^T \quad . \tag{A.16}$$

Stress tensors:

$$\hat{\mathbf{T}} \to \hat{\mathbf{T}}^\star = \overline{\mathbf{Q}}\hat{\mathbf{T}}\overline{\mathbf{Q}}^T \quad , \tag{A.17}$$

$$\hat{\mathbf{P}} \to \hat{\mathbf{P}}^\star = \overline{\mathbf{Q}}\hat{\mathbf{P}}\overline{\mathbf{Q}}^T \quad . \tag{A.18}$$

The transformation rules under rigid body rotations superposed only on the actual or only on the plastic intermediate configuration are obtained by setting in the relations above $\overline{\mathbf{Q}} = \mathbf{1}$ or $\mathbf{Q} = \mathbf{1}$, respectively.

Appendix B

Reduced forms for the specific free energy function ψ_e

Let ψ_e be given by (3.20). Then the following applies.

Theorem:
The free energy ψ_e is unaltered under arbitrary rigid body rotations superposed on both the actual and the plastic intermediate configuration, i.e.

$$\psi_e = \overline{\psi}_e\left(\mathbf{F}_e, \mathbf{\Phi}\right) = \overline{\psi}_e\left(\mathbf{F}_e^\star, \mathbf{\Phi}^\star\right) \qquad , \tag{B.1}$$

if and only if ψ_e obeys the representations

$$\psi_e = \overline{\psi}_e\left(\mathbf{F}_e, \mathbf{\Phi}\right) = \overline{\overline{\psi}}_e\left(\hat{\mathbf{\Gamma}}_e, \mathbf{\Phi}\right) = \tilde{\psi}_e\left(\mathbf{\Phi}^T\hat{\mathbf{\Gamma}}_e\mathbf{\Phi}\right) \qquad . \tag{B.2}$$

Proof:
First it can be shown that (B.1) implies (B.2). The relations in Appendix A and (3.21) will be used to obtain

$$\psi_e = \overline{\psi}_e\left(\mathbf{F}_e^\star, \mathbf{\Phi}^\star\right) = \overline{\psi}_e\left(\mathbf{Q}\mathbf{F}_e\overline{\mathbf{Q}}^T, \overline{\mathbf{Q}}\mathbf{\Phi}\right) \qquad . \tag{B.3}$$

Here, $\mathbf{Q} = \overline{\mathbf{Q}}\mathbf{R}_e^T$ is set, so that

$$\psi_e = \overline{\psi}_e\left(\overline{\mathbf{Q}}\mathbf{R}_e^T\mathbf{R}_e\hat{\mathbf{U}}_e\overline{\mathbf{Q}}^T, \overline{\mathbf{Q}}\mathbf{\Phi}\right) = \overline{\psi}_e\left(\overline{\mathbf{Q}}\hat{\mathbf{U}}_e\overline{\mathbf{Q}}^T, \overline{\mathbf{Q}}\mathbf{\Phi}\right) \qquad . \tag{B.4}$$

For $\overline{\mathbf{Q}} = \mathbf{1}$ it can be shown

$$\psi_e = \overline{\psi}_e\left(\sqrt{\hat{\mathbf{C}}_e}, \mathbf{\Phi}\right) =: \overline{\overline{\psi}}_e\left(\hat{\mathbf{\Gamma}}_e, \mathbf{\Phi}\right) \qquad , \tag{B.5}$$

which confirms $(B.2)_2$. On the other hand, choosing $\overline{\mathbf{Q}} = \mathbf{\Phi}^T$ in Eq. (B.4), then

$$\psi_e = \overline{\psi}_e\left(\mathbf{\Phi}^T\hat{\mathbf{U}}_e\mathbf{\Phi}, \mathbf{1}\right) \qquad . \tag{B.6}$$

Note that

$$\left(\mathbf{\Phi}^T\hat{\mathbf{U}}_e\mathbf{\Phi}\right)^2 = \mathbf{\Phi}^T\hat{\mathbf{C}}_e\mathbf{\Phi} = 2\mathbf{\Phi}^T\hat{\mathbf{\Gamma}}_e\mathbf{\Phi} + \mathbf{1} \qquad , \tag{B.7}$$

which indicates that $\mathbf{\Phi}^T\hat{\mathbf{U}}_e\mathbf{\Phi}$ may be expressed in terms of $\mathbf{\Phi}^T\hat{\mathbf{\Gamma}}_e\mathbf{\Phi}$. Thus, following from (B.6), ψ_e can be recasted as a function of $\mathbf{\Phi}^T\hat{\mathbf{\Gamma}}_e\mathbf{\Phi}$, which implies the representation $(B.2)_3$. In order to proof that (B.2) leads to (B.1), it should be observed that (B.2) implies

$$\overline{\psi}_e\left(\mathbf{F}_e^\star, \mathbf{\Phi}^\star\right) = \tilde{\psi}_e\left(\mathbf{\Phi}^{\star T}\hat{\mathbf{\Gamma}}_e^\star\mathbf{\Phi}^\star\right) \qquad , \tag{B.8}$$

or, by virtue of the property $\mathbf{\Phi}^{\star T}\hat{\mathbf{\Gamma}}_e^\star\mathbf{\Phi}^\star = \mathbf{\Phi}^T\hat{\mathbf{\Gamma}}_e\mathbf{\Phi}$, following from the relations in Appendix A and (3.21),

$$\overline{\psi}_e\left(\mathbf{F}_e^\star, \mathbf{\Phi}^\star\right) = \tilde{\psi}_e\left(\mathbf{\Phi}^T\hat{\mathbf{\Gamma}}_e\mathbf{\Phi}\right) \qquad . \tag{B.9}$$

In view of (B.2), the last equation takes the form (B.1), which completes the proof of the theorem. □

Bibliography

[1] ABAQUS, *version* 6.3, 2003.

[2] ABAQUS Standard User's Manual, *version* 6.3, 2003.

[3] N. Aravas, E. C. Aifantis. On the geometry slip and spin in finite plastic deformation. *International Journal of Plasticity*, 7:141–160, 1991.

[4] N. Aravas. Finite elastoplastic transformations of transversally isotropic metals. *International Journal of Solids and Structures*, 29:2137–2157, 1992.

[5] N. Aravas. Anisotropic plasticity and the plastic spin. *Modelling Simulation in Material Science and Engineering*, 2:483–504, 1994.

[6] P. J. Armstrong, C. O. Frederick. A mathematical representation of the multiaxial Bauschinger effect. *General Electric Generating Board*, report RD/B/N **731**, 1966.

[7] R. J. Asaro. Advances in Applied Mechanics, Volume: 23, Chapter: Micromechanics of Crystals and Polycrystals, pp. 1-115. Academic Press, san Diego, 1983.

[8] R. J. Asaro, J. R. Rice. Strain localization in ductile single crystals. *Journal of the Mechanics and Physics of Solids*, 6:309–338, 1977.

[9] G. Backhaus. Zur Fließgrenze bei allgemeiner Verfestigung.*ZAMM*, 48:99–108, 1968.

[10] A. Baltov, A. Sawczuk. A rule of anisotropic hardening. *Acta Mechanica*, 1:81–92, 1964.

[11] E. W. Billington, A. Tate. *The Physics of Deformation and Flow*, McGraw-Hill, New York, 1981.

[12] J. P. Boehler. Representations for isotropic and anisotropic non-polynomial tensor functions. In *Applications of tensor functions in solid mechanics*, J. P. Boehler. CISM courses and lectures, No 292, 31–53, Springer, Wien–New York, 1987.

[13] G. E. Dieter. *Mechanical Metallurgy*, SI meteric edition, McGraw-Hill, London, 1988.

[14] J. Casey, P. Naghdi. A remark on the use of the decomposition $\mathbf{F} = \mathbf{F}_e\mathbf{F}_p$ in plasticity. *Journal of Applied Mechanics*, 47:672–675, 1980.

[15] J. Casey, P. Naghdi. On the characterization of strain-hardening in plasticity. *Journal of Applied Mechanics*, 48:285–295, 1981.

[16] J. Casey, P. Naghdi. A correct definition of elastic and plastic deformation and its computational significance. *Journal of Applied Mechanics*, 48:983–985, 1981.

[17] J. Casey, M. Tseng. A constitutive restriction related to convexity of yield surfaces in plasticity. *Zeitschrift für angewandte Mathematik und Physik*, 35:478–496, 1984.

[18] B. D. Coleman, M. E. Gurtin. Thermodynamics with internal state variables. *Journal of Chemistry in Physics*, 47:597–613, 1967.

[19] J. L. Chaboche, K. Dang-Van, G. Cordier. Modelization of the strain memory effect on the cyclic hardening of 316 stainless steel. *SMIRT-5, Division L*, Berlin, 1979.

[20] H. Cho, Y. F. Dafalias. Distortional and orientational hardening at large viscoplastic deformations. *International Journal of Plasticity*, 12:903–925, 1996.

[21] J. D. Comins, A. G. Every, P. R. Stoddart, W. Wang, X. Zang. NDE of solid surfaces and thin surface coatings by means of suface brillouin scattering of light. Presented at *The NDE (Non Destructive Evaluation) workshop*, Cape Town, April 2002.

[22] Y. F. Dafalias, E. P. Popov. A model of nonlinearly hardening materials for complex loading. *Acta Mechanica*, 21:173–192, 1975.

[23] Y. F. Dafalias, E. P. Popov. Plastic internal variables formalism of cyclic plasticity. *Journal of Applied Mechanics*, 98:645–651, 1976.

[24] Y. F. Dafalias. Il'iushin's postulate and resulting thermodynamic conditions on elastic-plastic coupling. *International Journal of Solids and Structure*, 13:239–251, 1977.

[25] Y. F. Dafalias. Anisotropic hardening of initially orthotropic materials. *ZAMM*, 59:437–446, 1979.

[26] Y. F. Dafalias. The plastic spin concept and a simple illustration of its role in finite plastic transformations. *Mechanics of Materials*, 3:223–233, 1984.

[27] Y. F. Dafalias. Issues on the constitutive formulation at large elastoplastic deformations. Part I: Kinematics. *Archives of Mechanics*, 69:119–138, 1987.

[28] Y. F. Dafalias, M. M. Rashid. The effect of plastic spin on anisotropic material behaviour. *International Journal of Plasticity*, 5:227–246, 1989.

[29] Y. F. Dafalias. The plastic spin in viscoplasticity. *International Journal of Solids and Structures*, 26(2):149–163, 1990.

[30] Y. F. Dafalias, E. C. Aifantis. On the microscopic origin of the plastic spin. *Archives of Mechanics*, 82:31–48, 1990.

[31] Y. F. Dafalias. On multiple spins and texture developement. Case study: Kinematic and orthotropic hardening. *Archives of Mechanics*, 100:171–194, 1993.

[32] Y. F. Dafalias. Plastic spin: Necessity or redundancy. *International Journal of Plasticity*, 14:909–931, 1998.

[33] Y. F. Dafalias. Orientational evolution of plastic orthotropy in sheet metals. *Journal of Mechanics and Physics of Solids*, 48:2231–2255, 2000.

[34] Y. F. Dafalias, D. Schick, Ch. Tsakmakis. A simple model for describing yield surface evolution during plastic flow. In *Deformation and failure in metallic materials*, Eds. K. Hutter and H. Baaser, Spinger, Berlin, 169–201, 2003.

[35] E. Diegele, W. Jansohn, Ch. Tsakmakis. Finite deformation plasticity and viscoplasticity laws exhibiting nonlinear hardening rules; Part I: Constitutive theory and numerical integration. *Computational Mechanics*, 25:1–12, 2000.

[36] R. Fosdick, E. Volkmann. Normality and convexity of the yield surface in non-linear plasticity. *Quarterly Journal of Applied Mathematics*, 51:117–127, 1993.

[37] E. v. d. Giessen. Continuum models for large deformation plasticity. Part I: Large deformation plasticity and the concept of a natural reference state. *European Journal of Mechanics A/Solids*, 8:15–34, 1989.

[38] E. v. d. Giessen. Continuum models for large deformation plasticity. Part II: A kinematic hardening model and the concept of a plastically induced orientation tensor. *European Journal of Mechanics A/Solids*, 8:89–108, 1989.

[39] A. E. Green, P. Naghdi. Some remarks on the elastic-plastic deformations at finite strains. *International Journal of Engineering Science*, 9:1219–1229, 1971.

[40] P. Haupt, Ch. Tsakmakis. On the application of dual variables in continuum mechanics. *Continuum Mechanics and Thermodynamics*, 1:165–196, 1989.

[41] P. Haupt. Foundation of Continuum Mechanics. In *IUTAM International Summer School on Continuum Mechanics in Environment Sciences and Geophysics*. Udine, June 1992.

[42] O. Häusler. Anisotropes plastisches Fließen bei großen Deformationen. Ph.D thesis. FZKA 6351, Forschungszentrum Karlsruhe GmbH, Institut für Materialforschung, 1999.

[43] O. Häusler, D. Schick and Ch. Tsakmakis. Description of plastic anisotropy effects at large deformations. Part II: The case of transverse isotropy. *International Journal of Plasticity*, 20:199–223, 2004.

[44] S. S. Hecker. Yield surfaces in prestrained aluminum and copper. *Metallurgical Transactions*, 2:2077–2086, 1971.

[45] S. S. Hecker. Influence of deformation history on yield locus and stress-strain behaviour of aluminum and copper. *Metallurgical Transactions*, 4:985–989, 1973.

[46] D. E. Helling, A. K. Miller, M. G. Stout. An experimental investigation of the yield loci of 1100-0 aluminum, 70:30 brass, and an overaged 2024 aluminum alloy after various prestrains. *Journal of Engineering Materials and Technology, ASME*, 108:313–320, 1986.

[47] G. A. Henshall, D. E. Helling, A. K. Miller. Improvements in the MATMOD equations for modeling solute effects and yield-surface distortion. In *Unified Constitutive laws of plastic deformation*, Eds. A. S. Krausz, K. Krausz, Academic Press, New York, 153–227, 1996.

[48] W. Hermann, H. G. Sockel, J. Han, A. Bertram. Elastic properties and determination of elastic constants of nickel-base superalloys by a free beam technique. In *Superalloys 1996*, Eds. R. D. Kissinger, D. J. Deye, D. L. Anton, A. D. Cetel, M. V. Nathal, T. M. Pollock, D. A. Woodford, The Minerals, Metals & Materials Society, 1996.

[49] R. Hill. On constitutive inequalities for simple materials -II. *Journal of the Mechanics and Physics of Solids*, 16:315–322, 1968.

[50] R. Hill, J. R. Rice. Elastic potentials and the structure of inelastic constitutive laws. SIAM, 25:448–461, 1973.

[51] N. Huber. Zur Bestimmung von mechanischen Eigenschaften mit dem Eindruckversuch. Ph.D thesis. FZKA 5850, Forschungszentrum Karlsruhe GmbH, Institut für Materialforschung, 1996.

[52] N. Huber, D. Munz, Ch. Tsakmakis. Determination of Young's modulus by spherical indentation. *Journal of Materials Research*, 12:2459–2469, 1997.

[53] N. Huber, Ch. Tsakmakis. Determination of constitutive properties from spherical indentation data using neural networks. Part I: The case of pure kinematic hardening in plasticity laws. *Journal of the Mechanics and Physics of Solids*, 47:1569–1588, 1999.

[54] N. Huber, Ch. Tsakmakis. Determination of constitutive properties from spherical indentation data using neural networks. Part II: Plasticity with nonlinear isotropic and kinematic hardening. *Journal of the Mechanics and Physics of Solids*, 47:1589–1607, 1999.

[55] N. Huber, A. Konstantinidis, Ch. Tsakmakis. Determination of Poisson's ratio by spherical indentation using neural networks. Part I: Theory. *Journal of Applied Mechanics*, 68:218–223, 2001.

[56] N. Huber, Ch. Tsakmakis. Determination of Poisson's ratio by spherical indentation using neural networks. Part II: Identification method. *Journal of Applied Mechanics, ASME*, 68: 224–229, 2001.

[57] N. Huber. Anwendungen Neuronaler Netze bei nichtlinearen Problemen der Mechanik. Habilitationsschrift. FZKA 6504, Forschungszentrum Karlsruhe GmbH, Institut für Materialforschung, 2000.

[58] K. Ikegami. Experimental plasticity on the anisotropy of metals. In *Proceedings of the Euromech Colloquium 115*, Ed. J. P. Boehler, Éditions du Centre National de la Recherche Scientifique, Paris, 201–227, 1982.

[59] H. Ishikawa. Subsequent yield surface probed from its current center. *International Journal of Plasticity* 13:533–549, 1997.

[60] H. Ishikawa, K. Sasaki. Yield surface of SUS304 under cyclic loading. *Journal of Engineering Materials and Technology, ASME*, 110:364–371, 1988.

[61] H. Ishikawa, K. Sasaki. Deformation induced anisotropy and memorized back stress in constitutive model. *International Journal of Plasticity*, 14:627–646, 1998.

[62] W. Jansohn. Formulierung und Integration von Stoffgesetzen zur Beschreibung großer Deformationen in der Thermoplastizität und -viskoplastizität. Ph.D thesis. FZKA 6002, Forschungszentrum Karlsruhe GmbH, Institut für Materialforschung, 1997.

[63] A. S. Khan, X. Wang. An experimental study on subsequent yield surface after finite shear prestraining. *International Journal of Plasticity*, 9:889–905, 1993.

[64] A. S. Khan, S. Huang. Continuum theory of plasticity. Wiley, New York, 1995.

[65] Z. L. Kowalewski, M. Śliwowski. Effect of cyclic loading on yield surface evolution of 18G2A low-alloy steel. *International Journal of Mechanical Sciences*, 39:51–68, 1997.

[66] J. Kratochvil, O. W. Dillon jr. Thermodynamics of elastic-plastic materials as a theory with internal state variables. *Journal of Applied Physics*, 40:3207–3218, 1969.

[67] E. Krempl. Models of viscoplasticity - some comments on equilibrium (back)stress and drag stress. *Acta Mechanica*, 69:25–42, 1987.

[68] E. H. Lee, D. T. Liu. Finite strain elastic-plastic theory particulary for wave analysis. *Journal of Applied Physics*, 38:19, 1967.

[69] H. C. Lin, M. P. Naghdi. Necessary and sufficient conditions for the validity of a work inequality in finite plasticity. *The Quarterly Journal of Mechanics and Applied Mathematics*, 42:13–21, 1989.

[70] I.-S. Liu. On representations of anisotropic invariants. *International Journal of Engineering Sciences*, 20:1099–1109, 1982.

[71] B. Loret. On the effect of plastic rotation in the finite element deformation of anisotropic elastoplastic materials. *Mechanics of Materials*, 2:287–304, 1983.

[72] B. Loret, Y. F. Dafalias. The effect of anisotropy and plastic spin on fold formations. *Journal of the Mechanics and Physics of Solids*, 40:417–439, 1992.

[73] J. Lubliner. Normality rules in large-deformation plasticity. *Mechanics of Materials*, 5: 29–34, 1986.

[74] J. Lubliner. Large-deformation plasticity. In *Plasticity Theory*, chapter 8, 438–470, Macmillan Publishing Company, New York, 1990.

[75] M. Lucchesi, M. Silhavy. Il'iushin's conditions in non-isothermal plasticity. *Archives of Rational Mechanics and Analysis*, 113:121–163, 1991.

[76] R. Mahnken, E. Stein. The identification of parameters for visco-plastic models via finite-element methods and gradient methods. *Modelling and Simulation in Material Science and Engineering*, 2:597–616, 1994.

[77] D. Marquis. Modélisation et identification de l'écrouissage anisotrope des métaux. *General Electric Generating Board*, report RD/B/N **731**, 1979.

[78] G. Maugin. In *The Thermodynamics of Plasticity and Fracture*, chapter 5, Cambridge University Press, New York, 1992.

[79] J. Miastkowski. Analysis of the memory effect of plastically prestrained material. *Archiwum Mechaniki Stosowanej*, 20:257–276, 1968.

[80] J. Miastkowski, W. Szczepiński. An experimental study of yield surfaces of prestrained brass. *International Journal of Solids and Structures*, 1:189–194, 1965.

[81] Z. Mroz. On the description of anisotropic workhardening. *Journal of the Mechanics and Physics of Solids*, 15:163ff, 1967.

[82] P. M. Naghdi. Stress-strain relations in plasticity and thermoplasticity. In *Proc. Second Symp. Naval Structural Mechanics*, Eds. E. H. Lee and P. S. Symonds. Pergamon, Oxford, 121–169, 1960.

[83] P. M. Naghdi, J. A. Trapp. On the nature of normality of plastic strain rate and convexity of yield surfaces in plasticity. *Journal of Applied Mechanics*, 42, E, 1:61–66, 1975.

[84] J. Ning, E. C. Aifantis. Anisotropic yield and plastic flow of polycrystalline solids. *International Journal of Plasticity*, 12:1221–1240, 1996.

[85] R. W. Ogden. *Non-linear elastic deformation*. Ellis Harwood Ltd., Chichester, 1984.

[86] W. Oliferuk, W. Świątnicki, M. Grabski. Rate of energy storage and microstructure evolution during the tensile deformation of austenitic steel. *Materials Science and Engineering*, A161:55–63, 1993.

[87] P. Perzyna. The constitutive equations for rate sensitive plastic materials. *Quarterly of Applied Mathematics*, 20:321–332, 1963.

[88] A. Phillips. The foundations of plasticity. *Experiments. Theory and selected applications, CISM*, Udine, 189–271, 1979.

[89] A. Phillips, P. K. Das. Yield surfaces and loading surfaces of aluminum and brass: an experimental investigation at room and elevated temperatures. *International Journal of Plasticity*, 1:89–109, 1985.

[90] A. Phillips, H. Moon. An experimental investigation concerning yield surfaces and loading surfaces. *Acta Mechanica*, 27:91–102, 1977.

[91] A. Phillips, J. L. Tang. The effect of loading path on the yield surface at elevated temperatures. *International Journal of Solids and Structures*, 8:463–474, 1972.

[92] W. H. Press, S. A. Teukolsky, W. T. Vetterling, B. P. Flannery. Numerical recipes in fortran, second edition. Cambridge University Press, 1992.

[93] D. W. A. Rees. Yield functions that account for the effects of initial and subsequent plastic anisotropy. *Acta Mechanica*, 43:223–241, 1982.

[94] A. J. M. Spencer. Deformation of fibre-reinforced materials. Oxford Press, Clarendon, 1972.

[95] A. J. M. Spencer. Isotropic polynomial invariants and tensor functions. *Applications of tensor functions in solid mechanics*, J. P. Boehler. CISM courses and lectures, No 292, 31–53, Springer, Wien–New York, 1987.

[96] A. R. Srinivasa. On the nature of the response functions in rate-independent plasticity. *International Journal of Non-Linear Mechanics*, 32:103–119, 1997.

[97] M. G. Stout, P. L. Martin, D. E. Helling, G. R. Canova. Multiaxial yield behaviour of 1100 aluminum following various magnitudes of prestrain. *International Journal of Plasticity*, 1:163–174, 1985.

[98] W. Trampczynski. The experimental verification of the unloading technique for the yield surface determination. *Archives of Mechanics*, 44:171–190, 1992.

[99] C. Truesdell, W. Noll. The nonlinear field theories in mechanics. In *Handbuch der Physik*, volume III/3, Ed. S. Flügge. Springer, Berlin–Heidelberg–New York, 1965.

[100] Ch. Tsakmakis. Über inkrementelle Materialgleichungen zur Beschreibung großer inelastischer Deformationen. Ph.D thesis. Technische Hochschule Darmstadt, Institut für Mechanik, 1987.

[101] Ch. Tsakmakis. On the loading conditions and the decomposition of deformation. In *Anisotropy and localization of plastic deformation*, Eds. J.-P. Boehler, A. S. Khan 335–356. Elsevier Applied Science, Springer, London–New York, 1991.

[102] Ch. Tsakmakis. Formulation of viscoplasticity laws using overstress. *Acta Mechanica*, 115: 179–202, 1996.

[103] Ch. Tsakmakis. Kinematic hardening rules in finite plasticity. Part I: A constitutive approach. *Continuum Mechanics and Thermodynamics*, 8:215–231, 1996.

[104] Ch. Tsakmakis. Remarks on Il'iushin's postulate. *Archives of Mechanics*, 49:677–695, 1997.

[105] Ch. Tsakmakis, A. Willuweit. A comparative study of kinematic hardening rules at finite deformations. *International Journal of Non-Linear Mechanics*, in press.

[106] Ch. Tsakmakis. Description of plastic anisotropy effects at large deformations. Part I: Restrictions imposed by the second law and the postulate of Il'iushin. *International Journal of Plasticity*, 20:167–198, 2004.

[107] P. Tuğcu, K. W. Neale. On the implementation of anisotropic yield functions into finite strain problems of sheet metal forming. *International Journal of Plasticity*, 15:1021–1040, 1999.

[108] P. Tuğcu, P. D. Wu, K. W. Neale. Finite strain alalysis of simple shear using recent anisotropic yield criteria. *International Journal of Plasticity*, 15:939–962, 1999.

[109] K. Wegener, M. Schlegel. Suitability of yield functions for the approximation of subsequent yield surfaces. *International Journal of Plasticity*, 12:1151–1177, 1996.

[110] J. F. Williams, N. L. Svensson. Locus of 1100-F aluminum. *Journal of Strain Analysis*, 5:128–139, 1970.

[111] J. F. Williams, N. L. Svensson. Effect of torsional prestrain on the yield locus of 1100-f aluminum. *Journal of Strain Analysis*, 6:263–272, 1971.

[112] H. C. Wu, H. K. Hong, J. K. Lu. An endochronic theory accounted for deformation induced anisotropy. *International Journal of Plasticity*, 11:145–162, 1995.

[113] Y. Yoshimura. Hypothetical theory of anisotropy and the Bauschinger effect due to plastic strain history. *Aeronautical Research Institute, University of Tokyo*, report No. 349, 221-247, 1959.

[114] Q.-S. Zheng. Theory of representations for tensor functions – A unified invariant approach to constitutive equations. *Applied Mechanics Review, ASME*, 47:221-247, 1994.

Lebenslauf

David Schick
Dellen 51a
24616 Brokstedt

Geburtstag:	22.01.1970
Geburtsort:	Ichenhausen, Deutschland

Schulbildung:

1976 – 1980	Grundschule Unterknöringen
1980 – 1990	Dossenberger-Gymnasium Günzburg
05/1990	Abitur

Akademischer und beruflicher Werdegang:

1990 – 1993	Studium der Physik an der Universität Augsburg
1993 – 1999	Studium der Physik an der Technischen Universität Darmstadt
05/1999	Abschluss: Diplom-Ingenieur für Physik an der Technischen Universität Darmstadt Diplomarbeit: "Entwicklung von Materialmodellen zur Simulation von kurzfaserverstäkten Thermoplasten". Deutsches Kunststoffinstitut, Darmstadt Betreuer: Dr.-Ing. T. Pflamm
1999 – 2000	Mitarbeiter der Fa. Tecosim GmbH, Rüsselsheim
05/2000 – 2003	Wissenschaftlicher Mitarbeiter am Institut für Mechanik, AG Kontinuumsmechanik (Materialtheorie), Technische Universität Darmstadt. Betreuer: Prof. Dr.-Ing. Ch. Tsakmakis.
seit 06/2003	Mitarbeiter der Fa. Menck GmbH, Kaltenkirchen

Hiermit versichere ich, dass die vorliegende Dissertation von mir selbständig und nur mit den angegebenen Hilfsmitteln angefertigt wurde.

Darmstadt,
den 13. Januar 2004

.....
(Dipl.-Ing. David Schick)